



ANZORS 26th Annual Scientific Meeting

06-08 October 2021

Online Conference

Program



Online event platform by [JT. Production Management](#) 2021, Australia



ANZORS 26th Annual Scientific Meeting

06-08 October 2021

CONTENTS

PRESIDENT’S WELCOME	3
OUR SPONSORS	4
COMMITTEE MEMBERS	5
KEYNOTE SPEAKERS	8
PROGRAM	10
ABSTRACTS	14
DAY 1.....	15
KEYNOTE 1 - Dr Sheanna Maine	15
PODIUM 1	16
PODIUM 2	22
PODIUM 3	28
PODIUM 4	35
KEYNOTE 2 - A/Prof Claire Clarkin	41
DAY 2.....	42
David Findlay Early Career Researcher (ECR) Award Finalists	42
KEYNOTE 3 - Prof Farshid Guilak	48
PhD Award Finalists	49
Minghao Zheng Orthopaedic Innovation Award Finalists	56
DAY 3.....	64
KEYNOTE 4 - Prof Saman Halgamuge	64
PODIUM 5	65
PODIUM 6	72
PODIUM 7	79
POSTERS DAY 2	86
POSTERS DAY 3	99
LIST OF REGISTERED DELEGATES	115



ANZORS 26th Annual Scientific Meeting

President's Welcome

Welcome to the 26th Annual scientific meeting of ANZORS (1995-2021). This is the first ANZORS meeting to be held completely online due to COVID restrictions, after last year's meeting was postponed to this year. My warm welcome to our attendees from Australia, New Zealand and overseas, I look forward to engaging with you throughout the conference. Once again we are able to offer awards, thanks to the support of our sponsors.

It is fantastic to see the ANZORS scientific program being such a multidisciplinary mix of basic, translational and applied orthopaedic research, which is the signature of this society. Complex problems need multidisciplinary teams to be tackled and this is what we do well at ANZORS. Please engage with each other and mingle. Importantly, orthopaedic research needs to receive the funding it deserves. Together we must advocate for it and for the government to distribute it in a more equitable way.

This conference is the last of my three-year tenure as the President of ANZORS - thanks to Tania Crotti, David Ackland and Dominic Thewlis for all their work in this exciting journey.

Just a few days after returning down under from the ORS 2020 meeting in Arizona (USA), where Australia was Guest Nation, Australia and New Zealand entered the international travel ban, which, to date (05th October 2021) is still in place. Online presence is crucial in this scenario, to keep society momentum going, nationally and internationally. All plans had to change. Overall: make the society prevail, with their Innovators, Early Career Researchers and PhD candidates, they have to come out no matter what, they are the future and they need to prosper, COVID or not. Let them flourish.

This is what I am honestly proud of, of the people that despite everything, came out. A society is not just made of the ones that get the awards, who of course are awesome. It is all the people, the vibe, the Q&A with "sorry I don't know" (yes, go with that answer if you honestly feel it is the right one, as it might be the right one at that point in time, if you are at the cutting edge of something!).

We need to adapt to unexpected circumstances "we might not be accustomed to" and it is pretty much an analogy to what "our bone and joints do in certain instances, in daily life". Orthopaedic research and musculoskeletal research in general has to learn from this and I hope it will.

Over the past three years our society has grown, we strengthened our relationship with other societies such as AOA, ORS, the International Combined Orthopaedic Research Societies (ICORS) and the International Federation of Musculoskeletal Research Societies (IFMRS). There are achievements we all have to be proud of, including ANZORS hosting the ICORS 2025 meeting in Adelaide. There is lots of work to be done and I look forward to working with the new President of ANZORS, Nathan Pavlos, the Secretary Martina Barzan and Treasurer Dane Turner, over the next three years.

Please enjoy and engage with the great science presented over the next three days in our conference program.

Egon Perilli

**President, Australian & New Zealand Orthopaedic Research Society
Assoc. Professor, Biomedical Engineering, Medical Device Research Institute,
College of Science and Engineering, Flinders University**



Thanks to our sponsors:

Gold Sponsor



Silver Sponsor



Bronze Sponsor





ANZORS 26th Annual Scientific Meeting

Committee Members

President

A/Prof Egon Perilli

Associate Professor in Biomedical Engineering, The Medical Device Research Institute, College of Science and Engineering, Flinders University

Secretary

A/Prof Tania Crotti

Postgraduate Coordinator Manager for the Adelaide Medical School, Co-leader of the Bone and Joint Laboratory, The Faculty of Health and Medical Sciences, The University of Adelaide

Treasurer

A/Prof David Ackland

Associate Professor, Department of Biomedical Engineering, The University of Melbourne

Immediate Past President

A/Prof Dominic Thewlis

Associate Professor, Centre for Orthopaedic & Trauma Research, The University of Adelaide



Organising Committee

A/Prof Egon Perilli

A/Prof Tania Crotti

A/Prof David Ackland

A/Prof Dominic Thewlis

Dr Martina Barzan

Dr Jiao Jiao Li

Dr Dane Turner

Online Platform

Online event platform by [JT. Production Management](#) 2021, Australia:

Melinda Caswell

Angeline Canta

Scientific Committee

(alphabetical surname order)

A/Prof David Ackland	The University of Melbourne, Australia
Dr John Arnold	The University of South Australia, Australia
Prof Gerald Atkins	The University of Adelaide, Australia
Dr Martina Barzan	Griffith University, Australia
Dr Stuart Callary	The University of Adelaide, Australia
A/Prof John Costi	Flinders University, Australia
A/Prof Tania Crotti	The University of Adelaide, Australia
Dr Dane Turner	Macquarie University, Australia
A/Prof Justin Fernandez	The University of Auckland, New Zealand
Prof David Findlay	The University of Adelaide, Australia
Dr Claire Jones	The University of Adelaide, Australia
Dr Jiao Jiao Li	The University of Sydney, Australia
Dr ZuFu Lu	The University of Sydney, Australia
A/Prof Saulo Martelli	Queensland University of Technology, Australia
Dr David Musson	The University of Auckland, New Zealand
A/Prof Nathan Pavlos	The University of Western Australia, Australia
A/Prof Egon Perilli	Flinders University, Australia
Dr Diana Perriman	Australian National University, Australia
Prof Peter Pivonka	Queensland University of Technology, Australia
Dr Dale Robinson	The University of Melbourne, Australia
Prof Bogdan Solomon	The University of Adelaide, Australia
A/Prof Kathryn Stok	The University of Melbourne, Australia
Prof Ashvin Thambyah	The University of Auckland, New Zealand
A/Prof Dominic Thewlis	The University of Adelaide, Australia
Prof Cory Xian	University of South Australia, Australia
Prof Jiake Xu	The University of Western Australia, Australia

ANZORS 26th Annual Scientific Meeting

Keynote Speakers

Dr Sheanna Maine

Griffith University, Brisbane, Pediatric Orthopedic Surgeon. Hip and knee pathologies, with a focus on paediatric lower limb deformity & reconstruction.

Dr Maine is an Adult Lower Limb Orthopaedic Surgeon with a specialist interest in Paediatric Orthopaedics and Knee surgery. She is a VMO at Brisbane Private Hospital and North West Private Hospital. Dr Maine currently practices at the Queensland Children's Hospital as a Paediatric Orthopaedic Surgeon and at Redcliffe Hospital in Adult Lower Limb Orthopaedic surgery.

After completing her Medical degree in 2002, Sheanna trained in Orthopaedic Surgery in QLD, achieving FRACS in 2010. She undertook a fellowship in Paediatric Orthopaedics at the Royal Childrens Hospital in Melbourne in 2012 where she worked in General Paediatric Orthopaedics, Limb Reconstruction and Paediatric Sports Medicine. In 2018, Sheanna completed an international Travelling Fellowship in the Patellofemoral Joint awarded by ISAKOS.

Sheanna is secretary of the Australian Limb Lengthening & Reconstruction Society and a faculty member of the Australian Paediatric Orthopaedic Society, having been an organizing committee member and instructional course lecturer for the past 5 years. She is the first female member of the Australian Knee Society.

Research has been an integral part of Sheanna's career having collaborated with Griffith University in investigating the consequences of lower limb malalignment on the patellofemoral joint, as well as joint reaction forces in the lower limb. She has published articles including a systematic review and book chapter relating to the patellofemoral joint and she has previously been awarded the Gordon Kerridge Prize and Allan Frederick Dwyer prize for clinical research by the Australian Orthopaedic Association.

Sheanna enjoys spending her spare time with her family and trains in Shotokan karate having competed for Queensland and Australia in two world cups. She has consequently developed a unique insight into the needs of the adolescent and adult athlete. Sheanna has also devoted her time to orthopaedics in developing countries and hopes to continue General Orthopaedic Outreach work in the Pacific islands when COVID 19 is finally under control.



A/Prof Claire Clarkin

Developmental and Skeletal Biology, University of Southampton, UK; Leader, Developmental Biology Theme, Biological Sciences, Faculty of Environmental and Life Sciences; Centre for Human Development, Stem Cells and Regeneration (Medicine).

Claire is Associate Professor in Developmental and Skeletal Biology, she is deputy lead for Developmental Biology Theme within the School of Biological Sciences (Faculty of Environmental and Life Sciences), part of the Centre for Human Development, Stem Cells and Regeneration and is an active member of Fortisnet within the Institute for Life Sciences.

Claire has specific interest in how blood vessels interact with tissues and organs during development, adulthood and disease. To date much of her research has focused on the musculoskeletal system and how age and gender impact blood vessel function within bone and influence skeletal pathology. Cross disciplinary approaches are at the central to the development of Claire's research hypotheses and current collaborations within Southampton include Faculty of Engineering and Physical Sciences, Faculty of Medicine and the Faculty of Arts and Humanities.





Prof Farshid Guilak

Past ORS President; Editor-in-Chief, Journal of Biomechanics; Assoc. Editor, Osteoarthritis & Cartilage; Professor, Dept. of Orthopaedic Surgery, Washington University, USA; Director of Research, Shriners Hospitals for Children - St. Louis; Co-director, Washington University Center of Regenerative Medicine.

Dr. Farshid Guilak is a Professor of Orthopaedic Surgery at Washington University, Director of Research for the St. Louis Shriners Hospitals for Children, and co-director of the Washington University Center of Regenerative Medicine. His laboratory is pursuing a multidisciplinary approach for developing new tissue engineering and stem cell-based therapies for musculoskeletal diseases, particularly arthritis.

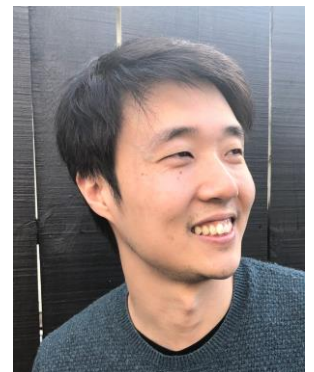
His laboratory has spearheaded the combination of genome engineering and synthetic biology to stem cells, in the context of tissue engineering and regenerative medicine. He has published over 370 articles in peer-reviewed journals and has co-edited four books. He is the editor-in-chief of the Journal of Biomechanics, Associate editor for Osteoarthritis & Cartilage, and serves on numerous other journal editorial boards. He has won several national and international awards for his research, including the Kappa Delta Award for orthopaedic research 3 times, as well as 4 separate awards for mentoring. He has also worked extensively in the translation of tissue engineering technologies and he is the Founder of Cytex Therapeutics, a startup company focusing on developing new regenerative medicine therapies for musculoskeletal conditions.



Dr Ju Zhang

Auckland (PhD Bioeng, 2013), New Zealand. As the founder of FormusLab, Dr Zhang will talk at the Early investigator event about his entrepreneurial post-PhD journey in the field of orthopaedic research.

Ju is the founder and CEO of Formus Labs and a passionate believer in the power of computational biomechanics to improve orthopedic practice. Ju has a PhD in Bioengineering from the Auckland Bioengineering Institute and conducted post-doctoral research at the ABI, Imperial College London, and Stanford University on the way to building Formus Labs.



Prof Saman Halgamuge

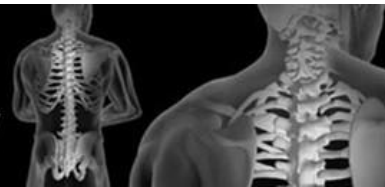
The University of Melbourne, FIEEE, Optimization & Pattern Recognition Research Group, Dept. of Mechanical Engineering. "21st Century Artificial Intelligence" and its potential in biomedical research.

Prof Saman Halgamuge received the B.Sc. Engineering degree in Electronics and Telecommunication from the University of Moratuwa, Sri Lanka, and the Dipl.-Ing and Ph.D. degrees in data engineering from the Technical University of Darmstadt, Germany. He is currently a Professor of the Department of Mechanical Engineering of the School of Electrical Mechanical and Infrastructure Engineering, The University of Melbourne, Australia. He is a Fellow of IEEE, a distinguished Lecturer of IEEE Computational Intelligence Society and listed as a top 2% most cited researcher for AI and Image Processing in Stanford database. His research interests are in AI, machine learning including deep learning, optimization, big data analytics and their applications in biomedicine and engineering.





Australian & New Zealand
Orthopaedic Research Society



PROGRAM

Day 1 (Wednesday October 06)

10:30-10:45 (Melbourne time)	ANZORS President's welcome: A/Prof Egon Perilli		
10:45-11:15 Session chair: A/Prof Egon Perilli	Keynote: Dr Sheanna Maine, Griffith University, Brisbane, Queensland, Australia "Challenges in Paediatric Orthopaedics"		
11:15-11:30 Morning tea & poster viewing			
11:30-12:30	First name	Surname	Abstract title
Podium 1 Session chair: Dr David Musson	Scott	Bolam	Obesity impairs enthesis healing after rotator cuff repair in a rat model
	Jun	Yuan	PINK1-mediated mitophagy in osteocytes contributes to glucocorticoid-induced osteocytic osteolysis
	Daniel	Wills	Healing of iliac crest cancellous autograft donor site in an adult ovine model
	Samantha	Hefferan	Histological characteristics of different human tendons
	Samuel	Bennett	Gene mining the dental and skeletal fields of the collaborative cross population
12:30-12:45 Break & poster viewing			
12:45-13:45	First name	Surname	Abstract title
Podium 2 Session chair: Prof Ashvin Thambyah	Sanaa	Zaki	Investigating the predictive utility of a mouse model of post-traumatic osteoarthritis for testing the symptom and disease modifying effect of therapeutic agents
	Maged	Awadalla	Knockout cystic fibrosis rat trabecular bone in the proximal tibia has a deficit through adolescence
	Iman	Roohani	Synthetic bone-like structures through omnidirectional ceramic bioprinting in cell suspensions
	Peilin	Chen	Fabrication of bioactive braided collagen rope with exceptional mechanical strength for anterior cruciate ligament reconstruction
13:45-14:15 Lunch break & poster viewing			
14:15-15:15	First name	Surname	Abstract title
Podium 3 Session chair: Dr Jiao Jiao Li	William	du Moulin	Shape differences in the semitendinosus following tendon harvesting for anterior cruciate ligament reconstruction
	Sophie	Rapagna	Relationships between cartilage thickness and subchondral bone in knee osteoarthritis and controls: a systematic mapping
	Pholpat	Durongbhan	A novel micro-computed tomography imaging protocol for reproducible quantitative morphometric analysis (QMA) of the mouse knee
	Aaron	Fox	Subscapularis muscle function following the Latarjet procedure
	Luca	Modenese	Personalised lower limb models generated using an automatic workflow: comparison with manually created models
15:15-15:30 Afternoon break & poster viewing			
15:30-16:30	First name	Surname	Abstract title
Podium 4 Session chair: A/Prof Tania Crotti	Mitchell	Almond	Double intramedullary and single extramedullary cortical button constructs for distal biceps tendon surgical repair
	Harshi	Rupasinghe	Tension band wiring versus a novel tension band suture fixation for the treatment of olecranon fractures: a comparative biomechanics study
	Dale	Robinson	The influence of graft positioning on glenohumeral joint contact in the Latarjet procedure for recurrent shoulder instability
	Adam	Kositsky	Knee flexor weakness after anterior cruciate ligament reconstruction with a semitendinosus tendon graft: is it just due to muscle size?
	Darcy	Thompson-Bagshaw	Characterising the response of human heads during a simulated head-first impact
16:30-17:00 Session chair: A/Prof Tania Crotti	Keynote: A/Prof Claire Clarkin, University of Southampton, Southampton, UK "Resolving Sexual Dimorphism of the Bone Vasculature"		
17:00-17:05 Close & thank you			

Day 2 (Thursday October 07)

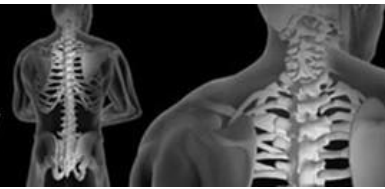
10:00-10:05	Day 2 Welcome: A/Prof Nathan Pavlos		
10:05-11:05	First name	Surname	Abstract title
David Findlay ECR Award Final, Session chairs: A/Prof Nathan Pavlos	Kai	Chen	Osteoblast-derived EGFL6 couples angiogenesis to osteogenesis during bone repair
	Damith	Senanayake	Wearable sensors for tele-medicine in orthopaedics: overcoming the challenge of converting raw IMU data into high accuracy joint angles
	Dzenita	Muratovic	Elevated levels of active transforming growth factor B1 in the subchondral bone relate spatially to cartilage loss and impaired bone quality in human knee osteoarthritis
	Carina	Blaker	Repeated mild knee injury events are associated with early osteoarthritic change
	Martina	Barzan	Accuracy and functional outcomes of juvenile proximal femoral osteotomies using virtual surgical planning and patient-matched surgical guides
11:05-11:45	<p>Session chair: A/Prof Nathan Pavlos</p> <p style="text-align: center;">Keynote: Prof Farshid Guilak, Washington University, St. Louis, USA</p> <p style="text-align: center;">“Gene Therapy for Obesity and Aging in Osteoarthritis”</p>		
11:45-12:05 Morning tea and poster viewing			
12:05-13:05	First name	Surname	Abstract title
PhD Award Final, Session chair: Sophie Rapagna	Jacob	Trend	Examining a role for VEGF in the regulation of osteocyte lacunae orientation
	Lauren	Wearne	Micro-CT imaging a press-fit tray implanted in human tibia: a zero-strain digital volume correlation analysis at organ level
	Amy	Ribet	Proteomics of the osteoclast secretory lysosome unmasks new regulators of bone resorption and skeletal bone mass
	Alexis	Brierty	The variability of foot motion in children with congenital talipes equinovarus (CTEV) being considered for tendon transfer surgery
	Kieran	Bennett	The mechanical response of trabecular bone within the tibial plateau due to external joint loading
13:05-13:45 Lunch break and poster viewing			
13:45-14:35	First name	Surname	Abstract title
Minhao Zheng Orthopaedic Innovation Award Final, Session chair: Dr Martina Barzan	Ben	Ferguson	CT-based FEA and multiobjective optimisation methods for determining optimal placement of fixation plate for scaffold-based mandibular reconstruction
	Faseeh	Zaidi	Remote patient monitoring with wearable sensors following knee arthroplasty
	Scott	Bolam	Enhancement of tendon-bone healing with a combined growth factor hydrogel in a rat chronic rotator cuff injury model
14:35-14:50	First name	Surname	Abstract title
Posters – Set 1, Session Chair: Dr Joe Lynch	Bailey	Deverell	Irinotecan's effect on trabecular long bone in a rat model of breast cancer
	Jonghoo	Sung	Delayed fracture healing in Zucker diabetic fatty (ZDF) rats is associated with persistent up-regulated pro-inflammatory marker expression
	James	Crowley	Lateral fenestration of lumbar intervertebral discs in rabbits: development and characterisation of a preclinical model
	Melanie	Amarasooriya	In vivo kinematics of the scaphoid in scapholunate instability using 4D CT-preliminary results
	Buddhi	Herath	Design workflow for 3D printable patient-specific Voronoi bone scaffolds
14:50-15:20 Break and poster viewing			
15:20-15:35	First name	Surname	Abstract title
Posters – Set 2, Session Chair: Dr Joe Lynch	Lachlan	Huntington	Double screw fixation in an unstable scaphoid fracture model: a biomechanical comparison of two screw configurations
	Hugo	Wiggins	High tibial osteotomy and distal femoral osteotomy using patient -specific instruments: pilot data from a biomechanical study of the lower limbs, pelvis and lumbar spine
	Sara Sadat	Farshidfar	Biomechanical improvements in gait following medial pivot knee implant surgery
	Yihang	Yu	The effect of spine cage position on the mechanical response of the superior lumbar endplate after lumbar interbody fusion
	Joseph	Cadman	Failure of tendon grafts fixed with 3mm tenodesis screws: does screw placement make a difference?
	Sara Sadat	Farshidfar	The effect of modelling parameters in the development and validation of knee joint models on ligament mechanics: a systematic review
15:35-15:45 Afternoon break & poster viewing			
15:55-16:55	<p>ANZORS AGM</p> <p>All delegates welcome (and encouraged) to attend</p>		
16:55-17:55	<p>New Investigator Breakout New Investigator Breakout: register if you haven't vet (free)!</p> <p>Dr Ju Zhang, founder of FormusLab: “Entrepreneurial post-PhD journey in the field of orthopaedic research”</p>		

Day 3 (Friday October 08)

10:25-10:30	Day 3 Welcome: A/Prof David Ackland		
10:30-11:00 Session chair: A/Prof David Ackland	Keynote: Prof Saman Halgamuge, The University of Melbourne, Victoria, Australia “21st Century Artificial Intelligence and its Potential in Biomedical Research”		
11:00-11:15 Morning tea and poster viewing			
11:15-12:15	First name	Surname	Abstract title
Podium 5	Azadeh	Kian	EMG-driven model predictions of glenohumeral joint force show high agreement with instrumented implant data after targeted model calibration
Session chair: Dr Dale Robinson	Ian	Al'Khafaji	The role of the ligamentum teres in normal function of the hip joint
	Dominic	Thewlis	Patient-reported and functional outcomes in patients following primary and revision total hip arthroplasty
	Ryan	Quarrington	Estimating facet joint apposition with specimen-specific computer models of subaxial cervical spine kinematics: the effect of axial compression and distraction during shear and bending motions
	Marco	Branni	Quantifying orthotropic mechanical properties in entire human femurs
12:15-12:45 Lunch and poster viewing			
12:45-13:20	First name	Surname	Abstract title
Posters – Set 3	Emma	Brown	Multi length scale structural investigation of articular cartilage: how structure influences the swelling response of mildly degenerate bovine articular cartilage
Session chair: Dr Dane Turner	Josh	Workman	Reference point indentation for the detection of early osteoarthritis
	Daniel	Wills	The thermal profile of self-tapping screws: the effect of insertion speed, power insertion, and screw geometry on heat production at the bone-screw interface
	Lianzhi	Chen	A population-based study on total knee replacement attributable to obesity in Australia
	Ross	Hamilton	Scoping review of imaging techniques to assess muscle damage post-total hip arthroplasty
	Joe	Lynch	In-vivo kinematics during step-up and down in three total knee replacement designs: a randomised clinical trial
Posters – Set 4	Peggy	Miller	Dangers of being an outlier; mortality risk in hip fracture patients based off the orthopaedic ward. A cohort study
Session chair: Dr Dane Turner	Megan	Roser	Preliminary outcomes for patients undergoing vertebral body tethering for idiopathic scoliosis
	Reinier W.A.	Spek	3D printed handheld models do not improve recognition of specific characteristics and patterns of three-part and four-part proximal humerus fractures
	Thomas	Robertson	CT measured acetabular bone density following total hip arthroplasty: a scoping review and meta-analysis
	Yuan	Chai	Two novel designs of improving patella resection tools
	Stuart	Callary	Establishing an evidence-based approach to improve the stability of acetabular components used at revision surgery
13:20-13:30 Lunch and poster viewing			
13:30-14:30	First name	Surname	Abstract title
Podium 6	Francesca	Bucci	Does sex influence knee passive kinematics?
Session chair: Dr Stuart Callary	Arjun	Sivakumar	Changes in post-operative lower limb biomechanics after femoral nailing of proximal femur fractures
	Azadeh	Nasseri	Effects of pubertal maturation on anterior cruciate ligament forces during a landing task in females
	David	Shen	Prosthetic impingement risk factors and impact on patient outcomes in hip resurfacing arthroplasty
	Kerry	Costi	Comparison of AOANJRR hip arthroplasty data with a hospital based registry
14:30-14:40 Afternoon break and poster viewing			
14:40-15:40	First name	Surname	Abstract title
Podium 7	Stuart	Callary	Factors influencing femoral periprosthetic fracture around cemented stems
Session chair: Dr Claire Jones	Sam	Mischewski	Venous thromboembolism following surgical intervention for below knee fractures: a systematic review of the risk and benefits of preventative strategies
	Fraser	Francis-Pester	Patients with anterior shoulder instability adopt compensatory scapula motion during upper limb function
	Kiran	Rajesh	Hip fracture and dementia: prevalence, clinical profile, in-hospital outcomes and readmissions
	Pouya	Saeedian	Preoperative kinematics influences postoperative kinematics of the knee. A prospective randomised clinical trial of total knee arthroplasty
15:40-15:45	Announcement of Awards		
15:45-16:00	President's closing address Discussion of ANZORS 2022		



Australian & New Zealand
Orthopaedic Research Society



ABSTRACTS

DAY 1

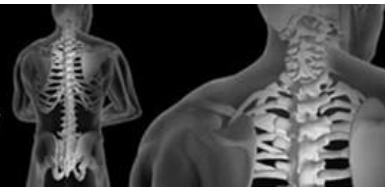
KEYNOTE 1 – Dr Sheanna Maine

Griffith University, Brisbane, Queensland, Australia

“Challenges in Paediatric Orthopaedics”



Australian & New Zealand
Orthopaedic Research Society



DAY 1

PODIUM 1



OBESITY IMPAIRS ENTHESIS HEALING AFTER ROTATOR CUFF REPAIR IN A RAT MODEL

S.M. Bolam^{1,2}, Y.E. Park¹, S. Konar¹, K. Callon¹, J. Workman³, A.P. Monk^{2,4}, B. Coleman⁵, J. Cornish¹, M.H. Vickers⁶, J.T. Munro^{1,2}, D.S. Musson^{1,7}

1. Department of Medicine, University of Auckland, Auckland, NZ; 2. Department of Orthopedics, Auckland City Hospital, Auckland, NZ; 3. Department Chemical and Materials Engineering, University of Auckland, Auckland, NZ; 4. Auckland Bioengineering Institute, University of Auckland, Auckland, NZ; 5. Department of Orthopedics, Middlemore Hospital, Auckland, NZ; 6. Liggins Institute, University of Auckland, Auckland, NZ; 7. Department of Nutrition, University of Auckland, Auckland, NZ

email: s.bolam@auckland.ac.nz

Introduction: Obesity associated with poor outcomes and increased risk of failure after rotator cuff (RC) repair surgery. The effect of diet-induced obesity (DIO) on entheses healing has not been well characterized and whether its effects can be reversed with dietary intervention is unknown. We hypothesized that DIO would result in inferior entheses healing in a rat model of RC repair, and that dietary intervention in the peri-operative period would improve entheses healing.

Methods: A total of 78 male Sprague-Dawley rats were divided into three weight-matched groups from weaning and fed either: control diet (CD), high fat diet (HFD), or HFD until surgery, then CD thereafter (HF-CD). After 12 weeks the left supraspinatus tendon was detached, followed by immediate surgical repair. At 2 and 12 weeks post-surgery, animals were culled and RCs harvested for biomechanical and histological evaluation. Body composition and metabolic markers were assessed via DEXA and plasma analyses, respectively.

Results and Discussion: DIO was established in the HFD and HF-CD groups prior to surgery, and subsequently reversed in the HF-CD group after surgery. At 12 weeks post-surgery, plasma leptin concentrations were higher in the HFD group compared to the CD group (5.28 vs. 2.91ng/ml,

$P=0.003$). Histologically, the appearance of the repaired entheses was poorer in both the HFD and HF-CD compared to the CD group at 12 weeks (overall histological score 6.20 ($P=0.008$), 4.98 ($P=0.001$) and 8.68 out of 15, respectively). The repaired entheses in the HF-CD group had significantly lower (26.4 N, $P=0.028$) load-at-failure 12 weeks post-surgery compared to the CD group (34.4 N); while the HFD group was low, but not significantly different (28.1 N, $P=0.096$). Body mass at the time of surgery, plasma leptin and body fat percentage were negatively correlated with histological scores and plasma leptin with load-at-failure 12 weeks post-surgery.

Conclusions: DIO impaired entheses healing in this rat RC repair model, with inferior biomechanical and histological outcomes. Restoring normal weight with dietary change after surgery did not improve healing outcomes. This pre-clinical rodent model demonstrates that obesity is a potentially modifiable factor that impairs RC healing and increases the risk of failure after RC surgery. Circulating levels of leptin significantly correlated with poor healing outcomes. This adipose-secreted cytokine could be an important mediator impairing entheses healing in obese patients, which could be targeted with future treatments.

PINK1-MEDIATED MITOPHAGY IN OSTEOCYTES CONTRIBUTES TO GLUCOCORTICOID-INDUCED OSTEOCYTIC OSTEOLYSIS

^{1,2}Jun Yuan, ²Andrew Chi Pang Tai, ^{1,2}Minghao Zheng, ^{3,1,2}Junjie Gao

¹Centre for Orthopaedic Translational Research, Medical School, The University of Western Australia, Nedlands, Western Australia, 6009, Australia

²Perron Institute for Neurological and Translational Science, Nedlands, Western Australia, 6009, Australia

³Department of Orthopaedic Surgery, Shanghai Jiao Tong University Affiliated Sixth People's Hospital, Shanghai, 200233, China
email: jun.yuan@research.uwa.edu.au

INTRODUCTION

Cathepsin K (CTSK) is a cysteine protease mainly produced by osteoclasts and has the unique capacity to degrade type I collagen. Previous study has reported the existence of autophagy and increased production of cathepsin K in osteocytes after GC administration, raising the possibility that autophagy activation and osteocytic cathepsin K overproduction could be coupled events. It is demonstrated that GC as one stress factor has been reported to have the potential to demolish mitochondria homeostasis and the dysfunction of mitochondria are claimed to be associated with various diseases. Given the fact that inhibition of autophagy cannot stop the GC-induced bone loss, investigating the role of mitophagy in this pathological process and its relationship with cathepsin K will be of high significance.

METHODS

The osteocyte like cell line, MLO-Y4, were employed to observe the effects of GC on osteocytes. Confocal imaging was used to show the changes of mitochondria morphology. Then, PTEN-induced putative kinase 1 (PINK1) as the mitophagy marker was chosen to verify the existence of mitophagy. To validate the regulation of mitophagy on osteocytic osteolysis, MLO-Y4 cells were transfected with siRNA to knock down PINK1 expression and subsequent changes of genetic expression as well as protein levels of PINK1 and CTSK were determined by real-time PCR and western blotting, respectively.

Figure 1: A, B Analysis for mitochondria morphology changes in MLO-Y4 cells; **C.** Representative confocal images of MLO-Y4 cells after 24 hours treatment with vehicle or 10^{-6} M Dex, cells were stained for PINK1 (green) and MTR (red). Scale bar = 10 μ m; **D.** Quantification for fluorescence intensity of PINK1; **E.** Western blotting analysis of PINK1 protein level in MLO-Y4 cells treated with vehicle or 10^{-6} M Dex.

RESULTS AND DISCUSSION

Cofocal imaging revealed that the majority of mitochondria in the control group are tubular-like. However, increased mitochondrial fragmentations were observed in dexamethasone (Dex) treated group, in a dose dependent manner, which is similar to the CCCP-treated (positive control) group (Figure 1A, B). Meanwhile, we observed that more PINK1 puncta accumulated around mitochondria and an increasing fluorescence intensity of PINK1 staining following Dex (10^{-6} M) treatment compare with cells in vehicle-treated group (Figure 1C and D). We then analyzed the protein level of PINK1 under high GC stress by western blot, the immunoblotting result showed an increased production of PINK1 protein (Figure 1E). Examination of relationship between mitophagy and osteocytic osteolysis revealed that inhibition of mitophagy *via* knocking down *Pink1* gene abolished the GC-triggered cathepsin K production (Figure 2).

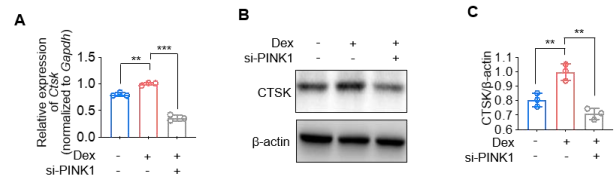
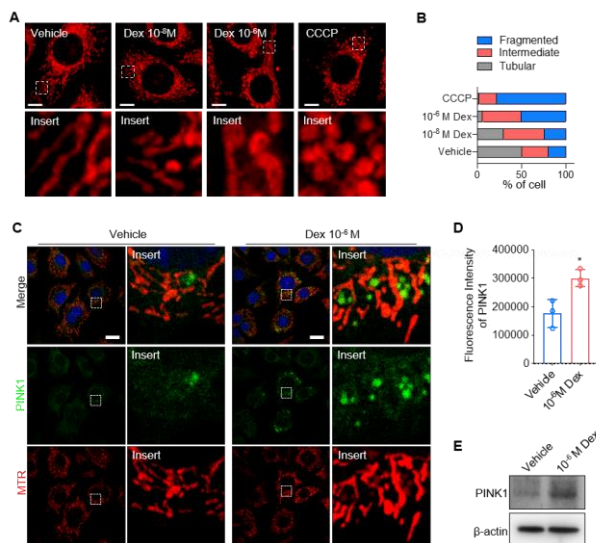


Figure 2: A. Evaluation of *Ctsk* gene expression in *Pink1* knock-down MLO-Y4 treated with vehicle or GC by RT-qPCR; **B, C.** Evaluation of cathepsin K protein levels in *Pink1* knock-down MLO-Y4 cells by western blotting.

CONCLUSIONS

In summary, our results provide the novel finding that GC-induced PINK1-mediated mitophagy substantially modulates the production of cathepsin K in osteocytes, thereby contributing to the GC-induced bone loss.

HEALING OF ILIAC CREST CANCELLOUS AUTOGRAFT DONOR SITE IN AN ADULT OVINE MODEL

Wills DJ¹, Crowley JD¹, Oliver RA¹, Wang T¹, Pelletier MH¹, Walsh WR¹

¹Surgical & Orthopaedic Research Laboratories, UNSW, Sydney, Australia.

email: d.wills@unsw.edu.au

Introduction

The iliac crest is a common donor site for harvesting of autogenous cancellous bone graft (1), however few studies have investigated normal healing of the harvest site. This study examined the healing of bone defects created in the iliac crest following manual harvesting of cancellous autograft in an adult ovine model.

Methods

Twelve skeletally mature ewes (4-5 years old) which were part of an interbody fusion study, were enrolled, with n=6 per group. The iliac crest was surgically exposed using a dorsolateral approach and bone rongeurs used to remove the dorsal cortex and harvest cancellous bone, maintaining the lateral and medial cortical shell and the associated musculature. Iliac crests were harvested and scanned with micro computed tomography (μCT) system (MILabs, Netherlands) with 40μm resolution followed by paraffin histology processing at 6 and 12 week timepoints to evaluate healing. μCT bone morphometry parameters of a central region within the defects and adjacent normal bone regions of similar volume were compared using a One-way ANOVA and post-hoc Tukey's test.

Results and Discussion

All animals recovered uneventfully following surgery. No adverse reactions were noted macroscopically, on μCT imaging or histology. The periosteal reaction was greater on the medial aspect of the iliac crest compared to the lateral in 8/12 cases. Mean trabecular bone volume (TBV) increased from $8.04 \pm 6.57 \text{mm}^3$ at 6 weeks to $17.59 \pm 9.54 \text{mm}^3$ at 12 weeks and was $20.69 \pm 3.79 \text{mm}^3$ in normal regions. TBV at 6 weeks was significantly less than that of normal regions ($p=0.018$), however no significant difference was shown between 6 and 12 weeks or 12 weeks and normal regions. Mean trabecular surface area (TSA) also progressively increased from $160.11 \pm 158.73 \text{mm}^2$ at 6 weeks to $224.80 \pm 125.15 \text{mm}^2$ at 12 weeks and was $281.15 \pm 26.39 \text{mm}^2$ in normal regions, however no statistical differences were detected between groups. Whilst no significant differences were detected between groups for bone morphometry variables, there were trends towards increased bone volume/total volume, trabecular thickness and trabecular number; and decreased bone surface area/bone volume, trabecular spacing and trabecular pattern factor over time.

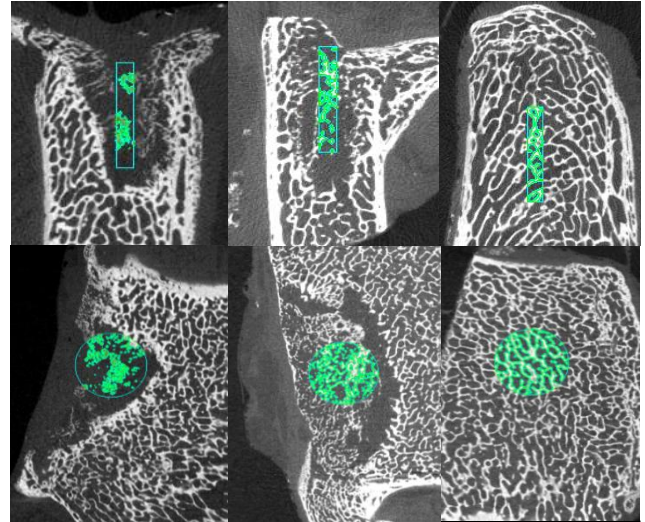


Figure – μCT imaging of iliac crest samples showing progressive bone formation over time within defect and dorsal bridging of the cortical shell. L to R 6, 12 weeks, normal. Bone morphometric analysis within the selected region of interest (green) were performed with IRW (Siemens Medical Solutions, Knoxville, TN, USA)

No variable returned to normal values within the timeframe of the study. Progressive filling of the defect and replacement of the dorsal cortical shell was present on μCT multiplanar reconstructions and histologically but healing at 12 weeks was incomplete.

Conclusion

Defect healing progresses with reformation of the dorsal cortical shell and internal trabecular structure following cancellous bone graft harvesting from the iliac crest, however is incomplete at 12 weeks. Recommended future work includes the comparison of this harvesting technique to that of a tricortical harvest.

References:

1. JBJS: 2002 - 84 - Issue 5 - p 716-720



HISTOLOGICAL CHARACTERISTICS OF DIFFERENT HUMAN TENDONS

^{1,3}Samantha Hefferan, ^{1,3}Carina Blaker, ^{1,3}Dylan Ashton, ⁴⁻⁶Nicholas Hartnell, ^{2,3}Christopher Little and ^{1,3}Elizabeth Clarke

¹Murray Maxwell Biomechanics Laboratory and ²Raymond Purves Bone and Joint Research Laboratories, Institute of Bone and Joint Research, Kolling Institute, Royal North Shore Hospital, Sydney, NSW, Australia

³Faculty of Medicine and Health, University of Sydney, Sydney, NSW, Australia

⁴Bowral and District Hospital, ⁵Southern Highlands Private Hospital, and ⁶Southern NSW Health District, NSW, Australia
email: samantha.hefferan@sydney.edu.au

INTRODUCTION

Tendons have one of the largest extracellular matrix to cell ratios of all tissues (65-80% collagen) with important structure-function characteristics for musculoskeletal functioning [1,2]. The pathophysiology of tendons is complex, and it is unclear whether these processes differ between different tendon types, underpinned by a lack of existing knowledge on normal variations between different healthy tendons. This study aims to characterise the histological structures of different human lower-leg tendons and identify variations between tendon type, region within a tendon (proximal versus distal), age and sex.

METHODS

Proximal and distal paired samples from nine different lower-leg tendons (Achilles, AT; tibialis anterior, TA; tibialis posterior, TP; fibularis longus, FL; fibularis brevis, FB; flexor hallucis longus, FHL; extensor hallucis longus, EHL; flexor digitorum longus, FDL; and plantaris, Plt) were retrieved from human cadavers (fresh-frozen; 5 male, 6 female; 68-99 years). Three histological sections were prepared for each sample following protocols modified from Smith et al. [3], one each for Haematoxylin and Eosin (H&E), Toluidine Blue (TB) and Picrosirius Red (PSR) staining. A total of 936 region-matched images (200x) were included for analysis (312 per stain). H&E images were used for automated image analysis (particle analysis macro; ImageJ-1.52a) to assess cell density and nuclear morphology, and further scored for structural characteristics of the collagen architecture. TB images were scored for proteoglycan content. PSR images were scored for additional structural characteristics and crimp wavelength (polarized light). Mixed-effects linear (macro outcomes) or ordered-logistic regression (scored outcomes) analysis models with Sidak's adjustment for multiple comparisons were used to determine the effects of tendon, region, age and sex on these outcomes (nine in total).

RESULTS AND DISCUSSION

Comparisons between tendon types found significant differences in crimp wavelength (Figure 1), average nucleus size, and nuclei circularity. When comparing all proximal versus all distal samples, differences were observed for cell density, nuclear size and circularity, fibre separation, proteoglycan content and staining intensity, collagen alignment and crimp wavelength (see Figure 1 for example). Males had significantly shorter crimp wavelength compared to females

($p=0.029$). Increasing age was found to decrease cell density ($p=0.002$), decrease fibre bundling ($p=0.001$) and decrease crimp wavelength ($p=0.045$).

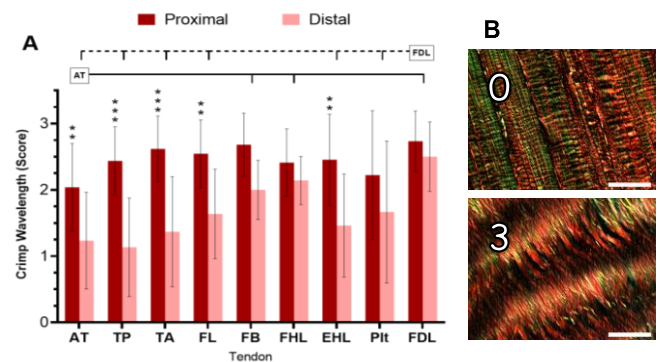


Figure 1. A) Crimp wavelength of proximal and distal samples for nine different human lower-leg tendons (mean±SD). Tick-marks indicate significant tendon type differences, comparing to the tendon identified in box ($p<0.05$). Significant proximal versus distal differences (per tendon) indicated by asterisks: * $p<0.05$; ** $p<0.01$; *** $p<0.001$. **B)** Example of end-range scores for crimp wavelength: 0 = very fine, 3 = very coarse. Picrosirius red (polarized light); 200x, scale bar = 100µm.

CONCLUSIONS

Numerous histological differences were observed with tendon type, region, age and sex, identifying important variations not previously assessed in human tendons. These findings could implicate potential differences in mechanical properties, injury risk and pathological predisposition between tendons, and could further knowledge of normal tendon variations, and provide a basis for understanding mechanisms of pathology.

ACKNOWLEDGEMENTS

The authors thank Sereen Assi, Susan Smith, Dr Patrick Haubruck and Dr Matthew McCann for their expertise and assistance. This work was supported by the Australian Orthopaedic Association Research Foundation Ltd; the Lincoln Centre for Bone and Joint Diseases; and the Ramsay Teaching and Research Trust Fund.

REFERENCES

1. Kjaer M, *Physiol Rev.* **84**:649-698, 2004.
2. Screen H, et al., *J Orthop Res.* **33**:793-799, 2015.
3. Smith M, et al., *Arthritis Rheumatol.* **58**:1055-1066, 2008.



GENE MINING THE DENTAL AND SKELETAL FIELDS OF THE COLLABORATIVE CROSS POPULATION

¹Samuel Bennett, ¹Eason Guo, ²Curtise Ng, ¹Jacob Kenny, ¹Jinbo Yuan, ³Grant Morahan, ¹Jennifer Tickner and ¹Jiake Xu

¹Molecular Laboratory, School of Biomedical Sciences, The University of Western Australia, Nedlands, WA.

²Discipline of Medical Radiation Sciences, Curtin University, Bentley, WA.

³UWA Centre for Medical Research, The University of Western Australia, Nedlands, WA.

Email: samuel.bennett@research.uwa.edu.au

INTRODUCTION

The Collaborative Cross (CC) is a purpose-built resource that was developed to enhance quantitative trait locus (QTL) and systems genetic analysis in mice [1]. Breeding programs of the CC were established at the University of North Carolina (UNC), Tel Aviv University (TAU), and The Gene Mine (Geniad) in Perth, WA. The Gene Mine consists of an octo-parental recombinant inbred panel of over 1000 strains generated and housed at the Animal Resources Centre, since 2004.

A primary aim of the CC and Geniad is to provide a stable, reproducible genetic reference platform for the qualitative and quantitative analyses of the causative gene-variants, epistatic mechanisms, and environmental factors that determine disease. Integration of phenotypic and genomic data over time and across a wide variety of fields is vital to achieving this aim. Research into the osteoporosis, osteoarthritis, and scoliosis fields of the CC has been initiated by our group. My project is investigating the molecular determinants of dental and skeletal phenotypes within the Geniad CC population. The aims are 1) to identify novel molecular determinants of dental and skeletal homeostasis and disease and 2) to correlate these findings with concomitant disease phenotypes including osteoporosis, osteoarthritis, and scoliosis in CC mice.

METHODS

Our aims will be achieved by screening of Geniad mice using conventional x-ray and micro computed tomography for dental, skeletal, scoliosis, and kyphosis phenotypes. Mapping of QTLs will subsequently be performed to identify candidate genes regulating these phenotypes. *In vitro* gene expression and bioinformatics analyses will then be used to verify and characterize candidate gene involvement.

RESULTS AND DISCUSSION

Table 1: Phenotypes observed across the scoliosis, kyphosis, and dental fields of the Geniad population.

	Phenotype						
	Total	Strains	Scoliosis	Kyphosis	Kyphoscoliosis	Dental	Hypodontia
Mice	1137	84	41	50	16	206	80

We have completed initial conventional x-ray screening of 1137 Geniad mice across 84 strains and observed a range of phenotypes, including a novel hypodontia phenotype (Table 1).

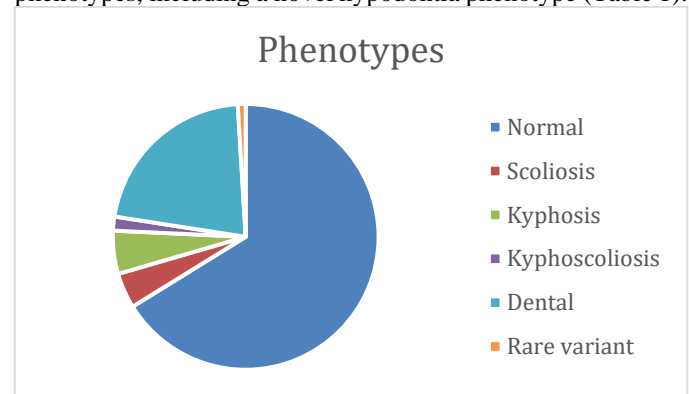


Figure 1: Proportion of phenotypes observed across scoliosis, kyphosis, and dental fields of the Geniad population.

CONCLUSIONS

In conclusion, the conventional x-ray screening results are consistent with the incidence of these pathologies in human populations, validating this approach, and indicating the need for further micro-CT analysis, identification, and mapping of QTLs, prior to the determination of candidate gene involvement for dental, skeletal, scoliosis and kyphosis phenotypes.

ACKNOWLEDGEMENTS

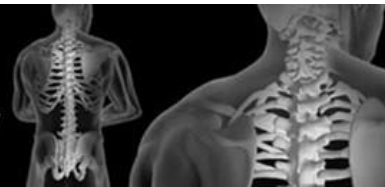
This research is supported by an Australian Government Research Training Program scholarship and UWA Project Grant (37005000).

REFERENCES

1. Threadgill DW and Churchill GA. *Genetics* **190**:291-294, 2012.



Australian & New Zealand
Orthopaedic Research Society



DAY 1

PODIUM 2



INVESTIGATING THE PREDICTIVE UTILITY OF A MOUSE MODEL OF POST-TRAUMATIC OSTEOARTHRITIS FOR TESTING THE SYMPTOM AND DISEASE MODIFYING EFFECT OF THERAPEUTIC AGENTS

^{1,2}Sanaa Zaki, ¹Sonia Nair, ²Carina Blaker and ²Christophor Little

¹Sydney School of Veterinary Science, Faculty of Science, University of Sydney; Camperdown, NSW, Australia

²Raymond Purves Bone & Joint Research Laboratories, Institute of Bone and Joint, Kolling Institute of Medical Research, Northern Clinical School, Faculty of Medicine and Health, University of Sydney; St Leonards, NSW, Australia

email: sanaa.zaki@sydney.edu.au

INTRODUCTION

Pre-clinical animal models form the foundation of translational drug-discovery, but how well models of osteoarthritis (OA) predict patient outcomes is unclear [1]. There is limited research directed towards evaluating how the effect size (ES) in a relevant pre-clinical model corresponds to the minimal clinically important difference (MCID) for a drug beneficial in human OA. Intra-articular corticosteroids (IAC) are a well-established therapy for short-medium-term relief of OA symptoms [2,3]. However, their impact on disease progression is of concern to clinicians, and to date little is known about how disease stage at the time of administration impacts long-term joint pathology. The aim of this study was to determine the predictive utility of the mouse medial-meniscus-destabilisation (DMM) model by measuring the effects of intra-articular triamcinolone-acetate (iaTCA) on pain and comparing this with well described ES responses in OA patients; and determining how these relate to end-stage disease.

METHODS

Male 10-week C57BL6 mice had unilateral DMM surgery to induce knee OA. At week -2, -4 or -8 post-surgery mice received 100mcg iaTCA or saline (n=12/treatment/time). Tactile allodynia, local hyperalgesia and hindlimb weight distribution (HLWD) were measured at baseline, week -2, -4, -8, -12 -16. The percentage response relative to baseline was calculated as an ES for comparing to clinical trial outcomes. Joints were harvested for histopathological assessment at week-16. Global joint pathology was quantified by scoring AC, synovium, subchondral bone, menisci & osteophyte pathology.

RESULTS AND DISCUSSION

iaTCA had significant short-medium-term benefit on all pain outcomes; ES and duration differing with administration time post-DMM. A greater reduction in tactile allodynia and local hyperalgesia occurred at week-2 and -4 (>90%) versus week-8 (70%) iaTCA. Duration of improvement was 4-8 weeks for iaTCA injected at week-4 and <4 weeks for week-2 and -8 iaTCA. Week-2 iaTCA resulted in early maximum resolution for allodynia (48hrs) and delayed maximum resolution for local hyperalgesia (2wks). Improvement in HLWD occurred with week-2 and -8 iaTCA only. Importantly the factors that modify efficacy in patients were reflected in this model e.g. reduced ES with worse OA pathology. iaTCA did not significantly affect late-stage disease synovitis or bone-pathology. AC damage was

significantly reduced for week-8 iaTCA compared to saline and week-2 iaTCA. Chondocyte hypertrophy/apoptosis was significantly increased for week-4 iaTCA; and was greater with week-2 and -4 iaTCA compared to week-8. Consistently, week 4 iaTCA injection resulted in increased joint pathology, and week 8 iaTCA injection resulted in decreased joint pathology at late-stage disease (week-16 DMM).

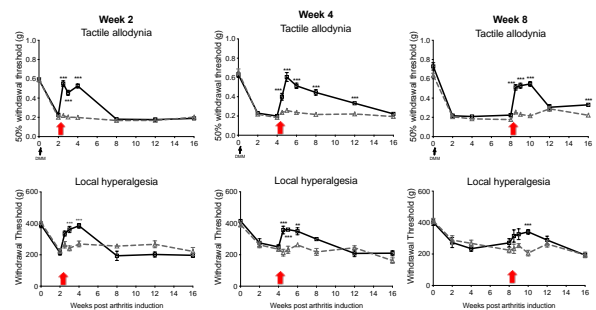


Figure 1: Pain measurements following iaTCA in DMM mice. Expressed as mean +/-SEM. **= $P < 0.01$, ***= $P < 0.005$

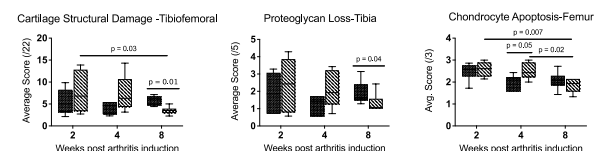


Figure 2: Mouse knee joint tissue histopathology scores at 16-weeks post DMM, following iaTCA injection at week-2, -4, -8.

CONCLUSIONS

As in people iaTCA modified OA pain, with effects dependent on disease stage. The effect on long-term pathology differed with time of iaTCA administration and was not predicted by clinical response. These findings provide direct evidence of the predictive utility of the DMM model for therapeutic outcomes in people and highlight the need for better patient selection to optimise therapeutic benefit and mitigate joint damage risk.

ACKNOWLEDGEMENTS

The Hillcrest Foundation through Perpetual Philanthropies.

REFERENCES

1. Hummel M, Whiteside GT. *OA&C*. **25**:376-384, 2017.
2. van Middelkoop, M. et al, *OA&C*. **24**(7)1143-1152, 2016.
3. Arden, N. K et al, *OA&C*. **16**(6), 733-739, 2008.



KNOCKOUT CYSTIC FIBROSIS RAT TRABECULAR BONE IN THE PROXIMAL TIBIA HAS A DEFICIT THROUGH ADOLESCENCE

¹Maged Awadalla, ¹Egon Perilli, ¹Saulo Martelli, ²Kaye S. Morgan, ²Marcus Kitchen, ^{3,4}Patricia Cmielewski, ^{3,4}Alexandra S. A. McCarron, ¹Karen J Reynolds, ^{3,4}David W. Parsons, and ^{3,4}Martin Donnelly

¹Medical Device Research Institute, College of Science and Engineering, Flinders University, Australia; ²School of Physics and Astronomy, Monash University, Australia ³Robinson Research Institute, and ⁴ Adelaide Medical School, The University of Adelaide, Australia

email: maged.awadalla@flinders.edu.au

INTRODUCTION

Patients with cystic fibrosis (CF) have an increased frequency of bone fracture compared to healthy subjects [1] and this is more pronounced in adolescent CF females, compared to their male counterparts and healthy females [1]. A CF rat model has recently been developed, which exhibits delayed or no CF-related pancreatic, gut and lung disease [2]; this enables to study bone growth during development without indirect secondary effects [2]. The CF model rats, similar to patients with CF, have a marked reduction in bone content in juvenile age (3-6 weeks) [3], however, it is unknown if this transfers into adolescence, a developmental stage where fractures are observed in CF humans. The aim of this study was to investigate proximal tibial trabecular growth in CF through adolescence.

METHODS

Wildtype (WT) and CF transmembrane regulator knockout Sprague-Dawley rats [2] (n=19 and 6, respectively) were used to investigate the effect of CF gene on trabecular bone in the proximal tibia. At the start of the study, the two groups did not differ in age (WT: 14.1±4.2weeks, CF: 17.2±6.8weeks, p-value=0.3 Mann-Whitney) and weight (WT: 242±46 g, CF: 233±66 g, p-value=0.9 Mann-Whitney). Micro-computed tomography (micro-CT) scanning was conducted at the Australian Synchrotron (Clayton, VIC) as part of an ongoing study under approval of the University of Adelaide animal ethics committee.

CF rats were sacrificed at various time points between 6 to 24 weeks of age (adolescence) using sodium pentobarbital overdose. Micro-CT scans of the tibiae were performed at 19 µm pixel size. The trabecular bone volume of interest (VOI) was selected starting 1 mm below the lower end of the growth plate, extending distally for 3 mm [4]. The following bone morphometric parameters were quantified: trabecular bone volume fraction (BV/TV), trabecular number, thickness and separation [4].

RESULTS AND DISCUSSION

In CF rats, both the BV/TV and trabecular number were lower (less than half) through adolescence compared to WT, despite showing similar growth rate to WT (slopes for WT and CF not significantly different from each other, p= 0.76 and p= 0.43, respectively) (Fig. 1). Trabecular separation in CF decreased

through adolescence, likely due to the increase in trabecular thickness, despite, however, not reaching WT values (Fig. 1).

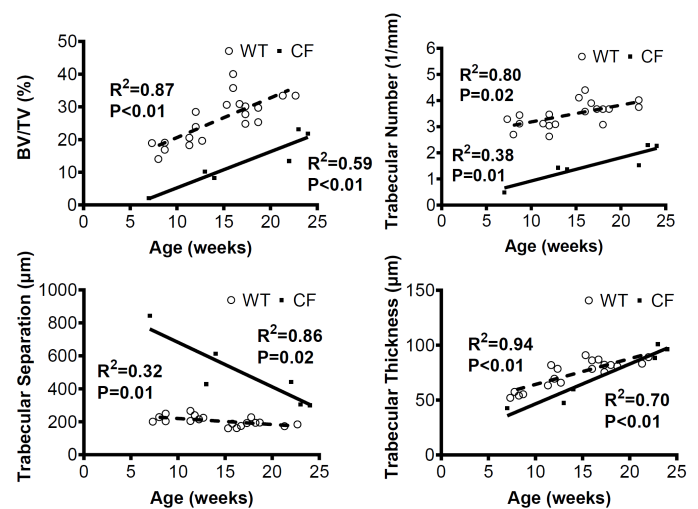


Figure 1. Trabecular bone growth in knockout CF rats during adolescence compared WT. BV/TV, bone volume fraction. Each dot in the scatter plot represents an individual rat.

CONCLUSIONS

CF rats enter adolescence with a lower BV/TV and trabecular number compared to WT, staying constantly lower throughout, despite their adolescent growth. These findings appear to be consistent with those reported using high-resolution peripheral quantitative computed tomography (HR-pQCT) in adolescent CF patients presenting lower bone volume fraction in the distal tibia compared to healthy [5], which ultimately can lead to an increased risk of fracture in that cohort [1, 5]. This rat model provides the opportunity to evaluate bone growth in CF during adolescence and evaluate the effect of current treatments on bone strength and fracture risk.

REFERENCES

1. Hendersom RC et al., *J Pediatr*, 125:208-212, 1994.
2. McCarron A et al., *Am J Pathology*, 2020.
3. Stalvey MS et al., *PLoS One*, 12:e0188497, 2017.
4. Perilli E et al., *Osteoporos Int*, 21:1371-82, 2010.
5. Putman MS et al., *Osteoporos Int*, 27(8): 2497-2505, 2016.

CONFLICT OF INTEREST DECLARATION

In the interests of transparency and to help reviewers assess any potential bias, all authors of original research papers are required to declare any competing commercial interests in relation to the submitted work. Referees are also asked to indicate any potential conflict they might have reviewing a particular paper.

If you have accepted any support such as funds or materials, tangible or intangible, concerned with the research by the commercial party such as companies or investors, choose YES below, and state the relation between you and the commercial party.

If you have not accepted any support such as funds or materials, choose NO.

Do you have a conflict of interest to declare? (DELETE TEXT as appropriate)

YES

If YES, please complete as appropriate:

1. The author(s) did receive payments or other benefits or a commitment or agreement to provide such benefits from a commercial entity.

State the relation between you and the commercial entity:

I am working on a project fully funded by DePuy Synthes to investigate total knee replacement implants.

2. A commercial entity paid or directed, or agreed to pay or direct, any benefits to any research fund, foundation, educational institution, or other charitable or nonprofit organization with which the authors are affiliated or associated.

I am working on a project fully funded by DePuy Synthes to investigate total knee replacement implants.



SYNTHETIC BONE-LIKE STRUCTURES THROUGH OMNIDIRECTIONAL CERAMIC BIOPRINTING IN CELL SUSPENSIONS

¹Sara Romanazzo, ¹Thomas Molley, ¹Stephanie Nemeč, ¹Kang Lin, ¹Rakib Sheikh, ¹Justin Gooding, ²Boyang Wang, ²Qing Li, ^{1,3}Kristopher Kilian, ^{1,3}Iman Roohani*

¹School of Chemistry, Australian Centre for Nanomedicine, University of New South Wales, NSW, Australia.

²School of Aerospace, Mechanical and Mechatronics Engineering, University of Sydney, Sydney, NSW 2006, Australia

³School of Life Sciences, Charles Perkins Centre, University of Sydney, Sydney, NSW 2006, Australia

email: iman.roohani@unsw.edu.au, i.roohani@sydney.edu.au

INTRODUCTION

Over the past years, there have been many efforts to mimic bone tissue in the form of 3D tissue engineered constructs for the regeneration of the damaged tissue, disease modeling, drug screening, or simply studying cell–cell crosstalk in the bone microenvironment [1]. Structurally, bone tissue is an organic–inorganic composite where metabolically active cells are embedded within a highly mineralized matrix in a hierarchical structural organization [2]. This has posed a significant challenge in developing a synthetic approach to replicate the heterogeneous environment of bone, which allows creating mechanically-stable mineralized constructs and at the same time enables embedding bone relevant cells and other temperature–chemical–radiation sensitive biomolecules. In this study, we demonstrate the first example of freeform printing of bone-mimetic constructs at room temperature with living cells, without harsh chemicals or radiation and postprocessing steps. This technique, labeled as ceramic omnidirectional bioprinting in cell-suspensions (COBICS, patented at PCT stage) provides solutions to the major challenges in generation of bone mimicked tissue engineering.

METHODS

A CaP based ink was formulated to achieve in-situ printability and setting in aqueous media (full cell culture medium, phosphate buffered saline and MQ-water). Ink integrity, minimum achievable layer size, printing fidelity and mechanical properties of printed structures have been tested and optimised. The ink biocompatibility was tested *in vivo* using a rabbit model and by using human bone marrow derived mesenchymal stem cells, adipose derived stem cells (ADSCs) and human derived osteoblasts. The printing technology consisted of the extrusion of fine filaments of the ink in a cell-laden Bingham fluid suspension of extracellular matrix colloids of gelatin microgels in presence of ADSCs. Live/dead assay, cytoskeleton staining, and RT-PCR analysis was performed to assess viability, and functionality of cells cultured in the COBICS system.

RESULTS AND DISCUSSION

This approach enabled unprecedented generation of mineralized constructs in a support bath containing live cells and microgels, mimicking the complex and hierarchical structure of native bone. The cells showed robust adhesion and

proliferation behaviour during printing, with greater than 95% viability after several weeks in culture. Lineage specification was dictated by proximity to the bone-mimicked constructs,

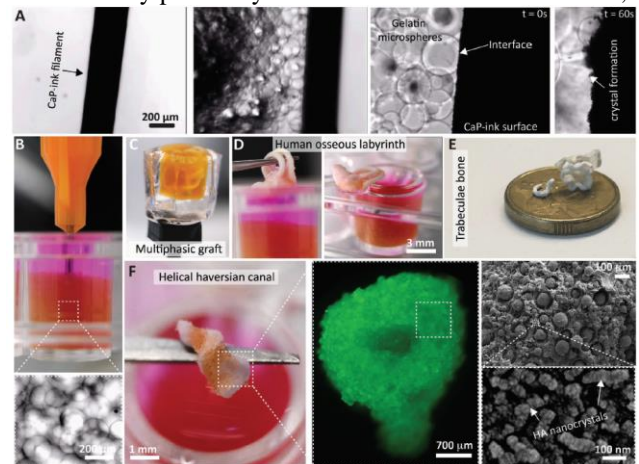


Figure 1: (A) A printed CaP-ink filament within a microgel bath and interfacial adhesion during nanocrystal formation; (B) front view of the printing process in a 96-well cell culture plate. Example of 3D constructs printed by COBICS: (C) a heterogeneous biphasic structure mimicking osteochondral tissue (D) human osseous labyrinth, (E) trabecular bone, and (F) helical Haversian canal. Magnification of printed BSA-FITC-labeled ink observed at epifluorescence microscope (F, middle) and at SEM to show formation of hydroxyapatite crystals postprinting (F, right).

close contact with the printed structure enhanced osteogenesis. The tendency for cells to differentiate at the interface of the constructs, while remaining multipotent in the intervening spaces, opens the potential for fabricating gradient tissue structures and intervening vasculature.

CONCLUSIONS

High-resolution printing of mineralised structures within a cell-laden matrix provides opportunities for “one-pot” generation of custom bone microenvironments for disease modelling and regenerative engineering, with scope for translation to *in situ* bone reconstruction during surgery.

REFERENCES

1. Hippler M, et al., *Adv. Mater.* **31**:808110, 2019.
2. Reznikov N, et al., *Nat. Rev. Mater.* **1**: 16041, 2016.



FABRICATION OF BIOACTIVE BRAIDED COLLAGEN ROPE WITH EXCEPTIONAL MECHANICAL STRENGTH FOR ANTERIOR CRUCIATE LIGAMENT RECONSTRUCTION

¹Peilin Chen, ¹Ziming Chen, ¹Lianzhi Chen, ¹Euphemie Landao-Bossonga, ^{1,2}Jun Yuan, ¹Rui Ruan, ¹Tao Wang and ¹Minghao Zheng

¹Centre of Translational Orthopedic Research, University of Western Australia, WA, Australia

²Perron Institute for Neurological and Translational Science

email: peilin.chen@research.uwa.edu.au

INTRODUCTION

Anterior cruciate ligament (ACL) is an important structure to provide stability and enable movement of knee joint. Unfortunately, high frequency of ACL injuries has led to tremendous burden on society. Currently, ACL reconstruction is a definite treatment for better functional restoration. Reconstruction with autologous grafting has been deemed to be most effective due to their preserved native tissue structure and non-immune response, however, donor site morbidity is a severe long-term complication. On the other hand, recently developed synthetic scaffold featured with their excellent mechanical property can provide satisfactory mechanical outcome. But the non-mammal origin of synthetic scaffold poses the risk of poor tissue integration and non-healing. Herein, to achieve both exceptional biocompatibility and mechanical strength, we develop a biotextile collagen rope scaffold with excellent biocompatibility and mechanical strength evidence in *in vitro* and *in vivo* studies.

METHODS

1. Collagen rope was compared to autograft (hamstring tendon) and native ACL in each following evaluation; observative time points for *in vivo* study was set at 6, 12, 18, and 26 weeks.

1. *In vitro* investigation: MTS assay for cell proliferation; QPCR and immunofluorescence for tenogenesis; Pre-implant ultimate load testing.

2. *In vivo* investigation: Histological staining (H&E and Goldner's Trichrome) for graft and enthesis evaluation; Cell morphology analysis (cell eccentricity and cell orientation); Polarized microscopic image of collagen bundles and collagen orientation analysis; post-implant ultimate loading testing; micro-CT analysis for bone tunnel healing.

RESULTS AND DISCUSSION

The *in vitro* data showed the 3D collagenous environment provided by natural collagen fibers for tenocyte and promote tenocytic morphological adaptation (figure 1). The results showed comparable mechanical properties between collagen rope and autograft. the remodelling and healing process *in vivo* is similar to the autograft of hamstring with better enthesis restoration in collagen rope group. Infiltrated ligament stem cells in collagen rope occurs as early as 6 weeks and there is gradually improved orientation of cells along the longitudinal axis of the graft. Ligament-like cells have adapted to elongated and spindle shapes after 18 weeks. Dynamical changes of

collagen bundles size were observed during remodeling process in both groups. After 18 weeks, collagen rope group exhibited greater collagen bundle size than autograft. At 26 weeks superior collagen orientation and bundles were indistinguishable from the native. Examination of bone tunnel by MicroCT showed better bone restoration on femur part than the tibial part in collagen rope group.

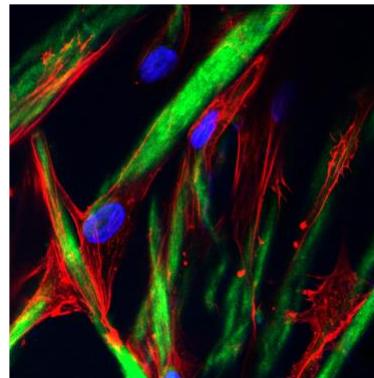


Figure 1: Tenocyte cultured on 3D collagen fibers.

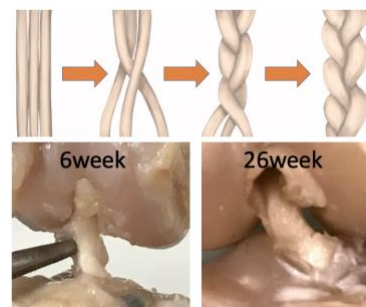


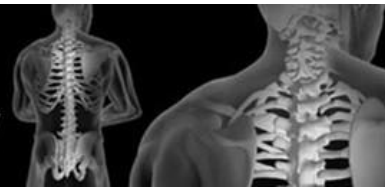
Figure 1: Fabrication of collagen rope (upper panel); ACL reconstruction with collagen rope (lower panel)

CONCLUSIONS

We developed a collagen rope by biotextile technique. Evaluation of the *in vitro* study showed an excellent biocompatibility and mechanical responsiveness. *In vivo* study demonstrated ideal cellular and collagenous component adaptive change to remodeling which are comparable to autograft. Collagen rope is ready for proof-of-concept clinical study.



Australian & New Zealand
Orthopaedic Research Society



DAY 1

PODIUM 3



SHAPE DIFFERENCES IN THE SEMITENDINOUS FOLLOWING TENDON HARVESTING FOR ANTERIOR CRUCIATE LIGAMENT RECONSTRUCTION

William du Moulin¹, Matthew Bourne¹; Laura E Diamond¹, Jason Konrath¹²; Christopher Vertullo¹³; David G Lloyd, and David J Saxby¹.

¹Griffith Centre of Biomedical and Rehabilitation Engineering (GCORE), Menzies Health Institute Queensland, Griffith University, Gold Coast Campus, Gold Coast, Australia

²Principia Technology, Crawley, Western Australia, Australia

³Knee Research Australia, Gold Coast, Queensland, Australia.

email: will.dumoulin@griffithuni.edu.au

INTRODUCTION

Anterior cruciate ligament reconstruction (ACLR) using a semitendinosus (ST) autograft, with or without gracilis (GR), results in donor muscle atrophy and retraction. Measures such as length, cross-sectional area, and volume may not fully describe the effects of tendon harvest on muscle morphology as these discrete measures lack spatial resolution and cannot characterize three-dimensional muscle shape. This study aimed to determine between-limb ST shape similarity and regional morphology in individuals with a unilateral history of ACLR using a ST-GR graft, and healthy controls.

METHODS

A secondary analysis of magnetic resonance imaging was undertaken from 18 individuals with unilateral history of ST-GR ACLR and 18 healthy controls. ST muscles were manually segmented, and shape similarity were assessed between limbs and groups using Jaccard index (0-1) and Hausdorff distance (mm). ST length (cm), peak cross-sectional area (CSA) (cm²), and volume (cm³) was compared between surgically reconstructed and uninjured contralateral limbs, and between the left and right limbs of control participants with no history of injury. For all comparisons Cohen's d was reported as a measure of effect size.

RESULTS AND DISCUSSION

Compared to healthy controls, the ACLR group had significantly ($p < 0.001$, $d = -2.33$) lower bilateral ST shape similarity. Furthermore, the deviation in muscle shape was significantly ($p < 0.001$, $d = 2.12$) greater in the ACLR group. Within the ACLR group, maximum Hausdorff distance indicated ST from the ACLR limb deviated (23.1 ± 8.68 mm) from the shape of the healthy contralateral ST, this was observed particularly within the distal region of the muscle. Compared to the uninjured contralateral limb (Figure 1.) and healthy controls, deficits in peak cross-sectional area and volume in ACLR group were largest in proximal ($p < 0.001$, $d =$

-2.52 to -1.28) and middle ($p < 0.001$, $d = -1.81$ to -1.04) regions.

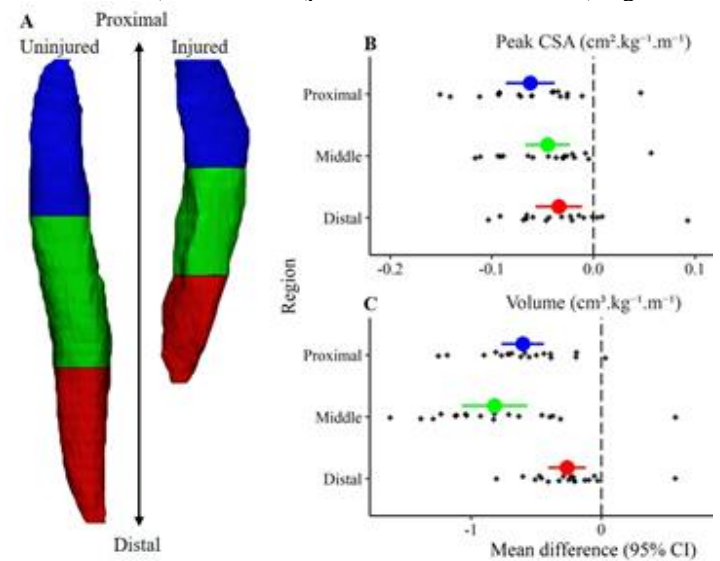


Figure 1: Mean difference of regional morphology in ACLR participant (injured - uninjured). A) A representative ACLR participant depicting ST muscle length in proximal (blue 100%-66%), middle (green 66%-33%), and distal (red 33%-0%) regions, B) normalised peak cross-sectional area (CSA), and C) normalised muscle volume across each region. 95% CI- 95% confidence interval of the mean difference.

CONCLUSIONS

Shape similarity analysis provided unique insight into regional adaptations in ST morphology post-ACLR. Findings highlight morphological features in distal ST not identified by traditional discrete morphology measures. ST shape was most different in the distal region of the muscle, despite deficits in CSA and volume being most pronounced in proximal and middle regions. ST shape following ACLR may affect force transmission and distribution within the hamstrings and contribute to persistent deficits in knee flexor and internal rotator strength. Future research should determine if ST shape change post-ACLR contributes to elevated risk secondary ACL injury.



RELATIONSHIPS BETWEEN CARTILAGE THICKNESS AND SUBCHONDRAL BONE IN KNEE OSTEOARTHRITIS AND CONTROLS: A SYSTEMATIC MAPPING

¹Sophie Rapagna, ^{1,2}Bryant C Roberts, ^{2,3}Lucian B Solomon, ¹Karen J Reynolds, ^{2,3}Dominic Thewlis, ¹Egon Perilli

¹Medical Device Research Institute, College of Science and Engineering, Flinders University, Adelaide, SA, Australia
²Department of Oncology & Metabolism, Insigneo Inst. for in silico Medicine, University of Sheffield, United Kingdom
²Centre for Orthopaedic & Trauma Research, The University of Adelaide, Adelaide, SA, Australia
³Department of Orthopaedics and Trauma, Royal Adelaide Hospital, Adelaide, SA, Australia

email: sophie.rapagna@flinders.edu.au

INTRODUCTION

Tibial cartilage and bone act as a functional unit, responding to daily stimuli together [1]. Nevertheless, relationships between the cartilage thickness and underlying bone microarchitecture, and whether they differ between osteoarthritic (OA) and healthy joints, has not yet been fully investigated.

Aim: to perform, in micro-CT scans of human tibial plateaus from people with end-stage OA and in controls, 1) a systematic spatial mapping (22 regions) of the cartilage and underlying bone morphology; 2) and examine region-specific relationships in these parameters.

METHODS

Participants: Tibial plateaus were retrieved during total knee arthroplasty surgery from 26 people with end-stage knee OA (68±7 years, mass 90±18 kg; varus-aligned (varus-OA; n=16), non-varus-aligned (non-varus-OA; n=10) and from 15 cadavers (62±13 years, mass 83±16 kg; controls) free of musculoskeletal disease in the examined joint. Joint alignment was measured from mechanical axis (pre-operative radiographs).

Micro-CT: The entire plateaus were micro-CT scanned (17 µm/voxel, model 1076, Skyscan-Bruker). Cartilage thickness (Cart.Th), subchondral bone plate thickness (SBPl.Th), porosity (SBPl.Po), and subchondral trabecular bone volume fraction (BV/TV) were analyzed in 22 sub-regions across the tibial condyles (square ROIs, 5 mm side, 3-5 mm length).

Statistics: For each tissue, within- and between-condyle regional differences were evaluated in each group (paired t-tests with Bonferroni adjustment for multiple comparisons). Region-specific relationships between cartilage thickness and subchondral bone parameters were investigated (Pearson's correlations). Statistical significance, p<0.05.

RESULTS AND DISCUSSION

In controls, Cart.Th, SBPl.Th and BV/TV were lowest in the external condylar ROIs and highest in the central and anterior ROIs. In varus-OA the cartilage was thinnest anteriorly in the medial condyle, with high SBPl.Th and BV/TV. In non-varus-OA, the cartilage distribution was similar to controls, but with higher SBPl.Th and BV/TV.

In controls, there were no significant relationships between cartilage thickness and the subchondral bone. In OA, however, several significant negative correlations were found (Cart.Th vs SBPl.Th, r=-0.40 to -0.72; Cart.Th vs. BV/TV, r=-0.41 to -0.78,

Fig. 1). In both controls and OA, strong positive correlations existed between SBPl.Th and BV/TV (r= 0.49 to 0.89) and negative between SBPl.Th and SBPl.Po (r= -0.40 to -0.77).

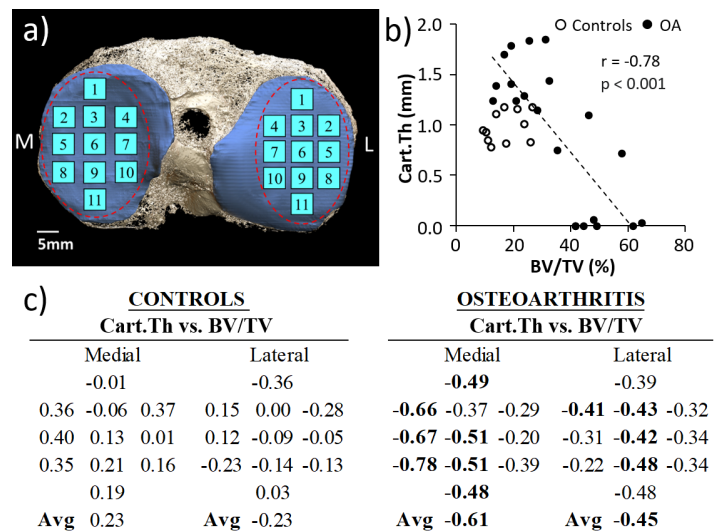


Figure 1: a) 3D micro-CT image, right tibial plateau, with the 22 cubic ROIs; b) scatter plot with line of best fit for “Cart.Th vs. BV/TV” for control and OA groups in ROI#8 of the medial condyle; c) r-values of region-specific correlations “Cart.Th vs. BV/TV” for control and OA groups. Bold values signify p<0.05.

CONCLUSIONS

This mapping revealed region-specific differences in cartilage thickness and subchondral bone microarchitecture, and relationships among them, depending on the group. Our findings may suggest a cartilage and bone response to habitual loading in OA, which might be altered compared to controls. This systematic approach to tissue mapping of the tibial plateau reveals patterns and region-specific relationships, which may aid in understanding and monitoring the progression of OA.

ACKNOWLEDGEMENTS

Arthritis Australia-Zimmer Australia (Grant in Aid 2013, Perilli E), Catalyst Grant DSD, Premier’s Research Industry Fund, SA (2013, Perilli E). D Thewlis is recipient of an NHMRC Career Development Fellowship.

REFERENCES

1. Imhof H, et al., *Invest Radiol.* **35**(10):581-8, 2000.



A NOVEL MICRO-COMPUTED TOMOGRAPHY IMAGING PROTOCOL FOR REPRODUCIBLE QUANTITATIVE MORPHOMETRIC ANALYSIS (QMA) OF THE MOUSE KNEE

¹Pholpat Durongbhan, ¹Mateus O. Silva, ¹Niloufar Ansari, ¹R. Y. Nigel Kour, ¹Catherine E. Davey and ¹Kathryn S. Stok

¹Department of Biomedical Engineering, The University of Melbourne, Australia
email: kstok@unimelb.edu.au

INTRODUCTION

Visualising and quantifying structural change related to osteoarthritis progression and treatment over time provides a promising non-invasive means to track disease. Recent studies have performed quantitative morphometric analysis (QMA) to assess bone, cartilage, and whole-joint changes in multiple pre-clinical animal models of osteoarthritis (OA) [1]. However, joint QMA is highly sensitive to the consistency of the joint pose and alignment due to its nature as a non-rigid link. This work aims to develop a novel micro-computed tomography (microCT) imaging protocol that allows reproducible whole-joint QMA measurements of the mouse knee by controlling the joint pose during image acquisition with a positioning device, and maintaining consistent joint alignment using an automated image processing workflow.

METHODS

A mouse positioning device compatible with the *in vivo* microCT animal bed (vivaCT80, Scanco Medical AG, Switzerland) was designed in-house and 3D printed with polylactic acid (Replicator 2X Experimental, MakerBot, USA), Figure 1. Seven healthy excess male mice (age 10–20 weeks) were sacrificed and collected from the Biomedical Sciences Animal Facility at the University of Melbourne. Mice were placed in the positioning device with their knees and ankles fixed, then scanned with microCT at 10 μm nominal voxel size (70 kVp, 57 μA). Each mouse was scanned 5 times, with repositioning between scans.

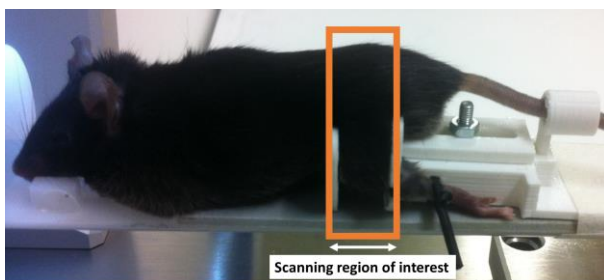


Figure 1: Mouse placed in positioning device for scanning.

Menisci and patellae were manually contoured and removed from the images, and the volume of interest defined between the epiphyseal plates of the femur and tibia, respectively.

Fully automated joint alignment was done by representing the tibia's rough shape and relative position using lower-order spherical harmonics descriptors (SPHARM), which describe objects of spherical topology as a weighted sum of spherical harmonic basis functions [2]. Principle component analysis was

performed on the resulting basic shape. The smallest and second smallest components were used as surrogates for the tibia shaft and anterior face, from which transformation matrices were calculated to align each joint to a common reference. The joint centre of mass was calculated from the aligned images, defined as a vector with orientations; α ($^\circ$); β ($^\circ$); and γ ($^\circ$), connecting the centres of mass of the femur and tibia [1]. Reproducibility was calculated as precision error expressed in both absolute value (PE_{SD}) and coefficients of variation ($PE_{\%CV}$), as well as intraclass correlation coefficient (ICC).

RESULTS AND DISCUSSION

The centre of mass angles for unprocessed and processed joints are plotted in Figure 2. ICC for β and γ improved from unprocessed (β : 0.793, γ : 0.557) to processed (β : 0.892, γ : 0.903) with only a slight drop for α (0.994 to 0.912); a value still indicating excellent reproducibility. Low precision errors (PE_{SD}) α : 4.08, β : 2.87, γ : 4.19; $PE_{\%CV}$) α : 6.81%, β : 3.03%, γ : 2.79%) were also obtained for processed samples.

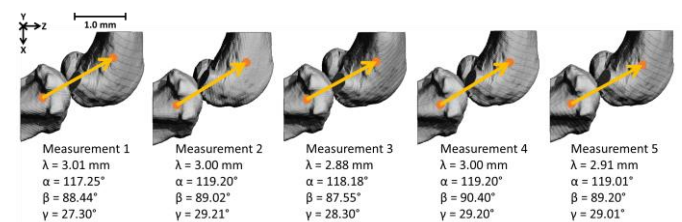


Figure 2: Vector length, l , and orientation α ($^\circ$); β ($^\circ$); and γ ($^\circ$) after alignment with SPHARM for five repeated measurements.

CONCLUSIONS

The novel positioning device enables highly reproducible imaging of the knee in preclinical animal models of osteoarthritis as demonstrated with QMA of whole-joint changes. The positioning device is simple to produce and deploy and the alignment software is easy to set up in any new research environment. Future work will focus on implementing this protocol in longitudinal experiments to observe joint changes due to progressing disease.

ACKNOWLEDGEMENTS

Funding by ARC Discovery Project (DP180101838).

REFERENCES

1. Stok, K.S. et al., *PLOS One*. 11(1): e0147564, 2016.
2. Brechbühler, C.M. et al., *Comput. Vis. Image Underst.* 61(2): 154–170, 1995.



SUBSCAPULARIS MUSCLE FUNCTION FOLLOWING THE LATARJET PROCEDURE

^{1,2}Aaron Fox, ^{3,4}Lukas Ernstbrunner, ²Janina Henze, ²Richard Page, ²Stephen Gill, ¹Jason Bonacci and ⁵David Ackland

¹Centre for Sport Research, Deakin University, Melbourne, VIC, Australia

²Barwon Centre for Orthopaedic Research & Education, Deakin University, Melbourne, VIC, Australia

³Department of Orthopedics, Balgrist University Hospital, University of Zurich, Zurich, Switzerland

⁴Melbourne Orthopaedic Group, Melbourne, VIC, Australia

⁵Department of Biomedical Engineering, The University of Melbourne, Melbourne, VIC, Australia

email: aaron.f@deakin.edu.au

INTRODUCTION

The Latarjet procedure is used to treat shoulder instability where significant bone loss, or glenoid and humeral bone defects are present [1]. The subscapularis muscle is split during the procedure to access the anterior glenohumeral joint, with the coracoid bone graft and coracobrachialis conjoint tendon routed through the split [2]. This physically deforms the subscapularis, however, the effect of this splitting approach on the mechanical stabilizing potential of the subscapularis remains poorly understood. We therefore aimed to examine the line of action of the subscapularis muscle following the Latarjet procedure.

METHODS

Seven (3 male, 4 female; mean age: 74.5y) fresh-frozen, entire upper extremities free of any joint or muscle injury were obtained from human cadavera. The proximal origins of the subscapularis were identified and divided into four equal regions. Radiopaque wires were sutured at the insertion and pulled towards the origin of each subscapularis region under physiological load, calculated using an EMG-driven musculoskeletal model [3] and applied using a customized cadaveric testing apparatus. Each specimen underwent a standard Latarjet procedure with the horizontal subscapularis split made at its middle [2]. Following the Latarjet procedure, specimens were radiographed in the scapular and transverse planes using X-ray fluoroscopy in four positions: (i) 0° abduction; (ii) 90° abduction; (iii) 90° abduction with maximum external rotation (ABER); and (iv) apprehension (ABER plus maximum horizontal abduction). Specimens were radiographed in each shoulder position with the coracobrachialis conjoint tendon both unloaded (0N) and loaded (40N). The orientation of the four subscapularis region lines of action were defined in the scapula and transverse planes, relative to the plane of the glenoid (see Figure 1).

RESULTS AND DISCUSSION

The lines of action in the mid-inferior and inferior subscapularis regions were more inferiorly and posteriorly directed when compared to literature values from anatomic (i.e. pre-operative) shoulders [4]. Loading of the coracobrachialis conjoint tendon had the greatest effect on the inferior subscapularis region in 90° abduction and ABER. The inferior region line of action became more inferiorly (mean difference = -5.96° and -11.11° in 90° abduction and ABER, respectively) and posteriorly

(mean difference = 6.53° and 16.24° in 90° abduction and ABER, respectively) directed with the conjoint tendon loaded. The response to conjoint tendon loading aligns with the proposed ‘dynamic sling’ mechanism of the Latarjet – where the coracobrachialis conjoint tendon produces a sling effect around the inferior subscapularis that hinders anterior humeral head translation. We found that conjoint tendon loading alongside the re-routed inferior subscapularis produced lines of action that could promote joint stability by countering superior and anterior humeral head translation at end range of movement (i.e. 90° abduction and ABER).

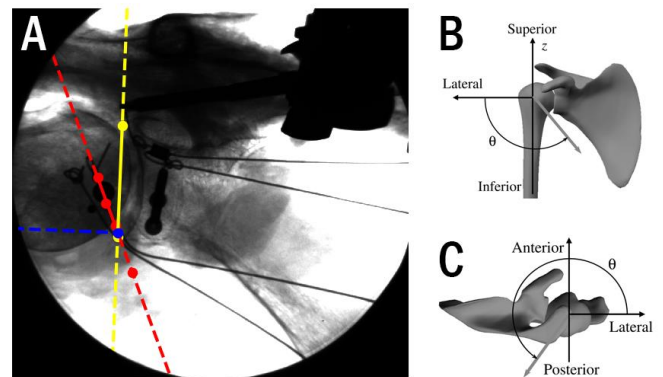


Figure 1: Scapula plane image at 90° abduction and 40N conjoint tendon load, with subscapularis region (red), glenoid plane axes (yellow and blue) digitised (A); Line of action definitions in the scapula (B) and transverse (C) planes.

CONCLUSIONS

The Latarjet procedure alters subscapularis lines of action in a way that can promote joint stability. The shift in subscapularis orientation may act to counter humeral head translation and increase joint compression in potentially unstable arm positions. Our findings suggest the Latarjet’s ‘dynamic sling’ effect may produce joint conditions favourable for maintaining joint congruency in patients with recurrent shoulder instability.

REFERENCES

1. Millett PJ, et al., *J Bone Joint Surg.* **87**:419-432, 2005.
2. Bhatia S, et al., *Arthroscopy*, **30**:227-235, 2014.
3. Kian A, et al., *J Biomech*, **97**: 109348, 2019.
4. Ackland D, et al., *J Anat*, **215**: 184-197, 2009.

CONFLICT OF INTEREST DECLARATION

In the interests of transparency and to help reviewers assess any potential bias, all authors of original research papers are required to declare any competing commercial interests in relation to the submitted work. Referees are also asked to indicate any potential conflict they might have reviewing a particular paper.

If you have accepted any support such as funds or materials, tangible or intangible, concerned with the research by the commercial party such as companies or investors, choose YES below, and state the relation between you and the commercial party.

If you have not accepted any support such as funds or materials, choose NO.

Do you have a conflict of interest to declare? (DELETE TEXT as appropriate)

YES

If YES, please complete as appropriate:

1. The author(s) did receive payments or other benefits or a commitment or agreement to provide such benefits from a commercial entity.

State the relation between you and the commercial entity:

DePuy Synthes agreed to provide the Latarjet kits free of charge for use in this study. The company was not involved in any process associated with the study design or conducting of research outside of providing these resources.

2. A commercial entity paid or directed, or agreed to pay or direct, any benefits to any research fund, foundation, educational institution, or other charitable or nonprofit organization with which the authors are affiliated or associated.

No payments were made or funds obtained from the conducting of this research.



PERSONALISED LOWER LIMB MODELS GENERATED USING AN AUTOMATIC WORKFLOW: COMPARISON WITH MANUALLY CREATED MODELS

¹Luca Modenese and ²Jean-Baptiste Renault

¹Department of Civil Engineering, Imperial College London, UK

²Aix-Marseille University, Marseille, France

email: l.modenese@imperial.ac.uk

INTRODUCTION

Many of the clinical applications envisioned for computational models of the musculoskeletal (MSK) system are in the field of orthopaedics, and consist, for example, of estimating internal joint loadings or simulating the effect of surgeries altering the patient's anatomy and biomechanics. Recent progress in MSK modelling has made possible the creation of highly personalized MSK models from standard medical images, so providing surgeons and physical therapists with a platform they can use to optimize treatments on a personalized fashion. Generating these personalized MSK models, however, remains a time-consuming procedure requiring hours of operator time even when following detailed codified approaches [1]. We recently developed a MATLAB toolbox called STAPLE (Shared Tools for Automatic Personalised Lower Extremity modelling) that implements fully automated workflows for model generation [2]. In this abstract, kinematic models created using STAPLE were evaluated against those created by human operators to quantify the differences in their joint coordinate systems (JCS) definition.

METHODS

Algorithms performing morphological analyses of the pelvis (2 algorithms), femur and tibia (5 algorithms each), patella (3 algorithms), talus and foot (1 algorithm each) were implemented in MATLAB r2020a. These methods, published in previous papers [3-5] or designed by the authors [2], can estimate anatomical joint axes and define the JCS of kinematic lower limb models. The implemented algorithms were applied to four datasets of segmented lower limb bone geometries with quality ranging from excellent to low (age range: 14-85 yo, height: 1.71- 1.8 m, mass: 45-87 kg) to obtain automatic OpenSim models. Manual models, created by experienced operators following [1], were also available for these datasets from previous research projects. The models included a free joint at the pelvis (6 degrees-of-freedom, DoF), a ball-and-socket hip joint (3 DoF) and hinge knee, ankle, subtalar and metatarsophalangeal joints (1 DoF), for a total of 13 DoF. The JCS origins and axes of the automatic and manual models were compared for all joints and their differences assessed against reported human inter-operator variability [6,7].

RESULTS AND DISCUSSION

Kinematic models, including a patellofemoral mechanism, were created automatically through a STAPLE workflow equivalent to [1] in around 30 seconds per dataset.

The automatic JCS origins differed on average by 1.8 ± 1.7 mm (X: 0.5 ± 0.5 mm; Y: 0.5 ± 0.6 mm; Z: 1.3 ± 1.7 mm) from those of the manual models. The average orientation differences of the JCS axes were also modest (X: $1.4^\circ \pm 1.1^\circ$, Y: $2.1^\circ \pm 2.5^\circ$, Z: $1.5^\circ \pm 2.4^\circ$). All these differences were within the inter-operator variability reported in [6,7], with larger differences for the lowest quality bone geometries. Different algorithms yielded distinct JCS definitions, especially at the proximal tibia, where knee Y axes varied up to 10° across the five available methods.

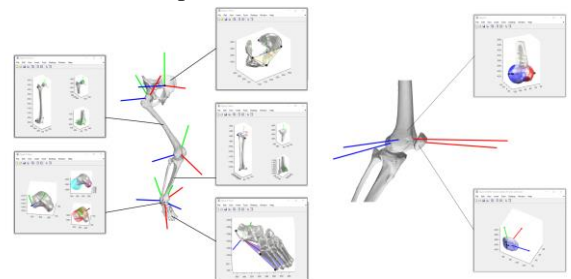


Figure 1: Overview of the algorithms applied to generate the lower limb model (left) and the patellofemoral joint (right).

CONCLUSIONS

The kinematic lower limb models generated with a fully automatic approach in negligible computing time were comparable to those created by human operators. The availability of multiple processing algorithms ensures flexibility for user-defined STAPLE workflows but requires caution in evaluating the resulting kinematic models. Overall, STAPLE is a promising platform for creating personalised biomechanical models and new features, such as the automatic generation of musculature models, will be previewed and discussed at the congress. STAPLE is an open-source package released at <https://simtk.org/projects/msk-staple> under a non-commercial license (CC-BY-NC).

ACKNOWLEDGEMENTS

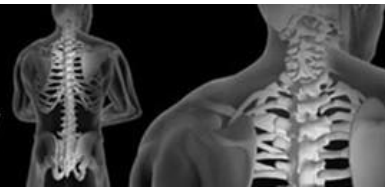
Imperial College Research Fellowship to LM.

REFERENCES

1. Modenese L, et al., *J Biomech.* **73**:108-118, 2018.
2. Modenese L, et al., *J Biomech.* **116**:110186, 2021.
3. Miranda DL et al., *J Biomech.* **43**:1623-1626, 2010.
4. Kai S, et al., *J Biomech.* **47**:1229-1233, 2014.
5. Renault JB et al., *J Biomech.* **80**:171-178, 2018.
6. Martelli S, et al., *CMBBE.* **18**:15555-1563, 2015.
7. Montefiori E, et al., *Ann Biom Eng.* **47**:2155-2167, 2019.



Australian & New Zealand
Orthopaedic Research Society



DAY 1

PODIUM 4

DOUBLE INTRAMEDULLARY AND SINGLE EXTRAMEDULLARY CORTICAL BUTTON CONSTRUCTS FOR DISTAL BICEPS TENDON SURGICAL REPAIR

¹Mitchell Almond, ¹David Ackland, ^{2,3}Lukas Ernstbrunner, ¹Harshi Rupasinghe, ²Olivia Jo, ³Robert Zbeda, ³Eugene Ek

¹Department of Biomedical Engineering, The University of Melbourne, Parkville, VIC; ²The Royal Melbourne Hospital, Parkville, VIC; ³Melbourne Orthopaedic Group, Windsor, VIC

Email: malmond@student.unimelb.edu.au

INTRODUCTION

The distal biceps tendon (DBT) contributes to flexion and supination of the forearm during normal elbow function, and rupture of this tendon significantly impairs upper limb function. Surgical repair of a torn DBT is the standard of care for restoring pre-injury elbow strength [1]. Previous studies have demonstrated inlay single extramedullary cortical button (SECB) repair constructs to be the biomechanically superior DBT surgical repair construct, but this technique presents significant intraoperative risk of posterior interosseous nerve (PIN) impaction [2, 3]. An onlay double intramedullary cortical button (DICB) repair construct has been proposed to reduce PIN impaction; however, its biomechanical performance and longevity are not fully understood. The aims of this study were to (1) examine gap formation, load to failure and construct stiffness of the DICB constructs for surgical repair of DBT tears in a cadaveric model, and (2) compare these results with those of conventional SECB surgical repair constructs.

METHODS

Twenty-two fresh-frozen upper limbs were harvested from male and female cadaveric specimens and transected at the mid-humerus and distal forearm. All soft tissue except the DBT and elbow joint capsule were dissected. The elbows of each specimen were randomised into one of two repair groups: onlay DICB repair, and inlay SECB repair.

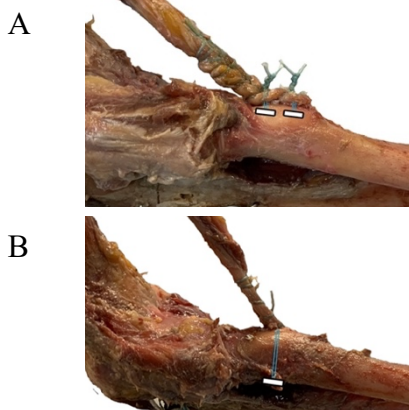


Figure 1: DICB (A) and SECB (B) constructs for the surgical repair of the DBT tears. Cortical button fixation positions are indicated by thick white lines.

Specimens were fixed to an Instron materials testing system by potting the humerus in a custom-made testing rig with dental plaster, allowing the elbow to move freely between 90° of flexion and full extension. All specimens underwent cyclic loading protocols to quantify gap formation. Specifically, a 60N pre-load force was applied to the constructs by attaching

a weight to the distal radius via an intramedullary rod. Specimens were cycled between 90° of flexion and full extension for 1000 cycles at 0.5Hz. Gap formation was measured during testing and used as a proxy for construct longevity under physiological loading. Following completion of cyclic loading, the elbow was fixed in 90° of flexion and the repair construct loaded to failure by displacing the biceps tendon at a rate of 4mm/sec. Construct stiffness was then calculated from the gradient of the resultant force-displacement graph. Analysis of variance was used to compare gap formation, load to failure and construct stiffness between repair groups.

RESULTS AND DISCUSSION

After 1000 cycles, DICB constructs exhibited a significantly smaller gap formation than SECB constructs (mean difference: 1.2mm, $p=0.003$). Three DICB specimens failed during cyclic loading testing prior to cycle 1000.

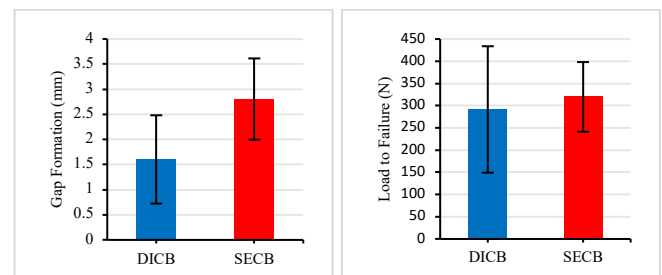


Figure 2: Mean ± one standard deviation for gap formation (left) and load to failure (right) of double intramedullary cortical button (DICB) and single extramedullary cortical button (SECB) biceps repair constructs.

There was no significant difference in mean failure loads of the DICB and SECB constructs (mean difference: 28.3N, $p=0.585$). Additionally, no significant differences were found in construct stiffness between DICB and SECB constructs (mean difference: 11.5N/mm, $p=0.515$).

CONCLUSION

This study provides preliminary evidence that the biomechanical performance and longevity of DICB constructs for surgical repair of the DBT is equivalent, or superior to, SECB repair constructs. Since DICB constructs mitigate the risk of intraoperative nerve impaction, this technique may result in improved clinical outcomes compared to the SECB repair technique.

REFERENCES

- Legg et al. *J Shoulder Elbow Surg*, 25(3), 341-348. 2016.
- Mazzocca et al. *Am J Sports Med*, 35(2), 252-258. 2007.
- Lo et al. *Arthroscopy*, 27(8), 1048-1054. 2011.

TENSION BAND WIRING VERSUS A NOVEL TENSION BAND SUTURE FIXATION FOR THE TREATMENT OF OLECRANON FRACTURES: A COMPARATIVE BIOMECHANICS STUDY

¹Harshi Rupasinghe, ^{2,3}Lukas Ernstbrunner, Mitchell Almond, ²Robert Zbeda, ²Eugene Ek, ¹David Ackland

¹Department of Biomedical Engineering, University of Melbourne, VIC; ²Melbourne Orthopaedic Group, Windsor, VIC;

³Royal Melbourne Hospital, Parkville, VIC

email: harshirs99@gmail.com

INTRODUCTION

Fractures of the olecranon account for approximately 1% of all upper extremity injuries and 10% of fractures associated with the elbow [1]. By disrupting the congruity within the ulna-humeral articulation and the elbow extensor mechanism, olecranon fractures impair elbow movement and stability. Tension band wire (TBW) fixation is a widely used surgical repair in the treatment of olecranon fractures. However, despite achieving sufficient union and restoration of elbow function, the metal construct can cause irritation and breakdown of surrounding soft tissue, resulting in a post-operative complication requiring re-operation rate. A novel, all-suture tension band construct was developed by the senior surgeon (L.E.) to reduce complication rates whilst maintaining sufficient inter-fragmentary compression. The purpose of this study was to assess the biomechanical performance of the tension band tape (TBT) construct and compare the results to those of the existing TBW construct. The TBT is a form of tension banding that maximises interfragmentary compression similarly to the existing TBW technique. Thus, we hypothesized that the novel construct would retain fracture reduction and have an ultimate load to failure comparable to that of TBW.

METHODS

Ten fresh-frozen matched-pairs of elbows were obtained from human cadavers and randomly allocated to receive one of two repairs: TBW or TBT fixation (Fig. 1). A standardized, transverse osteotomy of the olecranon was introduced using an oscillating saw. Each repaired specimen was dissected of all soft tissue, retaining only the elbow joint capsule and triceps tendon. The specimens were then fixed at 90° of flexion to an Instron materials testing system by potting the proximal humerus in dental plaster and clamping the distal ulna and radius. A sinusoidal force of amplitude 500N was then applied to the triceps tendon at 1Hz over 500 cycles, while fracture displacement (gap formation) was simultaneously evaluated with a calibrated high-speed camera. This was achieved by tracking the trajectories of bone-fixed markers on each side of the fracture.

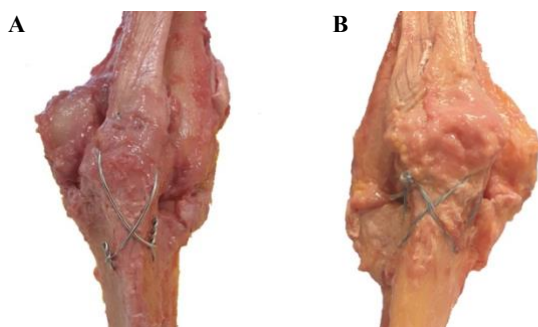


Figure 1: Olecranon surgical repair constructs including tension band wiring (A) and a novel tension band tape fixation (B).

Each specimen was then maximally loaded by displacing the triceps at a rate of 1mm/sec until construct failure, defined as a fracture displacement exceeding 4mm. Construct stiffness was calculated from the gradient of the force-displacement curve at 3mm of fracture displacement.

RESULTS AND DISCUSSION

Fracture displacement under cyclic loading was not statistically significant between TBW and TBT constructs ($p > 0.05$) (Fig. 2). Similarly, the difference in total fracture displacement after 500 cycles between TBW (1.8 ± 1.3 mm) and TBT constructs (1.9 ± 1.1 mm) was also not statistically significant ($p > 0.05$). Load to failure testing demonstrated that the TBW construct (1137.9 ± 285.8 N) on average, had a higher load to failure relative to the TBT construct (1126.4 ± 271.8 N), though this difference was also not statistically significant ($p > 0.05$). The TBT construct had a significantly greater mean construct stiffness than that of the TBW construct (mean difference: 142.6 N/mm) ($p = 0.05$).

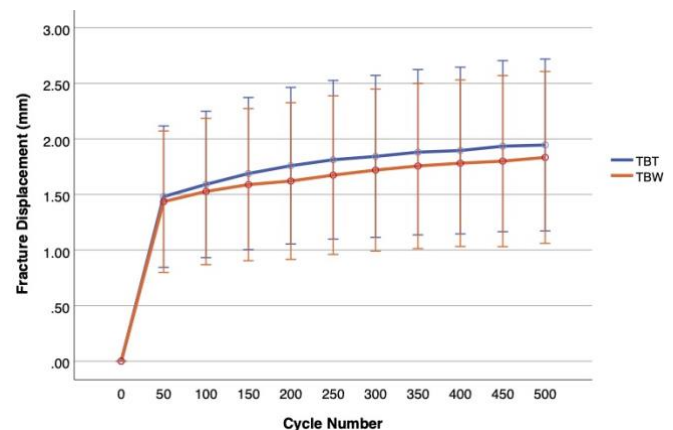


Figure 2: Fracture displacement (mean ± SE) during cyclic loading for TBW and TBT constructs.

CONCLUSION

Under cyclic loading and load to failure conditions, the novel TBT repair construct demonstrated comparable and superior performance to conventional TBW constructs, respectively. These findings suggest that TBT may achieve equivalent or greater longevity than that of conventional TBW techniques in olecranon fracture fixation in vivo. Since TBT has no metal components, this technique may ultimately mitigate irritation and soft-tissue breakdown, which is commonly reported in wiring-based techniques and a source of complication. The findings of this study will help inform clinical practice in surgical management of olecranon fracture fixation.

REFERENCES

1. Phadnis J, Watts AC. Tension band suture fixation for olecranon fractures. *Shoulder Elbow*. 2017; 9(4): 299-303.

THE INFLUENCE OF GRAFT POSITIONING ON GLENOHUMERAL JOINT CONTACT IN THE LатарJET PROCEDURE FOR RECURRENT SHOULDER INSTABILITY

¹Dale Robinson, ^{2,3}Lukas Ernstbrunner, ³Eugene Ek, and ³David Ackland

¹ Department of Biomedical Engineering, The University of Melbourne, Melbourne, VIC, Australia

² Department of Orthopedics, Balgrist University Hospital, University of Zurich, Zurich, Switzerland

³ Melbourne Orthopaedic Group, Windsor, Melbourne, Australia

email: d Robinson@unimelb.edu.au

INTRODUCTION

The Latarjet procedure is considered an effective surgical stabilisation procedure for anterior shoulder instability with glenoid bone loss, and involves augmenting the glenoid with a coracoid bone graft. Despite favourable long-term results, mediolateral mal-positioning of the graft and graft resorption remains common [1]. To identify and develop improved surgical planning to mitigate these complications, the aims of this study were twofold. Firstly, to establish the first biomechanical model of the Latarjet procedure that simulates physiological glenohumeral joint contact loading; and secondly, to assess the influence of medial-lateral graft mal-positioning on graft and glenoid cartilage loading.

METHODS

A finite element (FE) model of the right upper limb was created in Abaqus using the Visible Human Male (VHM) dataset [2]. The right scapula and humerus were meshed with tetrahedrons, and the articular surfaces of the glenoid and humeral cartilage were meshed with triangular shell elements with variable thickness based on their 3D geometries. Each cartilage surface was tied to the underlying bone. The bone material properties from a computed tomography (CT) scan of a healthy male were mapped into the FE model via non-rigid registration, and the cartilage material properties assigned based on previously published data [3].

The glenohumeral joint was positioned with the humerus at 90° of abduction and full external rotation (ABER), a critical joint position in the unstable shoulder occurring just prior to dislocation. At this joint angle, the humeral head was positioned such that its contact centre pressed against the anterior-inferior rim of the intact glenoid. Muscle forces derived from a rigid-body model of matching anatomy were applied as point loads on the humerus to generate joint compression [4]. Glenoid bone loss was simulated by removing the anterior region of the glenoid to reduce the overall glenoid surface area by 10%, as observed clinically [5]. A simulated Latarjet procedure was then performed by sectioning the distal 22 mm of the coracoid process and fixing this graft to the anterior region of the glenoid with two bicortical screws (Fig 1). The coracoid was positioned with its medial surface against the anterior aspect of the glenoid and its inferior surface parallel to the articular surface of the glenoid. Simulations of joint loading were then performed, and then repeated with the graft aligned relative to the glenoid bone,

simulating mal-positioning of the graft which occurs intraoperatively.

RESULTS AND DISCUSSION

When level with the glenoid bone, the humerus contacted both the glenoid cartilage and coracoid, with peak contact pressures of 18.7 MPa and 28.8 MPa, respectively. When the graft was placed level with the cartilage, the humerus only contacted the coracoid, with a peak contact pressure of 36.7 MPa.

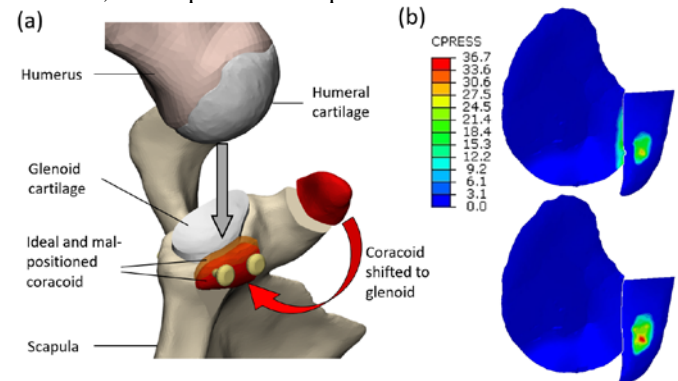


Figure 1: (a) FE model of Latarjet procedure. (b) Contour plot of contact pressure for the coracoid level with the glenoid bone face (upper) and level with the glenoid cartilage face (lower).

CONCLUSIONS

The findings of this study suggest that mal-positioning the graft laterally by an amount corresponding to the glenoid cartilage edge thickness (2 mm) causes all joint contact to occur on the graft. This localised and high contact pressure may lead to excessive bone strains and failure of the graft to integrate with the glenoid. Graft positioning closer to the glenoid bone surface may enhance load sharing between the glenoid and graft, which may ultimately encourage effective bone remodelling and graft integration without graft overload. The findings of this study provide guidance for intraoperatively alignment of the coracoid graft in Latarjet surgery for shoulder instability.

REFERENCES

1. Moroder et al. 2019, *AJSM*, 47(3): 688-694
2. Spitzer et al. 1996, *JAMAFU*, 3: 118-130
3. Büchler et al. 2002, *Clinbio*, 17(9-10): 630-639
4. Wu et al. 2017, *Gait and Post*, 54: 87-92
5. Shaha et al. 2015, *AMJ Sports Med*, 43(7):1719-1725



KNEE FLEXOR WEAKNESS AFTER ANTERIOR CRUCIATE LIGAMENT RECONSTRUCTION WITH A SEMITENDINOSUS TENDON GRAFT: IS IT JUST DUE TO MUSCLE SIZE?

¹Adam Kositsky, ¹Rod S. Barrett, ¹Laura E. Diamond, and ¹David J. Saxby

¹Griffith Centre of Biomedical and Rehabilitation Engineering (GCORE), Menzies Health Institute Queensland, Griffith University, Gold Coast, Queensland, Australia
email: adam.kositsky@griffithuni.edu.au

INTRODUCTION

The incidence of anterior cruciate ligament reconstruction (ACLR) in Australia is increasing despite already being the highest globally [1]. The semitendinosus (ST) tendon is by far the most preferred tissue harvested for ACLR, especially in Australia [2]. Although peak isokinetic knee flexion torque can be recovered following ACLR with an ST graft, weakness at deeper knee flexion angles is consistently reported [3]. As ST is a major contributor to knee flexor torque at high knee flexion angles [4], determining the mechanism(s) behind this deep flexion strength loss is important for successful rehabilitation. Here, we conducted a simulation study investigating the effects of muscle morphology changes post-ACLR with an ST graft on knee flexor strength.

METHODS

Preliminary data from five individuals (29 ± 7 years) that underwent ACLR with an ST-only graft (13 \pm 4 months post-surgery) and had confirmed tendon regeneration were included. Participants were positioned prone (hip neutral) and performed maximal voluntary isometric contractions on an isokinetic dynamometer (System 4 Pro, Biodex) at four knee angles (15°, 45°, 60°, 90°; 0° = full extension), with the order of joint angle and tested limb randomized. T₁ Dixon magnetic resonance images (MRI) were acquired on a 3T unit (Philips) from the iliac crest to mid-shank. ST muscle volume and length were measured from segmentations (Mimics v20, Materialise).

Simulations using the mean group data were performed using a musculoskeletal model [5,6] (OpenSim 4.1). The changes in muscle volume and length from MRI were used to adjust muscle parameters in the model. For volume, simulations were performed with the maximal isometric muscle force altered by ± 1 standard deviation of the between-leg ST volume deficit. Length-based simulations were performed based on the ± 1 standard deviation change in muscle length; the optimal fiber length was adjusted based on a change in either the number or length of sarcomeres in the anatomical position using a standard equation [7]. Baseline sarcomere data were obtained from previously published cadaveric data [7]. No adjustments were made for other knee flexor synergists. Activation for all involved agonist muscles was set at 1.

RESULTS AND DISCUSSION

ST muscle morphology in the ACLR leg was substantially altered (volume: $-25 \pm 3\%$; length: $-9 \pm 4\%$). Experimental

maximal voluntary isometric strength was recovered at lower flexion angles (15°: $-1 \pm 11\%$; 45°: $-3 \pm 13\%$) but not in more flexed positions (60°: $-20 \pm 10\%$; 90°: $-33 \pm 8\%$). Simulations demonstrate that muscle morphological changes do not explain strength loss at 90° (Figure 1).

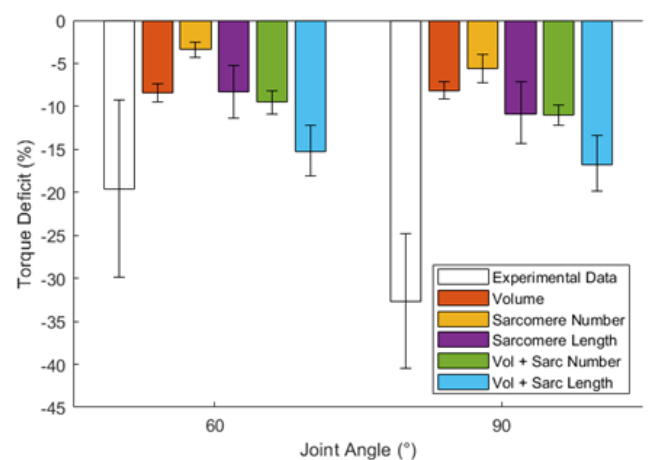


Figure 1: Experimental and simulated maximal voluntary isometric torque deficits at 60° and 90° of knee flexion.

CONCLUSIONS

Adjustments to the muscle parameters of ST based on MRI data did not simulate the reduction in flexion torque seen experimentally at 90°. Thus, it appears that factor(s) which were not accounted for in this model (e.g., regenerated tendon quality, neural inhibition, etc.) must also play a role in deep flexion strength deficits. As 90° may preferentially assess ST function given ST's large moment arm at this joint angle [4] and ST function is crucial for tasks such as sprinting [8], determining all mechanism(s) of torque loss may guide and enhance rehabilitation protocols post-ACLR with an ST graft.

REFERENCES

1. Zbrojkiewicz D, et al., *Med. J. Aus.* **208**:354-358, 2018.
2. Grassi A, et al., *Joints* **6**:177-187, 2018.
3. Ardern C, & Webster K, *Orthop. Rev.* **1**:e12, 2009.
4. Herzog W, & Read L, *J. Anat.* **182**:213-230, 1993.
5. Thelen, D, *J. Biomech. Eng.* **125**:70-77, 2003.
6. Lai A, et al., *Ann. Biomed. Eng.* **45**:2762-2774, 2017.
7. Ward S, et al., *Clin. Orthop. Relat. Res.* **467**:1074-1082, 2009.
8. Takahashi K, et al. *PLOS ONE* **16**:e0249670, 2021.



CHARACTERISING THE RESPONSE OF HUMAN HEADS DURING A SIMULATED HEAD-FIRST IMPACT

^{1,2}Darcy W. Thompson-Bagshaw, ²Ryan D. Quarrington and ^{1,2}Claire F. Jones

¹School of Mechanical Engineering, The University of Adelaide, South Australia, Australia

²Spinal Research Group, Centre for Orthopaedic and Trauma Research, Adelaide Medical School, The University of Adelaide, South Australia, Australia

email: darcy.thompson-bagshaw@adelaide.edu.au

INTRODUCTION

Tetraplegia can result from spinal trauma during head-first impacts, which are common in automotive rollovers and falls [1]. To understand the mechanisms of such spinal trauma and thereby develop injury prevention tools, biomechanical experiments are performed using cadaver material. Recent head-first impact cadaver models investigating neck trauma have omitted the head (e.g. [1]). However, the impact response of the head is likely important for biofidelic loading of the spine and should be considered in neck-only experiments. The response of the head to a vertex impact has not been characterised. The aim of this study is to assess the effect of vertex impact velocity on the stiffness and absorbed energy of the human head.

METHODS

Twelve fresh-frozen human heads (76±13 yrs; 7 male) were disarticulated from the neck at the occipital condyles, and the mandible was removed. Density-calibrated pre-test computed tomography (CT) scans were obtained to screen specimens for existing trauma. Mean vertex (apex of the sagittal suture) bone mineral density (BMD) and bone thickness were measured from computer segmented models developed from the CT scans, using MIMICS (Materialise NV, Leuven, Belgium). Specimens were fixed to a load cell (20 kN, K6D110, ME, Germany) at the base of a drop tower via a custom support mount that simulated the articular surfaces of the atlas and aligned the head with a horizontal Frankfort plane. Dental acrylic was used to ensure congruency between the mount and occipital condyles. A 17 kg carriage (50th percentile male upper torso mass), with a steel platen (400 cm²), was raised to predetermined heights and dropped via a frictionless rail to impact the specimen at 1 or 3 m/s (the latter is the minimum velocity thought to cause cervical trauma [1]). A linear encoder (10µm resolution, LM15, Rotary and Linear Motion Sensors, Slovenia) fixed to the carriage, was used to measure impact velocity and head deformation.

Stiffness was defined as the slope of the most-linear region of each force-displacement curve. Absorbed energy was defined as the area under the curve to the point of failure, where failure was identified by a sudden reduction in force and verified

against time-synchronised high-speed footage. Separate ANCOVA models were used to assess the effect of impact velocity on stiffness and absorbed energy; models were adjusted by gender, age, scalp thickness, vertex bone thickness, and vertex BMD. Fracture type was assessed from post-test CT scans.

RESULTS AND DISCUSSION

Stiffness and absorbed energy were significantly greater ($p < 0.05$) for 3 m/s impacts (4.48 kN/mm; 12 J), than for 1 m/s impacts (2.18 kN/mm; 7.2 J; Figure 1). None of the adjustment factors were significantly associated with the outcome measures. For 1 m/s impacts there was no evidence of cranial vault failure, but basilar fractures consistently occurred at 3 m/s.

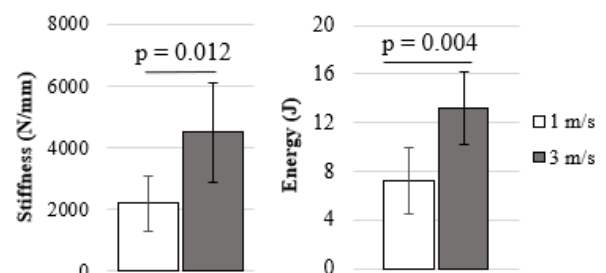


Figure 1: Mean stiffness and absorbed energy, at each impact velocity.

CONCLUSIONS

The stiffness and absorbed energy of cadaveric heads increased from 1 to 3 m/s during a vertex impact with anatomically relevant support conditions. Future head-first impact neck injury models could use this data to select materials to simulate the impact response of the head at the relevant loading rate, to ensure accurate transmission of loads to the cervical spine.

ACKNOWLEDGEMENTS

Project funding was provided by an Australian Research Council Discovery Project (DP190101209).

REFERENCES

1. Saari A, *J. Biomech Eng.* 135(11): 111003, 2013

DAY 1

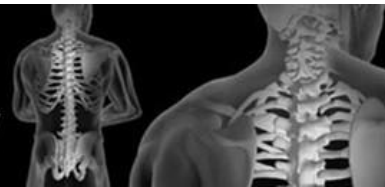
KEYNOTE 1 – A/Prof Claire Clarkin

University of Southampton, Southampton, United Kingdom

“Resolving Sexual Dimorphism of the Bone Vasculature”



Australian & New Zealand
Orthopaedic Research Society



DAY 2

David Findlay Early Career Researcher (ECR)

Award Finalists

OSTEOBLAST-DERIVED EGFL6 COUPLES ANGIOGENESIS TO OSTEOGENESIS DURING BONE REPAIR

¹Kai Chen, ^{1,2}Shijie Liao, ¹Vincent Kuek, ¹Jacob Kenny, ¹Jennifer Tickner, ¹Nathan Pavlos, ²Qian Liu, ³An Qin and ¹Jiake Xu

¹School of Biomedical Sciences, University of Western Australia, Perth, WA, Australia

²Department of Orthopedics, The First Affiliated Hospital of Guangxi Medical University, Nanning, Guangxi, China

³Shanghai Key Laboratory of Orthopedic Implants, Shanghai Ninth People's Hospital, Shanghai Jiao Tong University School of Medicine, Shanghai, China. Email: jiake.xu@uwa.edu.au

INTRODUCTION

Angiogenesis and osteogenesis are considered two indispensable and highly coupled steps involved in successful bone repair [1, 2]. However, the nature and identities of factors that regulate the coupling process remain largely elusive. We previously found that epidermal growth factor-like protein 6 (EGFL6) is an angiogenic factor that specifically and distinctively up-regulated during osteoblast differentiation [3]. In contrast with most currently known osteoblast-derived coupling factors, EGFL6 is highlighted with its little or low expression in other cells and tissues. This study aims to uncover the role of EGFL6 in bone repair.

METHODS

Primary bone marrow mesenchymal stem cells (MSCs) and osteoblastic cell line (MC3T3-E1) were transduced with lentiviral silencing or overexpression constructs targeting EGFL6. Cells were induced by osteogenic medium, followed by the evaluation of mineralization using alizarin red S (ARS) staining. Bone-related genes and protein expressions were examined by qPCR and Western Blot (WB) assay. EGFL6 global and osteoblast-specific knockout (KO) mice were established to examine the bone phenotype under physiological condition by using micro-CT scanning and bone histomorphometry analysis. Bone-specific type H vessels were identified using immunofluorescent staining of CD31 and Endomucin (EMCN). To evaluate EGFL6's role in bone repair, mono-cortical bone defect mice models were created to investigate the outcome of bone repair in both wildtype (WT) and KO mice.

RESULTS AND DISCUSSION

We found that overexpression of EGFL6 significantly enhances osteogenic capacity in vitro by augmenting bone morphogenic protein (BMP)-Smad and MAPK signaling, whereas downregulation of EGFL6 diminishes osteoblastic mineralization. Interestingly, osteoblast differentiation was not affected by the exogenous addition of EGFL6 protein, thereby indicating that EGFL6 may regulate osteoblastic function in an intracrine manner. Mice with osteoblast-specific and global knockout of EGFL6 surprisingly exhibit a normal bone phenotype under the physiological condition. However, EGFL6-deficiency leads to compromised bone repair in the

bone defect model which is characterized by the decreased formation of type H vessels as well as osteoblast lineage cells.

CONCLUSIONS

Taken together, our findings demonstrated that EGFL6 serves as an essential regulator to couple osteogenesis to angiogenesis during bone repair.

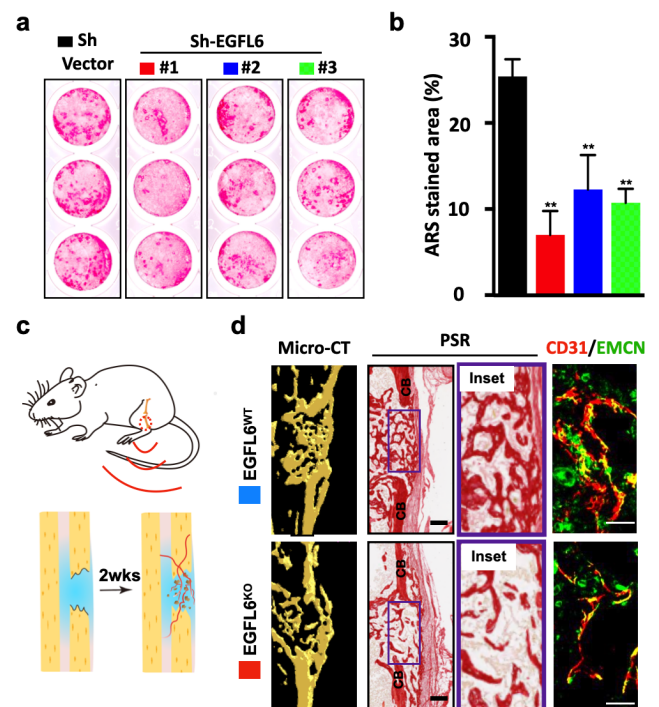


Figure 1: EGFL6 is required for bone defect healing. **a)** Alizarin Red S (ARS) staining of mesenchymal stem cells (MSCs) mineralization following transduction with lentiviral EGFL6 shRNA or a vector control. **b)** Quantification of **a)**. **c)** Schematic illustration of bone defect model. **d)** Bone histomorphometry analysis of bone defect repair in WT and EGFL6 KO mice. Bar graph is presented as mean \pm SD. ** $P < 0.01$ relative to the control group (Student's t-test). EMCN, Endomucin; PSR, picrosirius red.

REFERENCES

1. Kusumbe et al., *Nature*. 2014; 507: 323-8.
2. Ramasamy et al. *Nature*. 2014; 507: 376-80.
3. Chim et al., *J Biol Chem*. 2011; 286: 22035-46.



WEARABLE SENSORS FOR TELE-MEDICINE IN ORTHOPAEDICS: OVERCOMING THE CHALLENGE OF CONVERTING RAW IMU DATA INTO HIGH ACCURACY JOINT ANGLES

^{1,2}Damith A. Senanayake, ²Saman K. Halgamuge, ¹David C. Ackland

¹Department of Biomedical Engineering, University of Melbourne, VIC; ²Department of Mechanical Engineering, University of Melbourne, VIC, email: dackland@unimelb.edu.au

INTRODUCTION

Video motion capture systems such as Vicon and Optotrack are considered the gold-standard in clinical motion analysis; however, these systems have a restricted capture volume, are expensive, require considerable expertise in their use, and necessitate a patient visiting a motion analysis laboratory, which is expensive for the patient and Healthcare system, and may not always be practical. Inertial measurement units (IMUs), are a low-cost wearable sensor that measure acceleration and angular velocity, lending themselves well to wireless motion measurement in almost any location, including tele-medicine and tele-rehabilitation applications; however, utilising these data streams to obtain accurate joint angles in multi-degree-of-freedom joints remains an unsolved challenge. The aim of this study was to use deep neural networks, a form of artificial intelligence, to predict calculate knee and ankle kinematics during walking from raw IMU data, and compare the angle predictions with video motion analysis data, the reference standard

METHODS

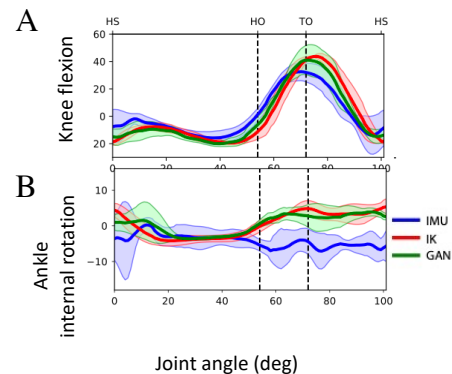
Nine healthy adults (age: 26.5 ± 6.2 years) were recruited and performed walking trials on a treadmill at 3 speeds for one minute (0.5 m/s, 1.0 m/s and 1.5 m/s). Three-dimensional trajectories of retro-reflective markers attached to each subject's lower limbs were simultaneously acquired using a 12-camera video motion capture system (Vicon, Oxfordmetrics, UK). Subjects also wore IMU sensors (Trigno, Delsys, USA) placed on the lateral mid-thigh, external mid-shank and lateral mid-foot of both lower limbs. IMU and video motion analysis data were acquired simultaneously and synchronised. Three-dimensional knee and ankle joint kinematics were calculated using three approaches: (i) inverse kinematics (IK) using the video motion analysis system (ii) IMUs, and (iii) deep neural network calculations derived from the IMU data. A generative adversarial network (GAN), a form of deep neural network, was trained to facilitate person-specific conversion of raw IMU data to knee and ankle joint angles in real time [1]. This was achieved by using IMU data as input to the GAN, which then emulated (simulated) knee and ankle joint angles derived from IK without requiring the video motion capture data. To evaluate GAN robustness, joint angle predictions were made for gait speeds not used in model training, and the results compared to IK. Comparisons between joint angles derived from IMUs,

video motion capture i.e. IK, and GANs were performed across entire gait cycles using statistical parametric mapping.

RESULTS AND DISCUSSION

There were significant differences between IK and IMU joint angle calculations for ankle eversion and internal rotation during walking at 0.5 m/s and 1.0 m/s ($p < 0.001$), suggesting lack of agreement between the two modalities; however, no significant differences in joint angles were observed between the GAN and IK at any speed or plane of joint motion ($p > 0.05$) (Fig. 1). When the GAN was trained using as few as 2 subjects at 1m/s, the RMS difference in angles between IK and GAN was 4.2° and 3.2° for knee flexion and ankle rotation, respectively (Figure 1). This finding demonstrates high-level of agreement with video motion analysis for both large in-plane and small out-of-plane joint motions. In contrast, RMS differences in joint angles between IK and IMUs were over 140% higher, 9.1° and 7.4° for knee and ankle joint angles, respectively.

Figure 1. Knee flexion angles (A) and ankle joint internal rotation angles (B) calculated using video motion capture (i.e. IK), IMU data, and generative adversarial networks (GAN) i.e. deep neural networks. Data are shown over one gait cycle for walking at 1 m/s.



CONCLUSIONS

This study reported a novel machine learning approach to real-time IMU-based joint angle calculation, with high knee and ankle joint angle predictability demonstrated across a range of contrasting speeds and planes of joint motion. The results provide a strong foundation for the use of IMUs in tele-medicine applications such as remote monitoring and rehabilitation in orthopaedics.

REFERENCES

1. Senanayake, D., et al. 2021. *J Biomech*, p.110552.



ELEVATED LEVELS OF ACTIVE TRANSFORMING GROWTH FACTOR B1 IN THE SUBCHONDRAL BONE RELATE SPATIALLY TO CARTILAGE LOSS AND IMPAIRED BONE QUALITY IN HUMAN KNEE OSTEOARTHRITIS

¹Dzenita Muratovic ¹Ryan D Quarrington ²Xu Cao ¹Gerald J. Atkins ^{1,3}Lucian B. Solomon ¹Julia Kuliwaba ¹David M. Findlay

¹Centre for Orthopaedic & Trauma Research, The University of Adelaide, Adelaide, SA, Australia.

²Department of Orthopaedic Surgery, Johns Hopkins University School of Medicine, Baltimore, USA

³Orthopaedic and Trauma Service, Royal Adelaide Hospital, Adelaide, SA Australia

email: dzenita.muratovic@adelaide.edu.au

INTRODUCTION

TGF β 1 is abundant in bone where it has multiple essential roles in development, homeostasis and repair, maintaining both bone volume and bone quality. Over-activity of transforming growth factor beta (TGF β 1) in subchondral bone has a direct causal role in rodent osteoarthritis (OA) which can be blocked by TGF β 1 neutralization; this relationship with OA progression has not been demonstrated in humans. Thus, the aim of this study was to investigate whether the level of active TGF β 1 in the subchondral bone associates with the structural, cellular and molecular parameters that are characteristic of human knee OA.

METHODS

Tibial plateaus were collected from 35 knee OA arthroplasty patients (15 men, aged 66 \pm 9 years; 20 women, aged 70 \pm 8 years). Bone core biopsies were collected from regions of the tibial medial condyle with relatively intact/moderately degenerated cartilage (CA+), and with severely degenerated/depleted cartilage (CA-). The concentration of active TGF β 1 protein were determined by ELISA, concentration and gene-specific mRNA expression were determined by quantitative real-time PCR, while parameters describing bone quality (bone microstructure, osteocyte-lacunar network and bone matrix vascularity) were obtained from synchrotron micro-CT images (*Figure A*). Finally, tissues were histologically processed to determine cartilage OARSI grade, density of tartrate resistant acid phosphatase positive (TRAP+) cells, osteocyte cell density and density of bone marrow micro-vasculature and collagen orientation by polarised-light microscopy.

RESULTS AND DISCUSSION

Subchondral bone in CA- regions is characterised by impaired bone matrix quality due to sclerotic microarchitecture, disorganised collagen, hyper-mineralisation, and high heterogeneity of the mineral distribution, contained increased concentrations of active TGF β 1 protein ($p < 0.05$), and increased RANKL/OPG mRNA ratio ($p < 0.05$), compared to adjacent CA+ areas. In addition, increased levels of active TGF β 1 protein in subchondral bone related directly to increased bone volume, increased osteocyte density, and bone matrix vascularity ($p < 0.05$ for all).

Together, these results support the hypothesis that increased active TGF β 1 occurs in human knee OA and that increased concentration of active TGF β 1 in the subchondral bone associates spatially with impaired bone quality and the degenerative severity of human OA.

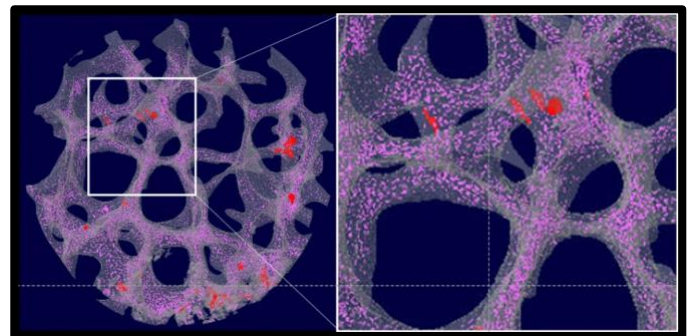


Figure 1: Synchrotron micro-CT images reconstructed into a 3D computer model, representing bone microstructure (grey), osteocyte lacunar density (pink) and vascular canal density (red) of trabecular bone.

CONCLUSIONS

Findings from this study are consistent with those obtained in rodent models of OA and may open up new options for therapeutic approaches for human OA, through the inhibition of TGF β 1 to prevent or reduce disease progression

ACKNOWLEDGEMENTS

The authors acknowledge funding from the National Health and Medical Research Council of Australia (NHMRC, Project Grant 18NHMRC_1138865), The Paul Scherrer Institut, Villigen, Switzerland for provision of the synchrotron radiation beamtime at the TOMCAT beamline of the Swiss Light Source, travel funding provided by the International Synchrotron Access Program (ISAP) managed by the Australian Synchrotron, part of ANSTO, and funded by the Australian Government. Dzenita Muratovic is recipient of Arthritis Australia 2021 Fellowship.



REPEATED MILD KNEE INJURY EVENTS ARE ASSOCIATED WITH EARLY OSTEOARTHRITIC CHANGE

^{1,2}Carina Blaker, ^{1*}Ben Ventura, ^{1*}Vanessa Lo Basso, ²Cindy Shu, ²Christopher Little and ¹Elizabeth Clarke

¹Murray Maxwell Biomechanics Laboratory and ²Raymond Purves Bone and Joint Research Laboratories, Institute of Bone and Joint Research, Kolling Institute, Faculty of Medicine and Health, University of Sydney, Northern Sydney Local Health District, St Leonards, NSW, Australia

*Equal contribution

email: carina.blaker@sydney.edu.au

INTRODUCTION

Mild knee injuries including contusions and low-grade sprains are common occurrences in sports players [1] and may increase the risk of subsequent injury [2]. The long-term impact of repeated mild knee injuries on joint health and function is an understudied area of research. This study used a mouse model of mild knee injury to investigate the effect of recurrent mild injuries and different recovery times on the risk of major injury (e.g. anterior cruciate ligament, ACL, rupture) and joint pathology associated with the onset of osteoarthritis.

METHODS

Ten-week-old male C57BL/6J mice were randomised to 4 groups: 1) naïve, no-injury (NI) control; 2) single injury (SI); 3) double injury separated by 2 weeks (DI-2w); 4) double injury separated by 4 weeks (DI-4w). Injury was induced by a single compressive load applied to the knee joint of anaesthetised mice. The injured knee was evaluated for changes in ACL biomechanics (maximum load and stiffness; n=10/group at 14-, 16- or 18-weeks-old) or osteochondral gene regulation in the patella and medial/lateral tibial epiphyses (RT-qPCR: Acan, Col1A1, Col2, Mmp-2,-3,-9, Timp-1,-3; n=6/group at 14-, 16-, 18- or 26-weeks-old). A small subset of animals were assessed at 26 weeks for signs of structural cartilage pathology (n=3/group). Data analysis was performed using mixed model regression for the biomechanical data and Kruskal-Wallis for gene expression.

RESULTS AND DISCUSSION

ACL failure load and stiffness were not different between groups, suggesting minimal direct damage to the ACL in this model. ACL stiffness at 18 weeks was significantly lower than earlier time points in all groups ($P \leq 0.008$) except DI-2w ($P \geq 0.759$). It is unclear if the absence of change in DI-2w is related to the timing of the second injury relative to the first injury.

The medial tibial epiphysis and patella demonstrated the most significant changes in osteochondral gene expression. In the medial tibial epiphysis, the fold change of Col2 increased significantly over time in both the SI and DI-2w groups ($P \leq 0.05$). In contrast, Mmp-3, -9 and Timp1 were significantly upregulated in DI-4w at 26 weeks compared with earlier time points ($P \leq 0.05$). In the patella, Col1A1, Mmp-2 and Mmp-3 were significantly downregulated over time in both DI groups ($P \leq 0.05$). At 26 weeks of age, Mmp-3,-9 and Timp-1 were

significantly higher in DI-4w compared with DI-2w ($P \leq 0.05$). These are genes which have been associated with the progression of osteoarthritis.

At 26 weeks all injury groups demonstrated signs of cartilage pathology (Figure 1), particularly in the medial tibiofemoral and patellofemoral compartments. Compared with the smooth surface of NI joints, SI cartilage was roughened; DI-2w cartilage was fibrillated and the lamellar surface lost; DI-4w joints were marked by regions of partial thickness, non-calcified cartilage loss and more pronounced focal lesions. These findings suggest that repeated injuries, even when separated by 4 weeks, have cumulative effects on joint tissue integrity.

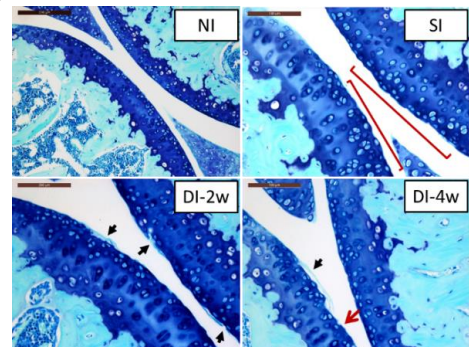


Figure 1: Sagittal toluidine-blue O sections of the knee. NI: smooth joint surface. SI: roughened joint surface (red bars). DI-2w: fibrillated articular cartilage (black arrows). DI-4w: fibrillated (black arrows) and loss of articular cartilage (red arrow).

CONCLUSIONS

In this model the risk of ACL failure was not affected by repeated mild knee injuries. However, other joint tissues were significantly affected with evidence of increased damage with repeated injury even when injury events were separated by longer times (4 vs 2 weeks). Gene expression and structural pathology findings reflected changes seen in the early stages of osteoarthritis. This suggests that even mild injury events are contributing to the onset and progression of osteoarthritis.

REFERENCES

1. Powell JW, et al., *J Athl Train.* **34**:277-284, 1999.
2. Driban JB, et al., *J Rheumatol.* **42**:1463-1469, 2015



ACCURACY AND FUNCTIONAL OUTCOMES OF JUVENILE PROXIMAL FEMORAL OSTEOTOMIES USING VIRTUAL SURGICAL PLANNING AND PATIENT-MATCHED SURGICAL GUIDES

¹Martina Barzan, ^{1,2}David Bade, ¹David Lloyd, ^{1,3}Derek Smith, ^{1,2}Christopher Carty

¹Griffith Centre of Biomedical and Rehabilitation Engineering, Griffith University, Gold Coast, QLD, Australia

²Department of Orthopaedics, Children's Health Queensland Hospital and Health Service, Brisbane, QLD, Australia

³Advanced Design and Prototyping Technologies Institute, Griffith University, Gold Coast, QLD, Australia

email: m.barzan@griffith.edu.au

INTRODUCTION

Proximal femoral osteotomies (PFO) are commonly implemented surgical procedures used to address hip joint dysfunction in juvenile patients (e.g., Perthes' disease, slipped capital femoral epiphysis, cerebral palsy) [1]. Surgical planning and execution using standard two-dimensional medical imaging protocols (i.e., x-ray) require a high degree of spatial intelligence and clinical experience, as most of these patients present with multiplanar femoral deformity and hip joint impingement.

In this medical device trial, we developed a novel platform for virtual surgical planning aimed at restoring hip joint anatomy and muscle function in juvenile patients with hip joint dysfunction. We also designed and manufactured patient-matched surgical guides using 3D printing to enable precise surgical execution. The aims of this investigation were to evaluate (a) the accuracy of PFO in juvenile patients when performed using patient-matched surgical guides, and whether PFO led to (b) reduced surgery time and radiation dose compared to traditional methods, and (c) improved gait function. We hypothesized that the use of surgical guides would enable accurate translation of the surgical plan in the operating theatre, would reduce surgery time and radiation dose, and that PFO would lead to improved function nine months post-surgery.

METHODS

Twelve patients (age: 11.7 ± 2.6 years) with proximal femoral deformities were recruited at the Queensland Children's Hospital as part of a Phase I clinical trial. Preoperatively, all patients had medical images (CT scan of their affected hip, MRI scan of their pelvis and full-length femurs) taken. Three-dimensional bones and glutei muscles were reconstructed using Mimics 23.0 (Materialise, Leuven). Musculoskeletal models of each patient's hips were created in OpenSim and used to virtually plan the surgery. The most appropriate fixation implants were selected and virtually placed on the femurs. Adhering to quality control guidelines [2], surgical guides were designed in 3-matic (Materialise, Leuven), and 3D printed in biocompatible Nylon (Formiga P110, EOS, Germany) for use in surgery. Surgery time, radiation time and dose were recorded after each surgery and compared against six similar procedures performed with traditional methods.

Using postoperative CT data, 3D models of the femurs were reconstructed and superimposed with the planned correction to calculate 3D accuracy. Each patient had pre- and post-surgery 3D gait analysis and the data were processed using PlugInGait (Vicon, Oxford, UK). Movement Analysis Profiles (MAP) and Gait Profile Scores (GPS) [3] were generated for each patient to compare pre- and post-surgery joint kinematics. The Minimal Clinically Important Difference (MCID) was defined as a change of 1.6° on the GPS [4].

RESULTS AND DISCUSSION

On average, the use of patient-matched surgical guides produced rotational corrections similar (3D angle: $8.8 \pm 4.5^\circ$) to the planned corrections (Figure 1). Importantly, compared to six similar procedures performed with traditional methods, virtual planning cases had reduced average radiation dose (-56 %) and time (-45 %), and surgery time (-27 %).

For patients who attended pre and post-surgery 3D gait analysis (8 patients, 10 surgeries) the overall GPS showed a mean improvement of 4.1° (>2 times the MCID) and a mean GPS improvement on the affected side of 5.3° (>3 times the MCID).

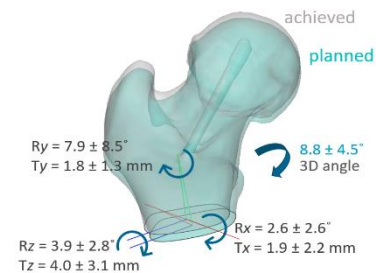


Figure 1: Planned versus achieved 3D accuracy assessment.

CONCLUSIONS

The use of virtual surgical planning and patient-matched surgical guides in PFO resulted in accurate surgical corrections, reduced radiation dose and time, and surgery time, and improved gait function nine months post-surgery.

REFERENCES

1. M'sabah DL, et al., *Orthop Traumatol Surg Res.* **99**:171-186, 2013.
2. Martinez-Marquez D et al., *PloS One*, **13**(4), 2018.
3. Baker R et al., *Gait & Posture*, **30**, 265-269, 2009.
4. Baker R et al., *Gait & Posture*, **35**, 612-530, 2012.

DAY 2

KEYNOTE 3 – Prof Farshid Guilak

Washington University, St. Louis, USA

“Gene Therapy for Obesity and Aging in Osteoarthritis”



Australian & New Zealand
Orthopaedic Research Society



DAY 2

PhD Award Finalists



EXAMINING A ROLE FOR VEGF IN THE REGULATION OF OSTEOCYTE LACUNAE ORIENTATION

¹Jacob Trend, ²Alisha Sharma, ¹Minsa Gurung, ¹Alice Goring, ²Philipp Schneider and ¹Claire Clarkin

¹Biological Sciences, University of Southampton, Southampton, UK

²Engineering and the Environment, University of Southampton, Southampton, UK

email: Jt4n19@soton.ac.uk

INTRODUCTION

Coupling of blood vessel development and bone formation is essential for the maintenance of bone homeostasis. Our previous work (1) has found that conditional loss of VEGF in osteocalcin-expressing cells (OcnVEGFKO) affects cortical microstructure in a sexually dimorphic manner with male OcnVEGFKO mice exhibiting pronounced pathology with increased vascularity of the bone cortex. This phenotype was coupled with elevated sclerostin (SOST) expression and increased production of unmineralised osteoid. Osteocytes are well characterised regulators of mineralisation and a pivotal source of SOST in bone. Herein, we have assessed how loss of VEGF expression impacts osteocyte lacunae spatial arrangements and describe development of novel analyses to map lacunae orientation in 3D using high resolution synchrotron radiation computed tomography (SR-CT).

METHODS

Littermate male and female wild-type (WT, n=3) and OcnVEGFKO (n=3) were sacrificed at 12 weeks of age. Long bones were extracted, soft tissue removed, fixed, and embedded in paraffin wax for scanning. The tibio-fibular junction was imaged using SR-CT at a resolution of 0.65 μ m and aligned using BoneJ's moment of inertia tool. Cortical microstructure was isolated with intracortical canals and osteocyte lacunae separated (1). For assessment of lacunae orientation an ellipsoid was fitted to each lacuna and the deviation of the ellipsoid's longest axis from the bone's longest axis calculated (Figure 1A).

RESULTS AND DISCUSSION

In male mice a greater proportion of lacunae were oriented horizontally in OcnVEGFKO (Figure 1B) mice than WT mice. More lacunae were placed in 80° (WT = 4.4% \pm 0.9%, OcnVEGFKO 9.8% \pm 0.09, $p < 0.0001$), 90° (6.7% \pm 1.7%, OcnVEGFKO 16.2 \pm 1.02, $p < 0.0001$), 100° (WT = 5.1 \pm 1.2%, OcnVEGFKO 10.8 \pm 0.52 $p < 0.0001$) and 110° (WT 3.4 \pm 0.55, OcnVEGFKO 7.5 \pm 0.44, $p = 0.0004$) orientation bins, suggesting a shift from vertically orientated lacunae as seen in WT mice, to horizontally aligned lacunae. In contrast no significant differences were found in female OcnVEGFKO mice versus WT (Figure 1C). While it is documented that loss of VEGF impacts bone mineral composition specifically in males (1), these findings suggest that osteocyte lacunae positioning is impacted in a sexually dimorphic manner and could relate to local extracellular collagen orientation (2). Finite element analyses have identified that bone populated with horizontally oriented lacunae possesses a decreased

Young's modulus (stiffness) versus bone populated with vertical lacunae (3) and therefore male OcnVEGFKO may be mechanically compromised at this site. Further, loss of VEGF leading to disruption of lacunar morphology may provide new insight into lacunar-vascular interactions.

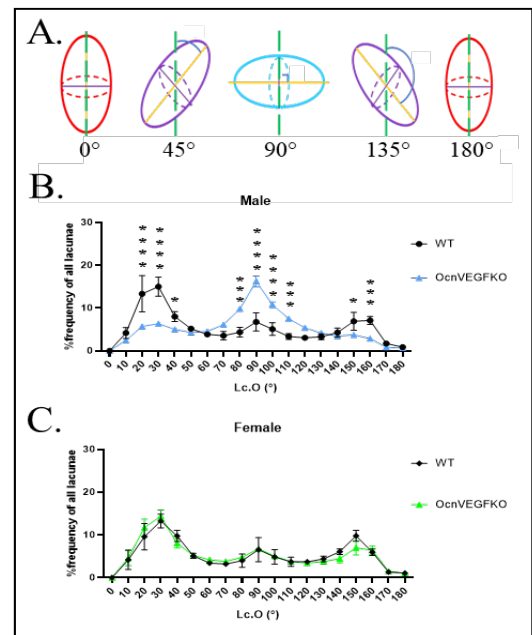


Figure 1: Loss of VEGF in bone disrupts lacunar orientation in male mice. The longest axis of osteocyte lacunae are mapped with vertical lacunae in red, and horizontal lacunae in blue (A.). Male OcnVEGFKO possess more horizontally aligned lacunae than male WT (B.) whereas female WT and female OcnVEGFKO possess similar proportions of lacunae in each orientation bin (C.). Data are shown as mean \pm SEM, * denotes $p < 0.05$, ** $p < 0.01$, *** $p < 0.001$, **** $p < 0.0001$ following two-way ANOVA and Sidaks multiple comparisons testing.

CONCLUSIONS

Our findings suggest that osteocyte lacunar orientation is impacted by loss of VEGF and is coupled to areas of poor mineralisation and mechanical instability. Whether osteocyte orientation may present a new clinical biomarker for fracture prediction sites requires further investigation.

REFERENCES

1. Goring A, et al., Journal of Bone and Mineral Research, 34(11), 2117-2132, 2019
2. Kerschnitzki M, et al., Journal of Structural Biology, 173(2), 303, 2011
3. Carpenter D et Anderson R, Osteocyte Lacunar Orientation Affects Bone Tissue Mechanics: A Finite Element and 3D Printing Study. 2019

MICRO-CT IMAGING A PRESS-FIT TRAY IMPLANTED IN HUMAN TIBIA: A ZERO-STRAIN DIGITAL VOLUME CORRELATION ANALYSIS AT ORGAN LEVEL

¹Lauren Wearne, ¹Sophie Rapagna, ¹Mark Taylor and ¹Egon Perilli

¹Medical Device Research Institute, College of Science and Engineering, Flinders University, Adelaide, SA, Australia
email: lauren.wearne@flinders.edu.au

INTRODUCTION

Achieving primary stability is crucial in tibial press-fit implant fixation [1]. However, experimental data on trabecular and cortical bone deformation during implantation is limited. Advancements in large-gantry micro-CT imaging and the development of digital volume correlation (DVC) allows such data collection. This pilot study assesses the DVC strain errors for a human tibia implanted with a titanium press-fit tray across four plausible scanning configurations using a cabinet micro-CT system. The aim is to optimise such analysis.

METHODS

Micro-CT Imaging: One cadaveric proximal tibia was resected, implanted with a titanium press-fit tray and micro-CT scanned (Nikon XT H225 ST) at $42\mu\text{m}/\text{pixel}$ (Fig.1 A-C), first in air with a longer (1: Air, 1h46m, 0.11°rst , 150kVp) and shorter (2: Air, 1h06m, 0.18°rst , 150kVp) scan time. Shorter scans were then repeated with the specimen placed in an aluminum cylinder (Al Tb) of 2mm wall thickness used for mechanical testing (3: Al Tb, 1h06m, 0.18°rst , 150kVp) and at higher voltage (4: Al Tb, 1h06m, 0.18°rst , 215kVp) [2]. Rescans were taken at each of the four configurations, with specimen repositioning in-between. 3D image co-registration of the rescans was performed (DataViewer, Bruker).

Masking of micro-CT Images: Regions external to the tibial cortex or across the tibial tray were masked (CT Analyser, Bruker). A custom script masked soft tissue or marrow that was not consistently present in rescans (MATLAB). Nine cubic volumes of interest (VOIs, 13.4mm side length) were selected from the resultant datasets via software (CT Analyser). Five VOIs contained only trabecular bone, four were centered on implant pegs (7mm \varnothing) with surrounding bone (Fig.1 D).

DVC Strain Analysis: DVC analysis (DaVis 8.3.1, LaVision, direct correlation) was performed on the VOIs. Nineteen DVC settings were assessed, including multistep progression (3-6 steps), final subvolume size (0.84-1.68mm) and subvolume overlap. Optimised DVC parameters (6-step multipass, 0% overlap, final subvolume size of 1.18mm) were applied to calculate the zero-strain error values across the entire proximal tibia. The strain mean absolute error (MAER) and its standard deviation (SDER) were calculated, as indicators of DVC's accuracy and precision, respectively [3].

RESULTS AND DISCUSSION

Across all 9 VOIs, the strain accuracy and precision at the four scanning configurations were comparable and within the range 223-540 $\mu\epsilon$ (MAER) and 88-261 $\mu\epsilon$ (SDER), respectively (Fig.1

D). In performing DVC analysis on the entire proximal tibia, strain accuracy was 536 $\mu\epsilon$ and precision 473 $\mu\epsilon$ (Fig. 1 E).

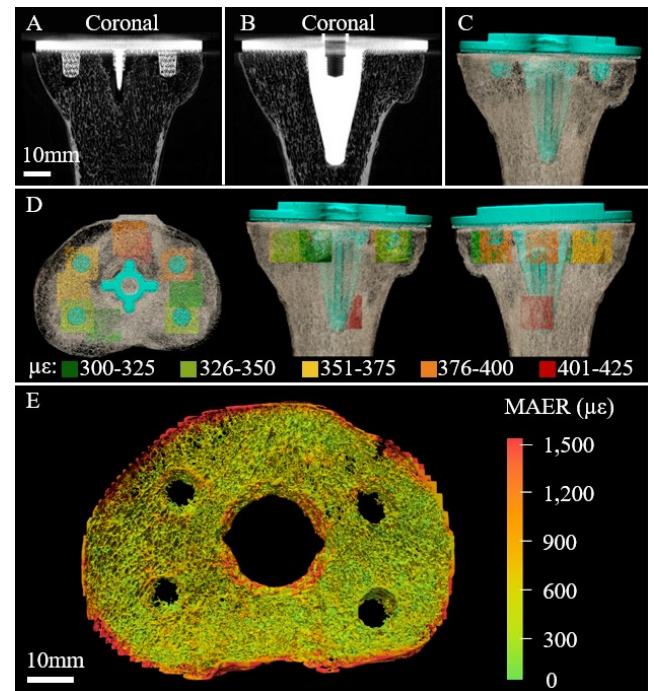


Figure 1: A-B) 2D micro-CT images ($42\mu\text{m}/\text{pixel}$), C) 3D micro-CT rendering of the proximal tibia with titanium implant, D) with the 9 VOIs used for zero-strain DVC (colour represents MAER); E) MAER across the proximal tibia (peg level).

CONCLUSIONS

Strain errors were sufficiently low for assessing bone within its elastic region ($< 10\%$ of the yield strain of bone, 7,000 $\mu\epsilon$), within subregions and at organ level [4]. Moreover, strain errors were comparable across the four scanning configurations considered. This indicates that the shorter scanning time, preferred for repeated scanning of biological specimens, is suitable for the planned mechanical testing configuration. This study will continue, performing micro-CT imaging of human tibiae implanted with press-fit prosthesis under load.

REFERENCES

1. Ryd L, et al., *J Orthop Res.* **17**:311-320, 1999.
2. Martelli S et Perilli E, *J Mech Behav Biomed.* **84**:265-272, 2018.
3. Tozzi L, et al., *J Mech Behav Biomed.* **67**:117-126, 2017.
4. Liu L et Morgan EF, *J Biomech.* **40**:3516-3520, 2007.

CONFLICT OF INTEREST DECLARATION

In the interests of transparency and to help reviewers assess any potential bias, all authors of original research papers are required to declare any competing commercial interests in relation to the submitted work. Referees are also asked to indicate any potential conflict they might have reviewing a particular paper.

If you have accepted any support such as funds or materials, tangible or intangible, concerned with the research by the commercial party such as companies or investors, choose YES below, and state the relation between you and the commercial party.

If you have not accepted any support such as funds or materials, choose NO.

Do you have a conflict of interest to declare? (DELETE TEXT as appropriate)

YES

If YES, please complete as appropriate:

1. The author(s) did receive payments or other benefits or a commitment or agreement to provide such benefits from a commercial entity.

This study is part of an ARC Centre of Excellence program, partially funded by DePuy Synthesis.

2. A commercial entity paid or directed, or agreed to pay or direct, any benefits to any research fund, foundation, educational institution, or other charitable or nonprofit organization with which the authors are affiliated or associated.



PROTEOMICS OF THE OSTEOCLAST SECRETORY LYSSOSOME UNMASKS NEW REGULATORS OF BONE RESORPTION AND SKELETAL BONE MASS

Amy B.P. Ribet¹, Benjamin Mullin¹, Daniel Yagoub¹, Laila N. Abudulai¹, Pei Ying Ng¹ and Nathan J. Pavlos¹

1. School of Biomedical Sciences, The University of Western Australia, Perth, WA, 6009

email: amy.ribet@research.uwa.edu.au

INTRODUCTION

Osteoclasts are central regulators of skeletal bone mass and are the only cell type capable of digesting bone. To achieve this, osteoclasts have evolved specialized hybrid endosome/lysosome-related organelles (ELROs) termed 'secretory lysosomes' that give rise to the bone-resorbing apparatus (i.e. the ruffled border) upon synchronous fusion with the bone-apposed plasma membrane [1]. Fusion of secretory lysosomes with the ruffled border equips its membrane with sets of nanoscale machinery that are requisite for extracellular acidification and bone digestion (e.g. the V-ATPase proton pump) [2]. Yet, despite their obvious importance in osteoclast resorptive function and thus fertile ground for the discovery of new anti-resorptive drug targets, our understanding of the molecular anatomy of osteoclast secretory lysosomes remains limited. In particular, compared to other ELROs (e.g. melanosomes in melanocytes), we still lack elementary information regarding the nature and number of membrane proteins that define secretory lysosome identity and function.

METHODS

Here, to expand the molecular inventory of membrane proteins operating on osteoclasts secretory lysosomes, we have combined biochemical organelle enrichment methods with high-resolution tandem mass spectrometry (nLC-ESI-MS/MS) to unbiasedly survey the osteoclast secretory lysosome membrane proteome.

RESULTS AND DISCUSSION

Using this approach, we unambiguously identified 4153 unique proteins. Of these 181 integral membrane proteins were functionally assigned as membrane transport proteins (transportome) and 390 as regulators of membrane trafficking (traffickome). Stratification of the 'transportome' and 'traffickome' for proteins that: (i) are significantly enriched on secretory lysosome membranes (LogFC > 1.5 and p < 0.05) and (ii) whose corresponding gene lead SNPs reached genome-wide significance (p < 5 x 10⁻⁸) when cross-referenced against the largest human cohort (n=400,000) of estimated bone mineral density (eBMD) (UKBioBank eBMD p < 5 x 10⁻⁸) established high-confidence lists of membrane transporters and trafficking proteins. By combining high-throughput siRNA gene knockdown studies in osteoclasts together with high-resolution confocal microscopy and novel genetic mouse models we demonstrate the power and utility of our proteomic screen to

unmask new and physiologically-relevant regulators of osteoclast bone resorptive function and skeletal homeostasis.

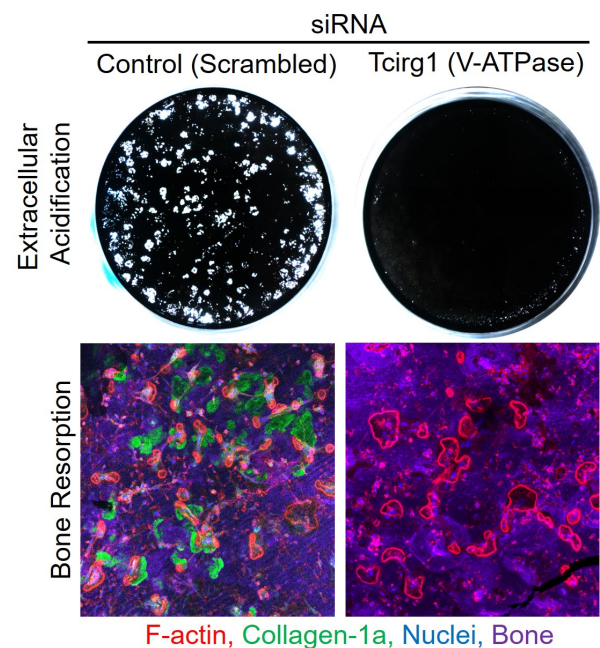


Figure 1: Functional validation of siRNA-mediated knockdown efficiency in bone-marrow derived osteoclasts using siRNAs targeting the osteoclast specific V-ATPase V0 proton pump subunit $\alpha 3$ (*Tc1rg1*) as an example. Knockdown of *Tc1rg1* potently suppressed extracellular acidification (osteoclast assay) and bone resorption (*collagen-1a* positive pits) *in vitro*. A non-targeting 'scrambled' siRNA served as a control.

CONCLUSIONS

Our work provides a roadmap for uncovering new regulators of osteoclast function and bone homeostasis that may serve as novel therapeutic targets for the treatment of osteoclast-mediated osteolysis and metabolic bone diseases.

ACKNOWLEDGEMENTS

This work is supported by project grant funding from the NHMRC (APP1143921 & APP1163933) to NJP

REFERENCES

1. Ng et al., *Biochem Soc Trans.* **47(2)**:639-650, 2019.
2. Ribet et al., *Front Cell Dev Biol.* **9**:644986, 2021.



THE VARIABILITY OF FOOT MOTION IN CHILDREN WITH CONGENITAL TALIPES EQUINOVARUS (CTEV) BEING CONSIDERED FOR TENDON TRANSFER SURGERY

Alexis Brierty^{1,2}, Sean Horan³, Claudia Giacomozzi⁴, Liam Johnson², David Bade^{1,2}, Christopher P Carty^{1,2,5}

¹Griffith Centre of Biomedical and Rehabilitation Engineering, Menzies Health Institute Queensland, Griffith University, QLD

²Queensland Children's Motion Analysis Service, Department of Orthopaedic Surgery Queensland Children's Hospital, QLD

³School of Allied Health Sciences, Griffith University, Gold Coast, QLD

⁴Italian National Institute of Health (Istituto Superiore di Sanità), Viale Regina Elena, 299, 00161 Roma RM, Italy

⁵Research Development Unit, Caboolture and Kilcoy Hospitals, Metro North Health, Caboolture, QLD

email: alexis.brierty@griffithuni.edu.au

INTRODUCTION

In children with congenital talipes equinovarus (CTEV), two common indications of relapse include hindfoot varus and forefoot supination during swing [1]. The most common surgical intervention for treatment of these relapses is the tibialis anterior tendon transfer (TATT), which is often prescribed following 2D visual assessment during gait and manual manipulation of the foot. Due to the complex musculoskeletal anatomy of the foot and ankle [2], this method of analysis may not be sufficient for identifying multiplanar changes.

The primary aim of this research was to assess the variability of foot motion in children with recurrent CTEV compared to a typically developed (TD) population using 3-dimensional motion analysis. Our secondary aim was to determine whether subgroups based on multi-segment foot model kinematics exist within the cohort.

METHODS

Seventeen participants with recurrent clubfoot being considered for TATT surgery were prospectively recruited. All participants were required to attend the Queensland Children's Motion Analysis Service (QCMAS) prior to intervention, where Plug-in-Gait and Oxford Foot Model kinematics, kinetics and plantar pressure were collected. Data analysis was performed using Vicon Nexus and dedicated Mathworks Matlab codes. Statistical analysis included Statistical Parametric Mapping (SPM) for time-series comparisons between cohorts, and k-means clustering for subgroup assignment.

RESULTS AND DISCUSSION

The results confirmed our hypothesis that patients with recurrent CTEV presented with more variable foot motion, with statistically significant increases in variability across all foot model (see Figure 1) and plantar pressure variables compared to the TD population. K-means clustering revealed two clear subgroups within the CTEV cohort: one group more impacted by hindfoot inversion (varus) and another group more impacted by hindfoot adduction and forefoot equinus (see Figure 1). There were no significant differences in kinetics or plantar pressures between the two identified subgroups. These differences in foot kinematics during gait raise the question of

whether or not the TATT is the most appropriate intervention for children in both groups. Further post-operative investigation is necessary to assess the outcomes in both groups following TATT surgery, and appropriate alternative treatment options.

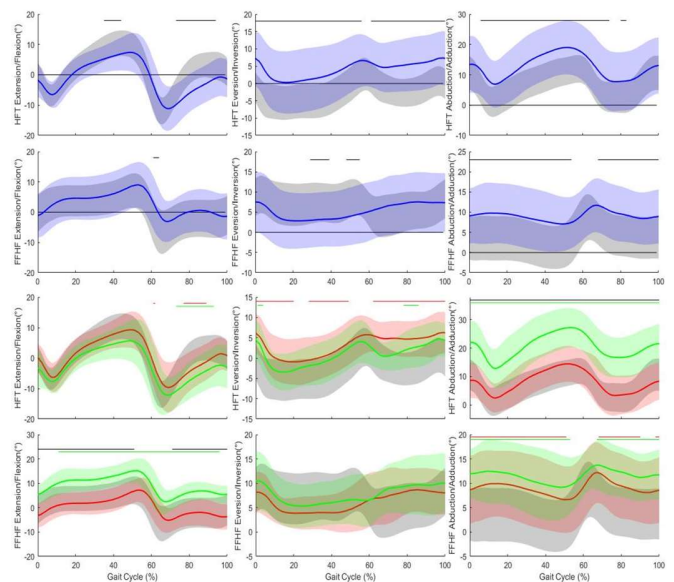


Figure 1: Ensemble means and standard deviations for all clubfoot participants (blue band) and the two clubfoot clusters (red and green bands) compared to the TD cohort (grey band) using the Oxford Foot Model (OFM). The colored lines indicate statistical significance.

CONCLUSIONS

Two clear subgroups were identified within the CTEV cohort being considered for TATT surgery. Further analysis is warranted to determine the effectiveness of TATT surgery for both groups and whether personalized surgical solutions are indicated on the basis of kinematic presentation.

REFERENCES

1. Staheli L, *Global HELP Organisation*, 2009
2. Ghanem I, et al., *Journal of Children's Orthopaedics* **13(2)**: 134-146, 2019.



THE MECHANICAL RESPONSE OF TRABECULAR BONE WITHIN THE TIBIAL PLATEAU DUE TO EXTERNAL JOINT LOADING

¹Kieran J Bennett, ²Lauren Wearne, ²Sophie Rapagna, ³Saulo Martelli, ¹Gerald J Atkins, ^{1,4}L Bogdan Solomon, ²Egon Perilli, ^{1,4}Dominic Thewlis

¹Centre for Orthopaedic and Trauma Research, Adelaide Medical School, The University Adelaide, Adelaide, SA, Australia

²Medical Device Research Institute, College of Science and Engineering, Flinders University, Adelaide, SA, Australia

³School of Mechanical Medical and Process Engineering, Queensland University of Technology, Brisbane, QLD, Australia

⁴Department of Orthopaedics and Trauma, Royal Adelaide Hospital, Adelaide, SA, Australia

email: Kieran.bennett@adelaide.edu.au

INTRODUCTION

The mechanical response of trabecular bone structures in the knee due to external load can currently only be implied from external measurement. Using a combination of large specimen micro-CT imaging and digital volume correlation (DVC), this behavior can be visualised and quantified. The aims of this study were to: (1) visualise the human proximal tibia bone microstructure while under an axial load using micro-CT imaging and, using these images, (2) calculate the strain distribution within the proximal tibia under load.

METHODS

Cadaveric knee specimens ($n=3$) were obtained. All soft tissues except for the articular cartilage and menisci were removed. The femur and tibia were mounted within a loading stage developed earlier [1]. The loading rig containing the specimen was positioned within a large-volume micro-CT scanner (Nikon XT H 225, Nikon Metrology, UK). Scans were performed at 46 μm isotropic pixel size in unloaded and then loaded conditions, with the proximal tibia and the distal femur contained in the field of view (86 x 86 mm, width x height). Axial loads equivalent to three bodyweights were applied to each specimen, based on the donor's mass at time of death. The angle of the femur was altered to obtain a 60:40 medial:lateral loading ratio. Loads were measured using a six degree-of-freedom load cell. Micro-CT cross-section images were reconstructed CTPro3D (Nikon Metrology). The loaded dataset was co-registered using DataViewer (Bruker) to the unloaded. Digital volume correlation (DVC) analysis was undertaken to calculate von Mises equivalent strains in four cylindrical volumes of interest (VOIs) (10x10 mm, diameter x length) located in regions of high and low loading [2] using DaVis (LaVision). The final DVC subvolume size was 34 voxel subvolume length. The VOIs were: anteromedial (AM), anterolateral (AL), posteromedial (PM), and posterolateral (PL).

RESULTS AND DISCUSSION

Within the four regions examined (Fig. 1), strains were within 1385-2170 $\mu\epsilon$. The highest strains were computed in the PM VOI (2170 \pm 640 $\mu\epsilon$ mean \pm SD).

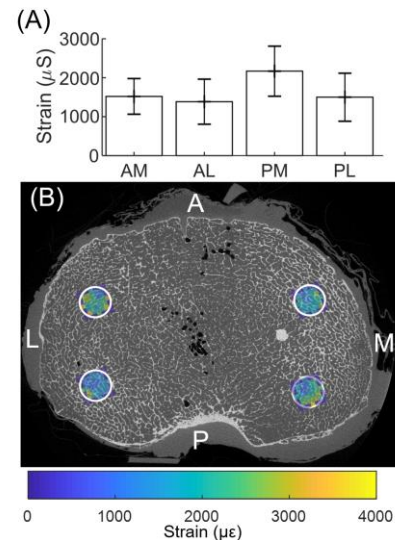


Figure 1: (A) Mean and standard deviation (error bars) of strains within the four cylindrical VOIs. (B) Micro-CT cross-section of a human proximal tibia, with strains under load in the VOIs.

CONCLUSIONS

Micro-CT scans of three proximal human tibiae were obtained, in unloaded and loaded conditions. Using DVC, the internal strains were quantified. These were within the physiological range reported in the literature [3] and were highest in the posteromedial region. The study will continue, with the final aim to inform computational models of bone mechanics.

ACKNOWLEDGEMENTS

This research program is supported by an Australian Government Research Training Program (RTP) Scholarship. A/Prof Thewlis receives fellowship funding from the NHMRC (CDF ID: 1126229). A/Prof Perilli and A/Prof Martelli receive funding from the ARC (ID: LE180100136, and IDs: DP180103146; FT180100338; IC190100020 respectively).

REFERENCES

1. Martelli S. *J. Mech Behav Biomed Mater.* **84**: 267-272, 2015
2. Roberts B.C. *Osteoarthr. Cartil.* **25**:1623-1632, 2017
3. Frost H.M. *Anat. Rec.* **1**:1-9 (1987)

DAY 2

Minghao Zheng Orthopaedic Innovation Award Finalists

CT-BASED FEA AND MULTIOBJECTIVE OPTIMISATION METHODS FOR DETERMINING OPTIMAL PLACEMENT OF FIXATION PLATE FOR SCAFFOLD-BASED MANDIBULAR RECONSTRUCTION

¹Ben M. Ferguson, ¹Ali Entezari, ²Jinguan Fang, ¹Qing Li.

¹School of Aerospace, Mechanical and Mechatronic Engineering, The University of Sydney, NSW 2006, Australia

²School of Civil and Environmental Engineering, University of Technology Sydney, Ultimo, NSW 2007, Australia

Email: Ben.Ferguson@sydney.edu.au

INTRODUCTION

A current challenge in bone tissue engineering is to create favourable biomechanical conditions conducive to tissue regeneration for a scaffold implanted in a segmental defect. This is particularly the case immediately following surgical implantation when a firm mechanical union between the scaffold and host bone is yet to be established via osseointegration. For mandibular reconstruction of a large segmental defect, the position of the fixation system is shown here to have a profound effect on the mechanical stimulus (for tissue regeneration within the scaffold), structural strength, and structural stiffness of the tissue scaffold-host bone construct under physiological load.

METHODS

This research combines computer tomography (CT)-based finite element (FE) modelling with multiobjective optimisation to determine the optimal height and angle to place a titanium fixation plate on a reconstructed mandible so as to enhance tissue ingrowth, structural strength and structural stiffness of the scaffold-host bone construct. To this end, the respective design criteria for fixation plate placement are to: (i) maximise the volume of the tissue scaffold experiencing levels of mechanical stimulus sufficient to initiate bone apposition (f_s), (ii) minimise peak stress in the scaffold (f_σ) so that it remains intact with a diminished risk of failure and, (iii) minimise scaffold ridge displacement (f_d) so that the reconstructed jawbone resists deformation under physiological load.

First, a CT-based FE model of a reconstructed human mandible implanted with a bioceramic tissue scaffold is developed to visualise and quantify changes in the biomechanical responses as the fixation plate's height and/or angle are varied. Next, surrogate modelling is implemented to generate bivariate cubic polynomial functions of the three biomechanical responses with respect to the two design variables (height, h and angle, α). Finally, as the three design objectives are found to be competing, bi- and tri-objective particle swarm optimisation algorithms are invoked to determine the most optimal Pareto solution, which represents the best possible trade-off between the competing design objectives.

RESULTS AND DISCUSSION

The volume of the scaffold experiencing appositional mechanical stimulus is observed to increase with the height of the fixation plate (see Figure 1). Also, as the principal load-transfer mechanism to the scaffold is via the fixation system,

there is a significant ingress of appositional stimulus from the buccal side towards the centre of the scaffold, notably in the region bounded by the screws.

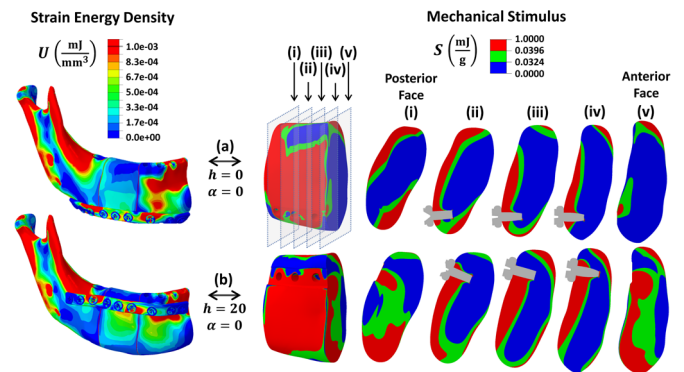


Figure 1: (left) Strain energy density distribution in the reconstructed half of the mandible and (right) mechanical stimulus distribution in the tissue scaffold where red indicates a bone apposition region, blue: resorption, and green: the lazy zone.

Figure 2 shows the most optimal point in tri-objective space is: $(f_{s,mo}, f_{\sigma,mo}, f_{d,mo}) = (-23.2\%, 2.18\%, 0.111 \text{ mm})$, which corresponds to $(h_{mo}, \alpha_{mo}) = (20.0 \text{ mm}, -3.5^\circ)$ in the $h\alpha$ -space.

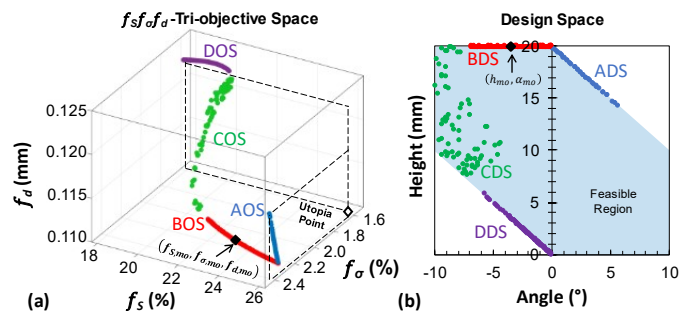


Figure 2: (a) The Pareto front in $f_s f_\sigma f_d$ -tri-objective space has four segments: AOS, BOS, COS, and DOS. (b) These Pareto front segments map to ADS, BDS, CDS, and DDS in $h\alpha$ -space.

CONCLUSIONS

It is recommended that consideration be given to placing the fixation system along the upper boundary of the mandible with a small clockwise rotation about its posterior end. The methodology developed here forms a useful decision aid for optimal surgical planning.

MINGHAO ZHENG ORTHOPAEDIC INNOVATION AWARD 2021, FINALIST

Orthopaedic Innovation Award Statement:

The outcome of this research is an innovative clinical planning tool used to inform and guide the decision-making process of a maxillofacial surgeon prior to undertaking a mandibular reconstruction procedure. Furthermore, this innovative research underpins the design and production of next-generation implants and scaffolds, which will be additively manufactured to be patient specific and enable surgeons to better reconstruct large bone defects. In addition, this research and methodology can be readily extended to include other orthopaedic surgical procedures such as spinal fusions or hip and knee reconstructions.



REMOTE PATIENT MONITORING WITH WEARABLE SENSORS FOLLOWING KNEE ARTHROPLASTY

^{1,3}Faseeh Zaidi, ²Scott M. Bolam, ³Ted C. Yeung, ^{3,4}Thor F. Besier and ^{2,3}Andrew Paul Monk

¹School of Medicine, Faculty of Medical and Health Sciences, The University of Auckland, Auckland, New Zealand

²Department of Orthopaedics, Auckland City Hospital, Auckland, New Zealand

³Auckland Bioengineering Institute, The University of Auckland, Auckland, New Zealand

⁴Department of Engineering Sciences, The University of Auckland, Auckland, New Zealand

email: szai535@aucklanduni.ac.nz

INTRODUCTION

Post-operative monitoring of patients following knee arthroplasty is essential to identify patients on a sub-optimal recovery course. Traditional patient-reported outcomes measures (PROMs) are highly subjective and are shown to poorly correlate with actual physical function. Inertial Measurement Units (IMUs) provide a low-cost, portable solution to obtain objective functional measures for three-dimensional gait analysis. The aim of our study was to demonstrate the feasibility and reliability of ankle-worn IMUs in monitoring post-operative recovery in knee arthroplasty patients.

METHODS

Fourteen patients undergoing primary knee arthroplasty for osteoarthritis were prospectively enrolled. Remote patient monitoring in the community was performed pre-operatively and weekly from post-operative weeks 2 to 6. IMU measures included: cumulative impact load, bone stimulus, impact load asymmetry. PROMs included: Oxford Knee Score (OKS), EuroQol Five-dimension with EuroQol visual analogue scale.

RESULTS AND DISCUSSION

On average, significant improvements were seen in the bone stimulus ($P=0.002$) and cumulative impact load ($P=0.035$) from post-operative week 2 by week 4 and week 6, respectively (Figure 1). The impact load asymmetry value trended towards equal impact loading between the operative and non-operative limb but did not reach significant difference ($P=0.308$) (Figure 1). Of note, PROMs scores (Oxford Knee Score) did not always reflect the same trend as the IMU-derived limb usage (Figure 2).

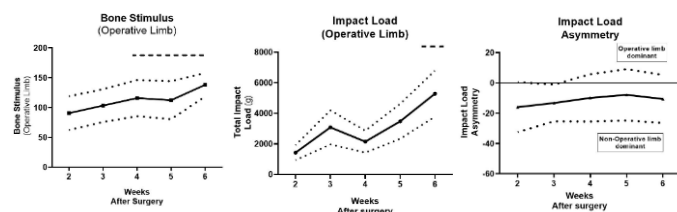


Figure 1: IMU Outputs (Bone Stimulus, Impact Load and Impact Load Asymmetry) presented as mean (solid line) \pm S.D (dotted line). Data were analysed by one-way ANOVA with

Tukey's post-hoc analysis ($P<0.05$, comparison vs. Post-op Week 2 Score [dashed bar above]).

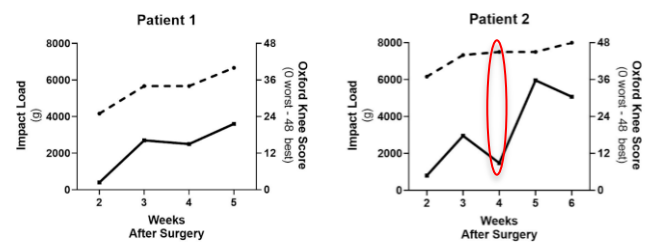


Figure 2: Individual data for Patient 1 and 2 with PROMs score (OKS, dashed line) and IMU Outputs (Impact load, solid line) over the post-operative period.

We present a scalable remote patient monitoring workflow system to quantitatively assess post-operative function in patients' recovery after knee arthroplasty. The simple use of an ankle bracelet system reliably captures data not previously available to the clinical team. Specifically, functional data (bone stimulus, impact load, impact load asymmetry) from the community are monitored and can be tracked over time. This represents a step change in monitoring post-operative knee replacement patients.

CONCLUSIONS

This study demonstrates the feasibility of a reliable, low cost and low-maintenance workflow system to remotely monitor post-operative progress in knee arthroplasty patients. By providing quantitative data, this complementary tool will be highly useful to clinicians to identify and intervene on 'at risk' outlier patients early in their recovery period. Quantitative measures from IMUs augment existing qualitative PROMs, to provide a more holistic overview of patient progress following knee arthroplasty.

ACKNOWLEDGEMENTS

We would like to thank VICON-IMeasureU (Vicon, Oxford, UK) for providing the IMU sensors and database/cloud computing infrastructure for this study.

This project was funded by NZ Medical Technologies Centre of Research Excellence (MedTech CoRE, New Zealand).

MINGHAO ZHENG ORTHOPAEDIC INNOVATION AWARD 2021, FINALIST

Orthopaedic Innovation Award Statement:

The purpose of this study was to assess the role of combining Inertial Measurement Units (IMU) with patient-reported outcome measures (PROMs) to provide a viable alternative to the current standard of post-operative care following knee arthroplasty. Through easily combining IMU data with established PROMs (such as the Oxford Knee Score) in the routine clinical pathway, this allows surgeons and care teams to better understand each patient's recovery trajectory after knee arthroplasty. As a result, we are able to identify patients on a sub-optimal recovery course and intervene early. The work has not been filed a patent.

CONFLICT OF INTEREST DECLARATION

In the interests of transparency and to help reviewers assess any potential bias, all authors of original research papers are required to declare any competing commercial interests in relation to the submitted work. Referees are also asked to indicate any potential conflict they might have reviewing a particular paper.

If you have accepted any support such as funds or materials, tangible or intangible, concerned with the research by the commercial party such as companies or investors, choose YES below, and state the relation between you and the commercial party.

If you have not accepted any support such as funds or materials, choose NO.

Do you have a conflict of interest to declare? (DELETE TEXT as appropriate)

YES

If YES, please complete as appropriate:

1. The author(s) did receive payments or other benefits or a commitment or agreement to provide such benefits from a commercial entity.

State the relation between you and the commercial entity:

Thor Besier was a co-founder of IMeasureU and remains a consultant to VICON-IMeasureU (Vicon, Oxford, UK). The sensors used in this research study is Vicon Blue Trident IMU sensors manufactured by VICON-IMeasureU.

The other authors declare no conflict of interest.

2. A commercial entity paid or directed, or agreed to pay or direct, any benefits to any research fund, foundation, educational institution, or other charitable or nonprofit organization with which the authors are affiliated or associated.

No



ENHANCEMENT OF TENDON-BONE HEALING WITH A COMBINED GROWTH FACTOR HYDROGEL IN A RAT CHRONIC ROTATOR CUFF INJURY MODEL

S.M. Bolam^{1,2}, S. Konar¹, M. Zhu^{1,2}, J. Workman¹, K. Lim³, T. Woodfield³, A.P. Monk^{1,2}, B. Coleman⁴, J. Cornish¹, J.T. Munro^{1,2}, D.S. Musson¹

1. University of Auckland, Auckland, New Zealand, 2. Auckland District Health Board (DHB), Auckland, New Zealand, 3. University of Otago, Christchurch, New Zealand, 4. Counties Manukau DHB, Auckland, New Zealand

Email: s.bolam@auckland.ac.nz

Background: Re-rupture rates after rotator cuff repair remain high because of inadequate biological healing at the tendon-bone interface. Single-growth factor therapies to augment healing at the enthesis have so far yielded inconsistent results. An emerging approach is to combine multiple growth factors over a spatiotemporal distribution that mimics normal healing. We propose a novel combination treatment of insulin-like growth factor 1 (IGF-1), transforming growth factor β 1 (TGF- β 1) and parathyroid hormone (PTH) incorporated into a controlled-release tyraminated poly-vinyl-alcohol hydrogel to improve healing after rotator cuff repair. We aimed to evaluate this novel growth factor treatment in a rat chronic rotator cuff tear model.

Methods: A total of 30 male Sprague-Dawley rats underwent unilateral supraspinatus tenotomy. Delayed rotator cuff repairs were then performed after 3 weeks, to allow tendon degeneration that resembles the human clinical scenario. Animals were randomly assigned to: [1] a control group with repair alone; or [2] a treatment group in which the hydrogel was applied at the repair site. All animals were euthanized 12 weeks after rotator cuff surgery and the explanted shoulders were analyzed for biomechanical strength and histological quality of healing at the repair site.

Results and Discussion: In the treatment group had significantly higher stress at failure (73% improvement, $P=0.003$) and Young's modulus (56%

improvement, $P=0.028$) compared to the control group (Figure 1). Histological assessment revealed improved healing with significantly higher overall histological scores (10.1 of 15 vs 6.55 of 15, $P=0.032$), and lower inflammation and vascularity.

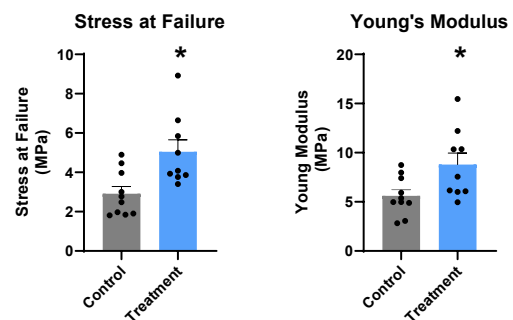


Figure 1: Biomechanical analysis showing a significantly higher stress at failure and Young's modulus and load at failure in the treatment group compared with the control group. Data are presented as mean \pm SEM where * $P < 0.05$.

Conclusions: This novel combination growth factor treatment improved the quality of healing and strength of the repaired enthesis in a chronic rotator cuff tear model. Further optimization and tailoring of the growth factors hydrogel is required prior to consideration for clinical use in the treatment of rotator cuff tears. This novel treatment approach holds promise for improving biological healing of this clinically challenging problem.

MINGHAO ZHENG ORTHOPAEDIC INNOVATION AWARD 2021, FINALIST

Orthopaedic Innovation Award Statement:

The failure rate after rotator cuff repair remains high (20-70%) due to inadequate tendon-to-bone healing. Using a novel growth factor hydrogel, we demonstrated improved strength and quality of healing at the tendon-to-bone interface in a rodent model. This growth factor delivery system could next be translated into humans. This novel approach holds promise for improving clinical outcomes and preventing surgical failure of this clinically challenging problem. A patent for this growth factor combination therapy has been filed.



DAY 3

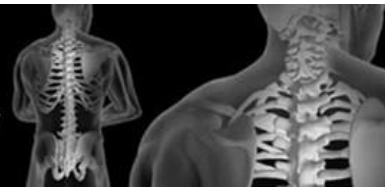
KEYNOTE 4 – Prof Saman Halgamuge

The University of Melbourne, Victoria, Australia

“21st Century Artificial Intelligence and its Potential in Biomedical Research”



Australian & New Zealand
Orthopaedic Research Society



DAY 3

PODIUM 5



EMG-DRIVEN MODEL PREDICTIONS OF GLENOHUMERAL JOINT FORCE SHOW HIGH AGREEMENT WITH INSTRUMENTED IMPLANT DATA AFTER TARGETTED MODEL CALIBRATION

¹Azadeh Kian, ²Claudio Pizzolato, ³Mark Halaki, ⁴Karen Ginn, ²David Lloyd, ⁴Darren Reed ¹David C. Ackland

¹Department of Biomedical Engineering, University of Melbourne, Australia

²Griffith Centre of Biomedical and Rehabilitation Engineering, Menzies Health Institute Queensland and School of Allied Health Sciences, Griffith University, Australia

³Discipline of Exercise & Sport Science, Sydney School of Health Sciences, Faculty of Medicine & Health, The University of Sydney

⁴Discipline of Anatomy & Histology, Faculty of Medicine and Health, The University of Sydney

email: dackland@unimelb.edu.au

INTRODUCTION

Computational models of the shoulder are used for evaluating the functional performance of implants, surgical planning, and development of targeted rehabilitation. Electromyography (EMG)-driven neuromusculoskeletal models employ EMG in the prediction of muscle and joint forces, but glenohumeral joint force calculations are known to be sensitive to chosen values of muscle-tendon parameters used in these models, which depends on model calibration [1]. The glenohumeral joint force is a clinically relevant quantity that has a significant bearing on joint stability and mobility, yet model predictions of this quantity are seldom validated. The aim of the present study was to employ an EMG-driven neuromusculoskeletal model to assess the influence of model calibration strategy on estimates of glenohumeral joint force. This was achieved by comparing the model estimates of joint force with instrumented shoulder implant data [2].

METHODS

Three healthy female adults were recruited for testing (age: 23.7 ± 6.4 years; body mass: 55.7 ± 3.2 kg; height: 165.0 ± 2.6 cm). The participants performed dynamic shoulder abduction at a rate of $60^\circ/\text{second}$ followed by three sets of tasks used to calibrate the model's muscle-tendon and EMG to activation parameters, which included: (i) general tasks including reaching and head touching as well as the submaximal isometric internal and external shoulder rotations (ii) sagittal plane tasks including active and passive shoulder flexion at $30^\circ/\text{second}$, sub-maximal isometric flexion and extension of the shoulder with the arm in 90° of flexion, and (iii) scapular plane tasks including active and passive abduction at $30^\circ/\text{second}$, sub-maximal isometric abduction and adduction of the shoulder with the arm in 90° of abduction.

Trajectories of 14 reflective markers attached to upper-limb bony landmarks were simultaneously collected using a video motion analysis system, and joint angles calculated using inverse kinematics. EMG data recorded using 5 surface electrode pairs (pectoralis major, biceps brachii, triceps brachii, upper and lower trapezius) and 12 intramuscular bipolar electrodes (rhomboid major, supraspinatus, infraspinatus, serratus anterior, teres major, latissimus dorsi, pectoralis minor, subscapularis, infraspinatus, anterior, middle and posterior deltoid). External forces during sub-maximal contractions were measured using an instrumented cable and pulley system.

Subject-specific EMG-driven neuromusculoskeletal models of each participant were created using a previously published model [1], and the model's EMG-to-activation and

musculotendon parameters were calibrated for each subject using data acquired from the three calibration task sets: (i) all calibration tasks (ii) sagittal plane tasks, and (iii) scapular plane tasks. In addition, an uncalibrated model was also employed using the default values for the musculotendon parameters. Muscle forces and resultant glenohumeral joint contact forces for abduction were computed, and joint forces compared to previously published instrumented implant data from two subjects [2].

RESULTS AND DISCUSSION

Model calibration strategy had a substantial influence on calculated glenohumeral joint forces during abduction (Figure.1). Calibrating EMG-driven neuromusculoskeletal models across a broad range of tasks in multiple planes produced glenohumeral joint forces that were most similar to those measured in instrumented implants, while models that were calibrated using tasks in one plane only, or not calibrated at all, produced joint forces that had great discrepancy with instrumented implant data. The RMS difference between calculated and measured glenohumeral joint force during abduction was 7.1%BW for implant 1 and 10.8%BW for implant 2.

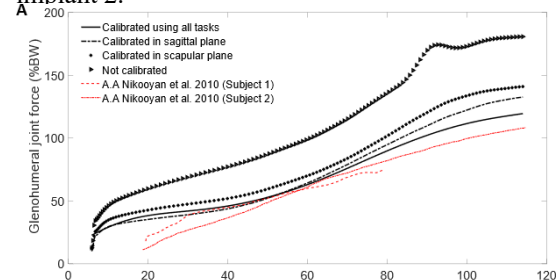


Figure 1: Mean glenohumeral joint force (%BW) estimated using the EMG-driven neuromusculoskeletal model during abduction and instrumented implant data for two subjects reported by Nikooyan et al. (2010) for the same task.

CONCLUSIONS

Calibration of EMG-driven neuromusculoskeletal models is critical for accurate prediction of glenohumeral joint forces, and the best possible calibration strategy, to achieve optimal model parameters, involves diverse tasks across a range of motion planes.

REFERENCES

1. Kian, A., et al. (2019). *Journal of Biomechanics* 97: 109348.
2. Nikooyan, A., et al. (2010). *Journal of Biomechanics* 43(15): 3007-3014.



THE ROLE OF THE LIGAMENTUM TERES IN NORMAL FUNCTION OF THE HIP JOINT

¹Ian Al'Khafaji, ¹John O'Donnell and ²David C. Ackland

¹Hip Arthroscopy Australia, Richmond, Victoria, Australia

²Department of Biomedical Engineering, The University of Melbourne, Melbourne, WA, Australia
Email: dackland@unimelb.edu.au

INTRODUCTION

The ligamentum teres (LT) is an intra-articular, extra-synovial ligament in the central compartment of the hip. It attaches to the fovea capitis of the femoral head, the transverse acetabular ligament (TAL), as well as the acetabular rim adjacent to the TAL. As the LT occupies the cotyloid fossa, it has been hypothesised that this ligament is crucial in maintaining a strong fluid seal of the hip [1], which is required for hip joint stability; however, this has never been proven. The purpose of this study was to quantify the role of the LT in maintaining fluid seal in a hip cadaver model of the LT intact and deficient hip.

METHODS

Fourteen fresh-frozen hemi-pelvis and lower extremity specimens (mean age: 64.6 ± 1.94 yrs) were harvested from 7 cadavers. All specimens were radiographed using x-ray fluoroscopy to screen for fracture, macroscopic hip joint abnormalities and evidence of prior surgery. Specimens were thawed for 24 hours prior to testing. The capsule and all extracapsular tissue surrounding the hip joint were removed by sharp dissection. To simulate LT deficiency, the LT was sharply released from its femoral and acetabular attachments and completely removed from the joint while leaving the cotyloid soft tissues in place.

Hip joint specimens were first tested in their native state (control case) followed by testing in the LT deficient state (test case). All specimens were mounted to a two-axis materials test system (Instron, Model 3521, Parker Hydraulics, USA) using customised fixtures (Fig. 1). The hip was positioned in neutral alignment, which was quantified by establishing ISB recommended joint coordinate systems using a four-camera video motion analysis system (Vicon, Oxfordmetrics, UK). A concentric compressive load of 100N between the femoral head and acetabulum was applied and held for 20 seconds to ensure presence of fluid seal and eliminate any residual joint displacement. The femur was then distracted from the pelvis at a rate of 0.33 mm/s until a maximum 8mm of translation was achieved. The cycle of compression and distraction was then repeated with the hip joint positioned in 20° of flexion as well as in 10° of extension. These hip joint positions were chosen as representative joint configurations that occur during walking. Peak distraction force, joint stiffness and distraction energy were compared between groups using paired t-tests, with significance level set at $p < 0.05$.

RESULTS AND DISCUSSION

In the neutral hip position, the LT deficient state displayed a significantly lower peak distraction force (mean difference: 33.5 N, $p=0.02$), stiffness (mean difference: 115.7 N/mm, $p=0.05$), and total energy (mean difference: 28.3 Nmm, $p=0.014$) compared to that in the intact control. In extension, the peak distraction force and total energy was significantly lower in the LT deficient hip compared to that in the control, while in flexion, the peak distraction force was significantly lower ($p < 0.05$).

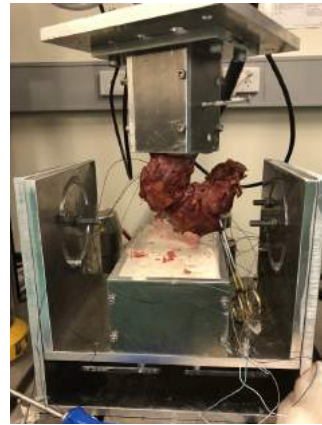


Figure 1: Illustration of cadaveric hip joint specimen potted in Instron testing system. Custom designed fixtures were developed to control hip flexion-extension and axial rotation of the hip joint.

CONCLUSIONS

Deficiency of the LT leads to a decreased distraction force and stiffness in the hip joint, indicating that the LT plays a role in maintaining hip stability via the biomechanical suction seal effect. The role of the LT in maintaining this hip suction seal appears to be most prominent when the hip is in neutral alignment or extended, indicating a greater resistance to distraction forces, particularly during the stance phase of gait. Future studies ought to explore the effectiveness of surgical LT reconstruction in maintaining the hip suction seal.

REFERENCES

1. Rosinsky, P.J., et al., *All About the Ligamentum Teres: From Biomechanical Role to Surgical Reconstruction*. JAAOS - Journal of the American Academy of Orthopaedic Surgeons, 2020. **28**(8).

CONFLICT OF INTEREST DECLARATION

In the interests of transparency and to help reviewers assess any potential bias, all authors of original research papers are required to declare any competing commercial interests in relation to the submitted work. Referees are also asked to indicate any potential conflict they might have reviewing a particular paper.

If you have accepted any support such as funds or materials, tangible or intangible, concerned with the research by the commercial party such as companies or investors, choose YES below, and state the relation between you and the commercial party.

If you have not accepted any support such as funds or materials, choose NO.

Do you have a conflict of interest to declare? (DELETE TEXT as appropriate)

YES

If YES, please complete as appropriate:

1. The author(s) did receive payments or other benefits or a commitment or agreement to provide such benefits from a commercial entity.
State the relation between you and the commercial entity:

2. A commercial entity paid or directed, or agreed to pay or direct, any benefits to any research fund, foundation, educational institution, or other charitable or nonprofit organization with which the authors are affiliated or associated.

This research was funded by Medacta, Switzerland.



PATIENT-REPORTED AND FUNCTIONAL OUTCOMES IN PATIENTS FOLLOWING PRIMARY AND REVISION TOTAL HIP ARTHROPLASTY

¹Bahl, J.S.; ¹Chai, H.; ¹Grace, T.M.; ^{1,2}Smitham, P.; ^{1,2}Solomon, L.B.; ^{1,2}Thewlis, D

¹Centre for Orthopaedic and Trauma Research, University of Adelaide, Adelaide, Australia;

²Department of Orthopaedics and Trauma, Royal Adelaide Hospital, Adelaide, Australia

email: dominic.thewlis@adelaide.edu.au

INTRODUCTION

Primary total hip arthroplasty (THA) is a highly successful procedure. In contrast, revision THA is a complex procedure, with reports of relatively poor patient-reported outcomes compared to primary THA [1]. However, there appears to be a discrepancy between patient reported outcomes of function and objectively measured function in THA [2]. As we move beyond the point where implant longevity is the major concern for device manufacturers, we must look at functional outcome for patients, which we have done in primary THA [2]. However, there have been no objective assessments of functional outcomes for revision THA. This study aims to quantify self-reported outcomes and walking gait function in patients following primary and revision THA.

METHODS

Forty-three patients undergoing primary THA for osteoarthritis and 23 patients undergoing revision THA were recruited, and followed longitudinally for 12 months. Reasons for revision were loosening (73%), dislocation (9%), and infection (18%). Patients completed the Hip dysfunction and Osteoarthritis Outcome Score (HOOS), and underwent gait analysis preoperatively, and at 3 and 12 months postoperatively. A 10 camera motion analysis system (Vicon) recorded marker trajectories (100 Hz) during walking at self-selected speeds. A generic lower-body musculoskeletal model (Gait 2392) was scaled using principal component analysis [1] and OpenSim 3.3 was used to compute joint angles. Independent samples *t*-test were used to compare patient reported outcomes between the primary and revision groups at each time point. Statistical parametric mapping was used to compare gait patterns between the two groups at each time point.

RESULTS AND DISCUSSION

Preoperatively, patients undergoing primary THA reported significantly worse pain ($p < 0.01$), symptoms ($p < 0.01$), function ($p < 0.01$), and quality of life ($p = 0.004$) (Table 1). No differences were observed at 3 and 12 months postoperatively ($p > 0.05$). The only observed difference in gait pattern was that patients with a revision THA had reduced hip extension at 3 months (Figure 1).

Table 1. HOOS outcome scores for primary and revision groups; Mean (SD).

		Preop	3m	12m
Pain	Primary	36 (16)	84 (15)	85 (20)
	Revision	64 (26)*	82 (19)	82 (19)
Symptoms	Primary	39 (17)	82 (16)	85 (16)
	Revision	65 (21)*	82 (16)	83 (20)
ADL	Primary	37 (63)	78 (23)	82 (20)
	Revision	63 (23)*	80 (17)	75 (20)
QOL	Primary	19 (17)	70 (26)	72 (29)
	Revision	38 (27)*	64 (22)	67 (16)

* $P < 0.05$; ADL = activities of daily living. QOL = quality of life

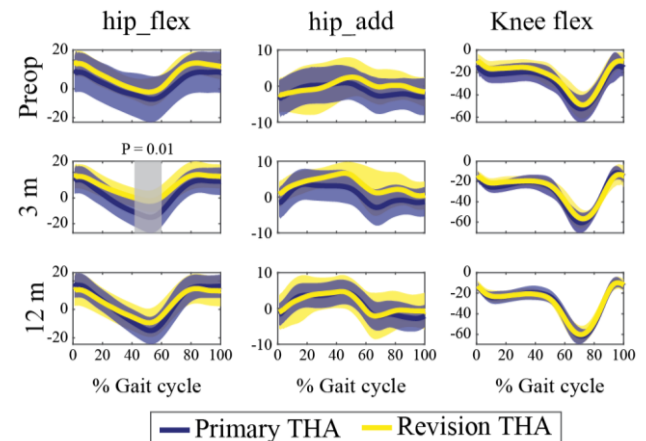


Figure 1. Hip and knee joint kinematics at each timepoint. Grey bar indicates a significant difference between primary and revision THA groups from the SPM analysis.

CONCLUSIONS

This study demonstrated no differences in patient-reported outcomes at 3 or 12 months postoperatively for primary vs. revision THA. Our data suggest that function recovers at a slower rate for patients after revision THA vs. primary THA, but this resolves by one year postoperative.

ACKNOWLEDGEMENTS

DT received funding from the NHMRC (ID: 1126229).

REFERENCES

- [1] Postler AE, et al. Hip International. 2017;27:180-6.
- [2] Bahl JS, et al. JBJS. 2021;103:1166-74.



ESTIMATING FACET JOINT APPPOSITION WITH SPECIMEN-SPECIFIC COMPUTER MODELS OF SUBAXIAL CERVICAL SPINE KINEMATICS: THE EFFECT OF AXIAL COMPRESSION AND DISTRACTION DURING SHEAR AND BENDING MOTIONS

¹Ryan Quarrington, ^{1,2}Darcy Thompson-Bagshaw, and ^{1,2}Claire Jones

¹Spinal Research Group, Adelaide Medical School, The University Adelaide, Adelaide, SA, Australia

²School of Mechanical Engineering, The University Adelaide, Adelaide, SA, Australia

email: ryan.quarrington@adelaide.edu.au

INTRODUCTION

Facet fracture occurs in up to 77% of traumatic cervical facet dislocations (CFD) but is rarely observed in experiments with cadaver tissue [1]. Muscle activation may superimpose an intervertebral compression load on traumatic intervertebral motions, increasing facet joint contact and thereby increasing the probability of fracture with dislocation. Computational models of experimental data can provide a non-invasive method to estimate joint biomechanics during spinal trauma and resulting from surgery. Existing models typically consider each vertebra as one rigid-body (vertebral body + posterior elements) and assume a uniform cartilage depth for each facet. However, facet deflection occurs during intervertebral motion [2], and cervical facet cartilage depth is not uniform [3].

The aim of this project was to use specimen-specific, multi rigid-body C6/C7 computational models with specimen-specific cartilage profiles to investigate the change in facet joint cartilage apposition when intervertebral axial distraction or compression is superimposed on intervertebral flexion (10°), anterior shear (1 mm), axial rotation (4°) and lateral bending (5°) motions.

METHODS

Twelve C6/C7 motion segments (70±13 yr, nine male) underwent high-resolution CT scanning. Specimens were subjected to non-destructive quasi-static anterior shear (AS; 1 mm), right axial rotation (AR; 4°), flexion (F; 10°), and left lateral bending (LB; 5°) motions using a six degree-of-freedom materials testing machine. Each motion was superimposed with: 1) neutral (50 N compression); 2) neck muscle contraction (300 N compression); and, 3) inertial intervertebral separation (2.5 mm distraction). Intervertebral kinematics and facet deflections were measured with motion-capture markers on the vertebral bodies, and the bilateral inferior facets of C6, respectively. The motion-capture data was applied to specimen-specific computer models, and facet cartilage apposition area (CAA) was calculated. For each test direction, linear mixed-effects models were used to compare CAA at peak motion between axial conditions.

RESULTS AND DISCUSSION

For all motions, CAA was significantly larger for the compressed condition, compared to the neutral and distracted conditions, and for neutral vs distracted ($p < 0.001$ for all). CAA was significantly larger for the 'loaded' left facet during axial rotation and lateral bending for all axial conditions ($p < 0.001$ for both).

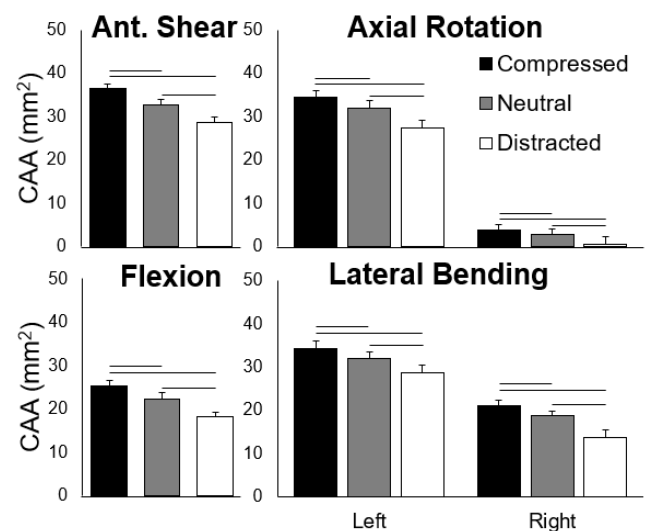


Figure 1: Cartilage apposition area (CAA) results for each motion/axial condition combination. Horizontal lines indicate statistical significance ($\alpha = 0.05$).

CONCLUSIONS

Simulated compressive neck muscle activation increased C6/C7 facet contact, compared to distraction, when superimposed on intervertebral shear and bending motions. This suggests that intervertebral compression forces may play a role in facet fracture associated with CFD.

REFERENCES

1. Foster, B. *IRCOBI* 2012.
2. Quarrington, R. J. *Biomech.* **72**, 116-124, 2018.
3. Womack, W. *Ost. Cartilage* **16**, 1018-1023.

QUANTIFYING ORTHOTROPIC MECHANICAL PROPERTIES IN ENTIRE HUMAN FEMURS

¹Marco Branni, ²Egon Perilli, ²Mark Taylor and ¹Saulo Martelli

¹School of Mechanical, Medical and Process Engineering, Queensland University of Technology, Brisbane, QLD, Australia

²Medical Device Research Institute, College of Science and Engineering, Flinders University, Adelaide, SA, Australia

email: marco.branni@qut.edu.au

INTRODUCTION

Finite Element (FE) models have become common tools for investigating the mechanical behavior of the human femur. However, a lack of standardization in assigning bone mechanical properties leads variable accuracy across laboratories [1]. This study aims to compare orthotropic apparent mechanical properties calculated using indirect fabric-based method against direct corresponding micro-FE calculations in entire proximal human femurs.

MATERIAL AND METHODS

Micro-CT images (29.81 $\mu\text{m}/\text{voxel}$) of four osteoporotic cadaveric femurs (76-81 years of age) were used [2]. Each image volume was subdivided into 5mm side-length contiguous trabecular cubes (Fig.1). A selection criterion based on morphometric parameters was implemented to guarantee bone homogeneity.

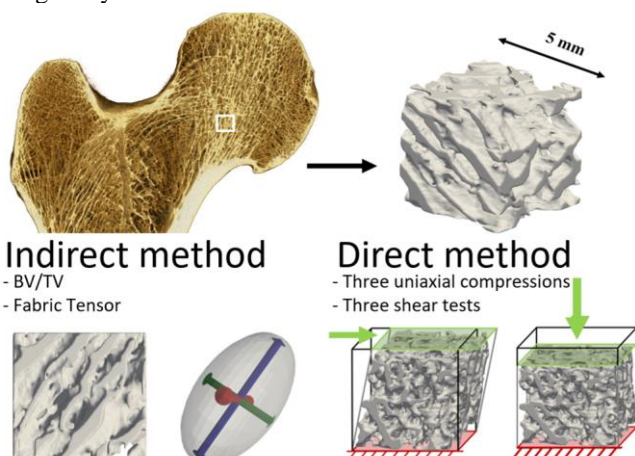


Figure 1: Orthotropic mechanical characterization.

Bone volume fraction (BV/TV), fabric tensor and degree of anisotropy (DA) were calculated using the Mean Intercept Length method (CT Analyser, Bruker, Belgium). Orthotropic stiffness matrix was determined by using fabric-elasticity relationships [3]. Micro-FE models were developed by converting bone voxels into linear hexahedra elements. Bone tissue material properties were modelled as isotropic linear elastic material ($E = 5.33 \text{ GPa}$) with a Poisson's ratio equal to 0.3. The orthotropic stiffness matrix was computed simulating in displacement control three uniaxial compression and three shear tests by homogenization procedure [4]. The stiffness

matrix obtained by the direct and indirect methods were compared using linear regression.

RESULTS AND DISCUSSION

The analysis was successfully completed for 1507 cubes from four femurs. The BV/TV and DA range were 8 – 47% and 1.08 – 2.05, respectively. The coefficient of determination was 0.85 and the slope was 1.25. The RMSE was lower than 7% of the maximum micro-FE predicted value (Fig.2).

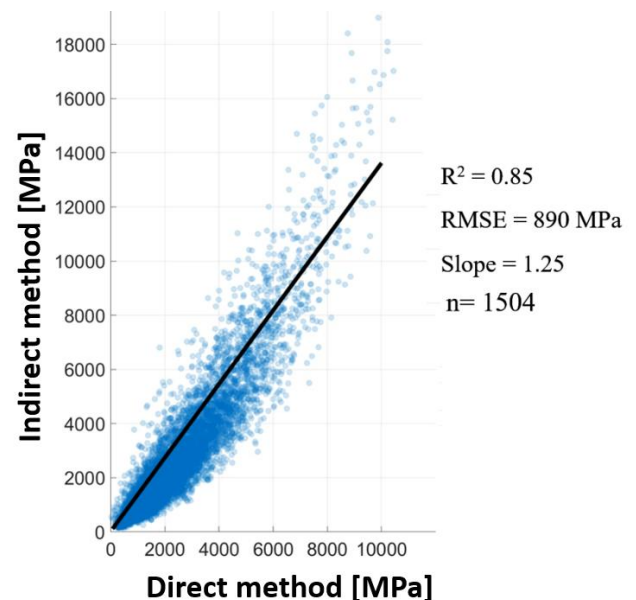


Figure 2: Linear regression analysis of stiffness matrix.

CONCLUSIONS

The procedure for determining the orthotropic stiffness matrix reveals a strong agreement between indirect and direct models. However, the indirect methods provided stiffer material properties than corresponding direct calculations. Further investigations are being performed to examine how these differences may influence stresses and strains continuum-FE models predictions.

REFERENCES

1. Kluess et al., *Comput Method Biom.* **22**: 1020-1031, 2019
2. Martelli et Perilli. *J Mech Behav Biome.* **84**:265-272,2018
3. Zysset et al, *J Biomech.* **36**:10:1469-1485, 2006
4. Van Rietbergen et al, *J Biomech.* **29**:1653-1657, 1996



Australian & New Zealand
Orthopaedic Research Society



DAY 3

PODIUM 6

DOES SEX INFLUENCE THE KNEE PASSIVE KINEMATICS?

¹Francesca Bucci, ¹Mark Taylor, ¹Rami Al-Dirini and ^{1,2}Saulo Martelli

¹Medical Device Research Institute, College of Science and Engineering, Flinders University, Adelaide, SA, Australia

²School of Mechanical Medical & Process Engineering, QUT, Brisbane, QLD, Australia

email: francesca.bucci@flinders.edu.au

INTRODUCTION

Women experience higher rates of knee ligament injuries than men [1], different anatomical features [2] and different knee kinematics during weight bearing activities [3]. However, kinematic differences between genders show mixed results [3]. Knee passive motion has been studied in large cohorts of male donors [4] and along selected axes of motion. The present study aims at studying gender differences of the knee passive kinematics over the six degrees of freedom in intact adult specimens.

METHODS

Twenty-nine healthy knee specimens (19 males and 9 females, between 43 and 82 years of age) were obtained from a body donation program (Science Care, Phoenix, USA); exclusion criteria included no reported history of knee surgery and osteoarthritis. Ethics approval was obtained from the institutional Ethics Committee. Specimens were CT scanned (SOMATOM force, Siemens, Germany; in-plane voxel size: 0.33 mm). Femoral and tibial bone surfaces were segmented with ScanIP (Simpleware, Exeter, UK). Custom 3D printed potting cups were created for the tibia and the femur. Reflective markers (12) were placed on dedicated features on the femur and tibial potting cups, and the assembly was CT scanned to determine the relative position of the marker and the knee. Two trials of complete flexion-extension movements were performed respectively by manually applying a medial a lateral pressure to the femoral cup [6-8N] for five repetitions each (Fig1). The marker trajectories were recorded using a 10-camera stereo-photogrammetric system (VICON, Oxford, UK). Anatomical bony landmarks were identified according to the ISB standards [5] using NMS Builder (IOR, Bologna, Italy). The anatomical joint coordinate system was created according to Gray et al. (2019) [6]. The knee kinematics for the six axes of motion was estimated using the Kinemat toolbox (MATLAB, MathWorks Inc., USA). The range of passive motion was the difference between the knee motion measured applying medial and lateral pressure. Mean and standard deviation were calculated and compared between genders using two tails t-test and statistical parametric mapping (SPM, Matlab toolbox, $\alpha = 0.05$); variations were reported as mean or peak differences.

RESULTS AND DISCUSSION

Tibio-femoral kinematics were consistent with earlier reports. The largest difference between medial and lateral force trials was 18° mean internal-external rotation (peak: 26°). Smaller

differences were found for adduction-abduction (peak: 5°) and medio-lateral translation (peak: 3mm) (Fig1). Females presented greater adduction-abduction angles than males by applying a medial force (mean diff.: 2°, $p < 0.05$), whereas no gender-specific differences were found for the remaining axes of motion (Fig1).

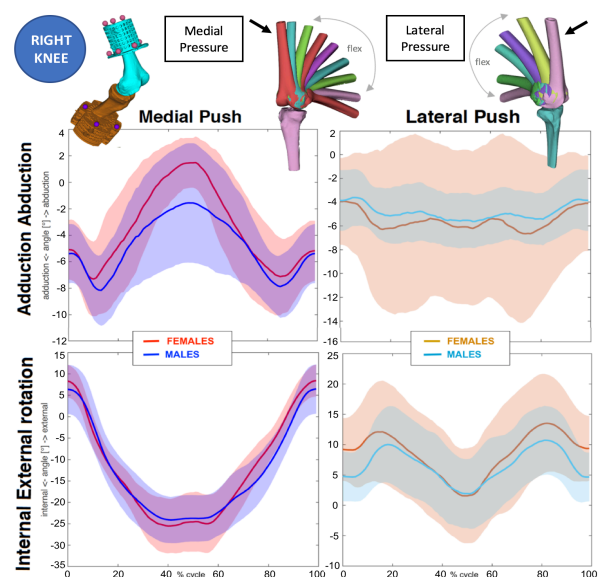


Figure 1: Knee gender passive kinematics differences.

CONCLUSIONS

Results demonstrate a gender-specific passive knee motion observed for the two medial and lateral extremes of the envelope of passive motion, obtained by applying medial and lateral pressure. Females display higher adduction-abduction and lower internal-external rotation than males, in partial agreement with literature [3]. These findings may complement current understanding of gender differences kinematics.

ACKNOWLEDGEMENTS

Australian Research Council (DP180103146)

REFERENCES

1. Arendt et al., *J.Athletic.Train*,34:86-92,1999.
2. Conley et al, *J.Am.Acad.Orthop.Surg.*,15:S31-6,2007.
3. Roger James et al, *Res.Q.Exerc.Sport*,75(1):31-38, 2005.
4. Cyr et al. *Proc.Inst.Mech.Eng.H.*, 228: 494-500, 2014.
5. Wu et al., *J.Biomech.*,35:543-548, 2002.
6. Gray et al., *J.Biomech.Eng.*,8:141, 2019.



CHANGES IN POST-OPERATIVE LOWER LIMB BIOMECHANICS AFTER FEMORAL NAILING OF PROXIMAL FEMUR FRACTURES

¹Arjun Sivakumar, ^{2,1}Mark Rickman and ^{1,2}Dominic Thewlis

¹Centre for Orthopaedic & Trauma Research, The University Adelaide, Adelaide, SA, Australia

²Department of Orthopaedics & Trauma, The Royal Adelaide Hospital, Adelaide, SA, Australia

email: arjun.sivakumar@adelaide.edu.au

INTRODUCTION

Intertrochanteric (IT) hip fractures are highly prevalent in the elderly [1] with 40% to 60% of patients losing the ability to function independently and unable to return to preinjury ambulatory levels. [2] While a handful of authors have reported postoperative spatiotemporal gait parameters [3,4] there exists no published literature on gait biomechanics in geriatric IT fracture patients to date. This study aims to investigate if the joint kinematics and powers of the lower limbs changed between six weeks and six months in elderly IT patients after internal fracture fixation.

METHODS

Twenty eight patients (n=28) sustaining IT fractures and treated with a proximal femoral nail (PFN) were prospectively enrolled. Patients were followed up at six weeks and six months postoperative where three-dimensional gait analysis data were collected. Analyses were performed in OpenSim 3.3. The gait2392 model was scaled using an atlas based statistical shape modelling method (MAPClient). [5] For the joints of the lower limbs, angles and powers were calculated according to ISB recommendations. [6] Statistical parametric mapping was used to analyze changes in joint angles and powers between timepoints. Changes in gait speed between timepoints were assessed with a paired t-test.

RESULTS AND DISCUSSION

There was a significant increase in gait speed of 0.2m/s between timepoints ($p < 0.001$). For joint angle at the hip, the SPM analysis showed improvements in peak extension during terminal stance (~35 to 55% gait cycle) ($p = 0.049$) and flexion during initial to mid swing (~65% to 80% gait cycle) ($p = 0.007$). Peak hip abduction also increased during mid to terminal stance (~25% to 40% gait cycle) ($p = 0.002$). Significant improvements in peak knee flexion ($p < 0.001$) as well as ankle plantarflexion and dorsiflexion ($p < 0.001$) were also shown across the gait cycle. The SPM analysis of joint powers showed an increase in hip power generation during the loading response to approximately midstance (~10 to 50% stance) and during terminal stance and pre swing (~80% to 95% stance) ($p < 0.001$).

At the knee, there were increased power absorption within the loading response ($p = 0.015$) and throughout terminal stance and pre swing (~85% to 95% stance) ($p < 0.001$). At the ankle joint, power absorption increased throughout single limb support phase of the ipsilateral foot, while power generation increased from approximately terminal stance (~80% stance) to toe off during pre-swing ($p < 0.001$).

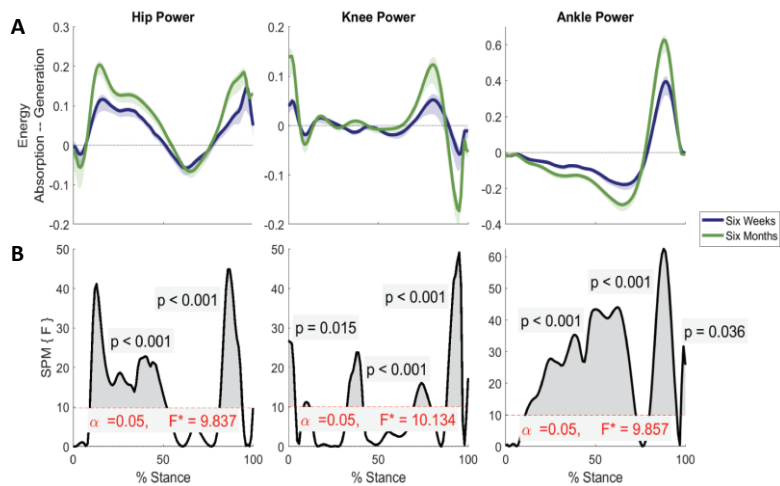


Figure 1: (A) Average joint powers at six weeks (blue) and six months (green) post-operative. (B) SPM(F) between six weeks and six months for hip, knee and ankle joint powers over stance.

CONCLUSIONS

The findings from this study are the first to highlight overall improvements in walking biomechanics after surgery from six weeks to six months.

REFERENCES

1. Sambrook, P. *The Lancet* 367, 2010-18, 2006.
2. Dyer, S.M. *BMC Geriatrics* 16, 158, 2016
3. Thingstad, P. *BMC Geriatrics* 15, 150, 2015
4. Gausden, E.B. *J. Orthop. Trauma* 32, 554-8, 2018
5. Zhang. *ISBMS* 8789, 182-192, 2014
6. Wu G. *J. Biomech* 35, 543-548, 2002

CONFLICT OF INTEREST DECLARATION

In the interests of transparency and to help reviewers assess any potential bias, all authors of original research papers are required to declare any competing commercial interests in relation to the submitted work. Referees are also asked to indicate any potential conflict they might have reviewing a particular paper.

If you have accepted any support such as funds or materials, tangible or intangible, concerned with the research by the commercial party such as companies or investors, choose YES below, and state the relation between you and the commercial party.

If you have not accepted any support such as funds or materials, choose NO.

Do you have a conflict of interest to declare? (DELETE TEXT as appropriate)

YES

If YES, please complete as appropriate:

1. The author(s) did receive payments or other benefits or a commitment or agreement to provide such benefits from a commercial entity.

State the relation between you and the commercial entity:

This project was funded through an investigator initiated research grant awarded by Smith & Nephew Inc Orthopaedic Division. Smith & Nephew had no input into the study.

2. A commercial entity paid or directed, or agreed to pay or direct, any benefits to any research fund, foundation, educational institution, or other charitable or nonprofit organization with which the authors are affiliated or associated.

N.A.



EFFECTS OF PUBERTAL MATURATION ON ANTERIOR CRUCIATE LIGAMENT FORCES DURING A LANDING TASK IN FEMALES

¹Azadeh Nasser, ¹David Lloyd, ¹Clare Minahan, ²Timothy Sayer, ²Kade Paterson, ³Christopher Vertullo, ²Adam Bryant, ¹David Saxby

¹Griffith Centre of Biomedical and Engineering Rehabilitation, Griffith University, Gold Coast, QLD, Australia

²Centre for Exercise, Health & Sports Medicine, University of Melbourne, Melbourne, VIC, Australia

³Knee Research Australia, Gold Coast, QLD, Australia

email: a.nasser@griffith.edu.au

INTRODUCTION

The Anterior cruciate ligament (ACL) rupture is a common knee injury resulting in substantial health care costs (i.e., surgical care and physical therapy) and elevated risk of early onset knee osteoarthritis. Rates of ACL rupture in young people have increased dramatically over past decades [1], with the resultant burden of early knee osteoarthritis falling on young people with the history of ACL injury. Sex- and age-specific differences in rates of ACL rupture have been observed [1]. There is a two to four times greater risk of sustaining ACL injury in female athletes compared to male athletes. Compared to pre-pubertal girls, late- to post-pubertal young women are at greater risk of ACL injury [2]. However, conclusive causal mechanism(s) for this increased risk of ACL injury in young females have yet to be presented. The purpose of this study was to determine the effects of pubertal maturation in females on ACL force during a dynamic motor task.

METHODS

Based on Tanner's classification system, 19 pre-pubertal, 19 early/mid-pubertal, 24 late/post-pubertal females performed standardized drop-land-lateral jump while three-dimensional body motion, ground reaction forces, and surface electromyography were acquired. These data were used to model external biomechanics, lower limb muscle forces, and knee contact forces, which were subsequently used in a validated computational model [3, 4] to estimate the ACL loading. Statistical parametric mapping analysis of variance was used to compare ACL force, and its causal contributors, between the three pubertal maturation groups during stance phase of the task.

RESULTS AND DISCUSSION

Compared to pre- and early/mid-pubertal females, late/post-pubertal females had significantly higher ACL force (mean differences 482 N and 355 N during 3%-30% and 55%-89% of stance; and 381 N and 296 N during 3%-25% and 62%-85% of stance, respectively). At the peak point of ACL force, contributions from the sagittal, and transverse plane loading late/post pubertal group compared to pre and early/mid pubertal groups (medium effect sizes ranging from 0.44 to 0.77). No differences were found between pre- and early/mid-pubertal

groups in ACL force or its contributors (Figure 1).

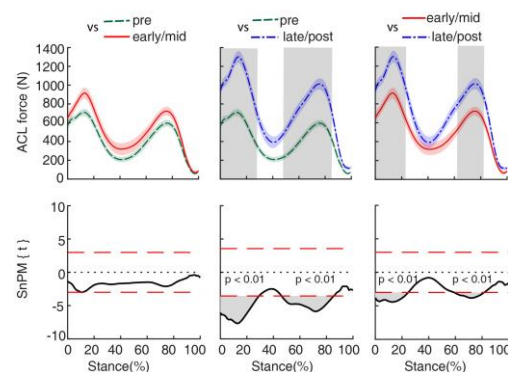


Figure 1: Comparisons of the ACL force during the stance phase of the task between pre-, early/mid-, and late/post-pubertal females performed with statistical non-parametric mapping (SnPM).

CONCLUSIONS

During a standardized drop-land-lateral jump, late/post-pubertal females generated higher ACL forces compared to less mature females across a large percentage of stance, including the instances of peak forces. The sagittal plane was the primary contributor to ACL force in all maturation groups but made relatively lower contribution in the late/post-pubertal group compared to less mature females. Results indicate ACL forces increased across pubertal maturation, and, given the cessation of ACL growth at ~10 years of age in females, may explain the dramatic rise in ACL rupture sustained by females 15-19 years of age. Quantifying ACL force can advance our understanding of the ACL loading mechanism thereby providing insight into better approaches to injury prevention.

REFERENCES

1. Zbrojkiewicz D, et al., *Med J Aust*, **208(8)**: 354-358, 2018.
2. Shea K.G, et al., *J Pediatr Orthop*. **24(6)**: 623-628, 2004.
3. Nasser A, et al., *Med Sci Sports Exerc*, **53(6)**: 1235-1244.
4. Nasser A, et al., *Comput Methods Programs Biomed*, **184**: 105098.



PROSTHETIC IMPINGEMENT RISK FACTORS AND IMPACT ON PATIENT OUTCOMES IN HIP RESURFACING ARTHROPLASTY

David Shen MD¹, Lukas Eckhard MD², Eric Jiang³, William L Walter MD PhD¹

¹Tom Reeve Academic Surgical Clinic, Royal North Shore Hospital, Sydney University, Sydney, Australia

²Department for Orthopaedics and Traumatology, University Medical Centre Mainz, Germany

³Data Analysis and Surgical Outcomes Unit, Royal North Shore Hospital, Sydney, New South Wales, Australia

email: david.b.shen@gmail.com

INTRODUCTION

Hip resurfacing arthroplasty (HRA) is a bone sparing surgical procedure for chronic hip pathologies such as osteoarthritis [1]. A phenomenon that may occur post resurfacing is prosthetic impingement (PI), defined as cortical bone loss at the head-neck junction as a result of acetabular cup to bone collision [2]. This study aims to determine the significance of impingement on patient outcomes and identify potential risk factors that may mitigate its occurrence.

METHODS

A consecutive series of 135 primary HRA (130 patients) were examined from a single surgeon between September 2005 and 2016. Mean radiographic follow up was 66 months (range 24 to 147). Anteroposterior radiographs were evaluated for signs of impingement then analysed using radiographic measurements such as head-neck ratio, lateral cup protrusion, stem medialisation and cup position. Clinically, patient reported outcome measures (PROMs), numeric pain scales and range of motion were assessed.

RESULTS AND DISCUSSION

Radiographic signs of impingement were present in 15.6% of patients and were seen at the superior aspect of the head-neck junction. The median post-operative Harris Hip Score (HHS) in the impingement group was 93 points (Interquartile range 88, 98) which was lower than the non-impingement group with a median of 96 points (IQR 92, 99), $p = 0.04$. Groin pain was higher in the impingement group with both activity ($U = 561.5$, $p = <0.005$) and rest ($U = 645$, $p = <0.005$).

Forward stepwise logistic regression shows an increased risk of prosthetic impingement with head-neck ratio (odds ratio 2.23, $p = 0.03$), and abduction (odds ratio 1.08, $p = 0.01$). These variables in combination with lateral cup protrusion and radiographic inclination using receiver operating characteristic (ROC) curves provides an excellent model of prediction with

an area under the curve of 0.81. Optimal cut-off points using Youden's index were generated for each of these risk factors.

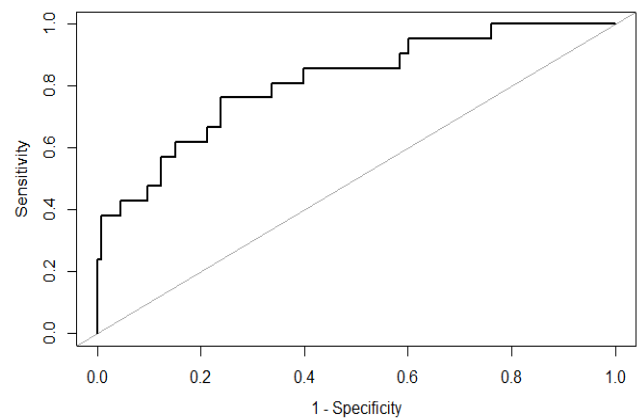


Figure 1: ROC curve using the combined risk factor model

CONCLUSIONS

Prosthetic impingement can cause significant post-operative pain and impact patient reported outcomes. The risk factors associated with this pathology such as head-neck ratio and abduction may be incorporated into pre-operative planning or at-risk assessments to mitigate patient-specific implant malposition.

REFERENCES

1. Australian Orthopaedic Association National Joint Replacement Registry, *Hip, Knee & Shoulder Arthroplasty: 2018 Annual Report*, Adelaide, Australia 2018.
2. J. Girard, et al., Femoral head to neck offset after hip resurfacing is critical for range of motion, *Clin. Biomech.*, **27**:165–169, 2012.

Table 1: Identified risk factors for prosthetic impingement from forward logistic regression analysis

Variable	Odds Ratio	Standard Error	P value
Lateral Cup Protrusion	1.07	0.04	0.11
Abduction	1.08	0.03	0.01
Head-Neck ratio	2.23	0.36	0.03
Radiographic Inclination	0.91	0.05	0.09



COMPARISON OF AOANJRR HIP ARTHROPLASTY DATA WITH A HOSPITAL BASED REGISTRY

Kerry Costi, Stuart Callary, Darcy Noll, Donald Howie, Bogdan Solomon

Centre for Orthopaedic and Trauma Research, The University of Adelaide and the Department of Orthopaedics and Trauma,
The Royal Adelaide Hospital (RAH), Adelaide, SA, Australia
email: kerry.costi@sa.gov.au

INTRODUCTION

Arthroplasty registries play a critical role in improving the outcome of joint replacement surgery. They provide unique community-based comparative data enabling individual surgeons to identify best practice for their own arthroplasty surgery [1]. Accurate documentation of arthroplasty procedures is also important for hospital audits to capture complications, reoperations and revision surgeries. The aim of this study was to compare the number primary total hip replacements (THR) and subsequent revisions captured by the AOANJRR relative to a hospital-based registry.

METHODS

A retrospective study was undertaken of 2123 primary THRs performed at the Royal Adelaide Hospital from May 2000 to December 2016. Data was retrieved from a hospital-based registry (OPMOD) including patient name, UR number, date of birth, gender, operation date, side of replacement, diagnosis, implants used and subsequent revision details where applicable. Data was sent to the AOANJRR [2] for cross matching purposes.

RESULTS AND DISCUSSION

Primary:

The AOANJRR matched 2087 of the 2123 primary THRs (98.3%). The date of operation was not a factor that influenced missing data, given that the 36 unmatched records spanned over 14 separate years.

Table 1: Primary and Revision THR matching using AOANJRR and hospital-based registry data

	Primary THR (n, %)	Revision THR (n, %)
Total	2123	98
Matched	2087 (98.3)	85 (86.7)
Identified by AOANJRR, confirmed to be non-THR	0	4 (4.1)
Not identified by AOANJRR	36 (1.7)	13 (13.3)

Revision:

The hospital-based registry recorded 98 revisions of the 2123 primary THRs. 85 revisions recorded by AOANJRR

matched the hospital-based registry. The AOANJRR identified an additional 4 revisions. Three were later confirmed to not be revision THR but open reduction internal fixations of femoral fractures. One was recorded as a revision of the opposite hip. Of the 13 additional hospital-based registry revisions, there were six head-liner exchanges, three acetabular component revisions and four femoral component revisions.

Of the 2087 primary THRs, osteoarthritis was recorded as the predominant diagnosis in 80% of the AOANJRR data and in 67% of the hospital-based registry. Osteonecrosis or AVN was similar in numbers. Differences were identified in some diagnosis particularly fracture neck of femur. There were 9 primary THRs missing diagnoses in the AOANJRR dataset.

This study confirms similar results to a smaller single surgeon cohort comparison study of 231 primary THRs [4]. Local verification and validation of arthroplasty data is important to ensure hospital staff are completing both AOANJRR and hospital operating forms correctly [3,4].

CONCLUSION

This study confirmed the excellent performance of the AOANJRR to capture 98.3% of the primary THRs from a public hospital over a 16 year period. Our review has identified that improved reporting of revision THRs is required due to the variation within revision procedures. Further investigation is required to improve the documentation of both primary and revision THR diagnosis.

ACKNOWLEDGEMENTS

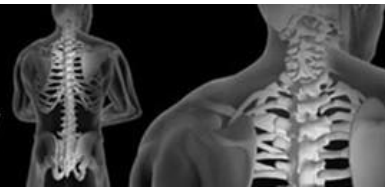
We thank the RAH, our Orthopaedic surgeons, nursing staff, the Orthopaedic Quality Assurance and Research Unit at the RAH and the staff at the AOANJRR for crossmatching Registry data to our dataset.

REFERENCES

1. Graves SE. *Acta Orthopaedica* 2010; 81(1):8–9.
2. AOANJRR Annual Report. Adelaide: AOA, 2019.
3. Barr CJ, BS, et al. *J of Arthroplasty* 27(10): 2012
4. Jang B, et al. *J of Ortho Surgery* 2013;21(3):347-50



Australian & New Zealand
Orthopaedic Research Society



DAY 3

PODIUM 7



FACTORS INFLUENCING FEMORAL PERIPROSTHETIC FRACTURE AROUND CEMENTED STEMS

Stuart Callary, Darcy Noll, Kerry Costi, Tania Carbone, Peter Smitham, Donald Howie, Bogdan Solomon
 Centre for Orthopaedic and Trauma Research, The University of Adelaide and the Department of Orthopaedics and Trauma,
 The Royal Adelaide Hospital, Adelaide, SA, Australia
 email: stuart.callary@sa.gov.au

INTRODUCTION

Peri-prosthetic femoral fracture (FPPF) is the third leading reason for revision in primary THR, according to the Australian Orthopaedic Association National Joint Replacement Registry [1] (AOANJRR) placing a significant burden on the patient, surgeon and the health care system. The reported incidence of femoral peri-prosthetic fractures (FPPF) varies between 0.4% and 3.5%. Recently, the burden of FPPF was suggested to be almost double the revision rate for fracture [2] as many centers now treating FPPF around cemented tapered stems with open reduction internal fixation (ORIF) [3]. A study of 82,972 cemented polished stems identified fracture as the leading cause of revision (41.5%), although the incidence was relatively low, 0.5% [4]. Therefore, the aim of our study was to determine the incidence of FPPF at our institution and investigate factors that may influence FPPF.

METHODS

Between May 2000 and December 2016, 2123 primary THRs were performed at our institution (1173 females, 950 males). The median age at primary THR was 69 years (range, 18-100). There were 2008 hips implanted with cemented stems and 115 hips with uncemented stems. Of the cemented stems, a cemented CPT 12/14 (Zimmer Biomet) implant was used in 1720 hips (86%). FPPF were confirmed using state hospital records, a hospital based joint replacement database (OPMOD), AOANJRR data request and radiographs. Multivariable binary logistic models investigated factors including age, gender, previous femoral fracture (prior to primary THR), head size and stem length.

RESULTS AND DISCUSSION

Of the 2123 cases at latest follow-up, 70 hips (3.3%) had a Vancouver B (77%) or C (33%) FPPF. 60 hips underwent were treated by ORIF, nine by revision THR and one was managed conservatively. There was a similar gender ratio, median time to revision and median age across both ORIF and revision groups (Table 1).

Revision due to FPPF at latest follow-up was 0.4% for all stems and 0.5% for CPT 12/14 stems. Incidence of FPPF within the first 24 months was 0.9% for all stems and 1.1% for CPT 12/14 stems. The incidence of FPPF at latest follow up was 3.3% for all stems and 3.7% for CPT 12/14 stems.

Adjusting for all variables, there was a statistically significant association between FPPF and Age ($p=0.0110$). For every one year increase in age the odds of having a FPPF increases by 3% (Odds Ratio=1.01). There was also a statistically significant association between FPPF and

previous femoral fracture of CPT 12/14 stems at both two years ($p=0.036$) and latest follow-up ($p=0.0185$). Patients with no previous femoral fracture are 52% less likely to have FPPF than those patients with a femoral fracture prior to primary THR (Odds Ratio=0.48).

Within the first 24 months the incidence of FPPF was 0.9% for all stems and 1.1% for CPT 12/14 stems as opposed to 0.38% [5]. The incidence of FPPF at latest follow up was much higher (3.3% all stems; 3.7% CPT 12/14 stems) than other reports (0.78% [1] and 0.5% [4]). However, our revision rate due to FPPF at latest follow-up (0.4% all stems; 0.5% CPT 12/14) is similar to previous reports. When interpreting the incidence of FPPF in the literature, it is important to consider the treatment methods (reoperation or revision) used by different institutions.

CONCLUSION

The incidence of FPPF may be under reported in studies that only report reason revision THR. Our study included reoperations of primary THRs performed at our institution. Older age and patients that had previous femoral fracture prior to primary THR were more likely to have a FPPF.

ACKNOWLEDGEMENTS

We thank the RAH for supporting this study, our Orthopaedic surgeons and nursing staff, the Orthopaedic Quality Assurance and Research Unit at the RAH and Suzanne Edwards from the University of Adelaide for statistical advice.

REFERENCES

1. AOANJRR Annual Report. Adelaide: AOA, 2019.
2. Constantin, H et al., ANZ J of Surg, 2019;89:1647-51.
3. Smitham, P et al., J Arthro, 2019;34(7):1430-34.
4. Hoskins W et al., J Arthro. 2018;33(5):1472-76.
5. AOANJRR Annual Report. Adelaide: AOA. 2017.

Table 1: Fracture cohort demographics

	Total	ORIF	Revision
M:F	37:33	32:28	5:4
Median Time to Revision (months)	47 (1 -197)	47 (1 -197)	10 (1-86)
Median Age at Primary (range, years)	73 (38 – 89)	74 (38 - 89)	71 (41 - 87)
Vancouver grade B1: B2: B3: C	8:46:0:15	8:37:0:15	0:9:0:0



VENOUS THROMBOEMBOLISM FOLLOWING SURGICAL INTERVENTION FOR BELOW KNEE FRACTURES: A SYSTEMATIC REVIEW OF THE RISK AND BENEFITS OF PREVENTATIVE STRATEGIES

¹Dr Sam Mischewski, ^{1,2}A/Prof Kerry Hitos

¹Sydney Medical School, The University of Sydney, Sydney, NSW, Australia.

²Westmead Research Centre for the Evaluation of Surgical Outcomes, Department of Surgery, Westmead Hospital, Sydney NSW, Australia

email: sam.mischewski@gmail.com

INTRODUCTION

Venous thromboembolism (VTE) is a significant risk for all orthopaedic surgery. In the past, research has largely focused on hip and knee fractures with the significance of events in below knee operatively managed fractures not fully appreciated. Symptomatic VTE rates in below knee fractures were historically recognised at 2.6-4.3% [1]. Current guidelines are conflicting and provide mixed recommendations on the prescription of VTE prophylaxis but generally do not support routine prescription in this demographic group of patients. Currently only low molecular weight heparin is licensed for use as chemical prophylaxis. There is a need to fully assess the current state of evidence for risks and benefits of prophylaxis in operatively managed below knee fractures.

Objective: To review the incidence of venous thromboembolism in operatively managed fractures below the knee and evaluate the efficacy of chemical and mechanical prophylaxis on VTE rates and associated adverse events.

METHODS

A systematic review was conducted as per the PRISMA guidelines. A search was performed of Embase, Pubmed, Cochrane and associated reference lists for any papers related to the effect of prophylaxis (both mechanical and chemical) on VTE rates and secondarily on adverse outcomes. Studies were included if the population involved operatively managed below knee orthopaedic trauma in patients over the age of 18 years old and intervention involved strategies for mechanical or pharmacological prevention in the perioperative setting. Outcomes of interest were both symptomatic and asymptomatic VTEs, including above and below knee deep vein thrombosis (DVT) and Pulmonary Embolism (PE), with secondary outcomes of interest including both major and minor post operative bleeding events, wound breakdown and death.

RESULTS AND DISCUSSION

From 330 articles returned from the protocolised search strategy at total of nine met the inclusion criteria. All articles were assessed for individual characteristics, risk of bias and results with synthesis conducted and reported [2-9]. Rates of asymptomatic VTEs in this population were significantly higher than previously thought, ranging from 1.9 to 12.6% [2, 3, 4]. Chemical prophylaxis reduced VTE rates with mixed

significance. Duration of prophylaxis decreased VTE rates when comparing 1 week to 6 weeks although not significantly [5]. The type of fracture was shown to significantly impact the rate and effectiveness of VTE prophylaxis, with tibial fractures showing significantly higher rates and possible benefit from prophylaxis [2, 4]. No information was available on mechanical prophylaxis. Major and minor bleeding events were not significantly increased with use of chemical prophylaxis, except for warfarin which showed a combined bleeding adverse event rate of 5.4% [1, 2]. Low molecular weight heparin remains the agent of choice, although aspirin and rivaroxaban showed comparable efficacy and adverse event rates based on the limited evidence available [3,7,8].

CONCLUSIONS

The use of VTE prophylaxis remains controversial following surgical intervention of below knee fractures. This study was unable to support or reject current guidelines on the prescription of pharmacological and mechanical VTE prophylaxis. This study shows significant difference in rates and effect based on fracture location and thus should not be considered a single entity. Further research into the duration and agent of prophylaxis as well as the efficacy and safety for tibial and ankle fractures is recommended. Of note rivaroxaban shows potentially beneficial efficacy and low adverse event rates though is currently not licensed in this population.

ACKNOWLEDGEMENTS

No source of external funding was sought or gained

REFERENCES

1. Solis G, et al., *Foot Ankle Int.* **23**(5):411-4, 2002.
2. Heijboer RRO, et al., *J Bone Joint Surg Am.* **101**(6):539-46, 2019.
3. Hoffmeyer P, et al., *Orthopedics.* **40**(2):109-16, 2017.
4. Goel DP, et al., *J Bone Joint Surg Br.* **91**(3):388-94, 2009.
5. Lapidus LJ, et al., *Acta Orthop.* **78**(4):528-35, 2007.
6. Pelet S, et al., *J Bone Joint Surg Am.* **94**(6):502-6, 2012.
7. Saragas NP, et al., *S Afr Med J.* **107**(4):327-30, 2017.
8. Hunter AM, et al., *Injury.* **51**(2):554-8, 2020.
9. Stavem K, et al., *Foot Ankle Surg.* **26**(6):681-6, 2020.
10. Zheng X, et al., *Foot Ankle Int.* **37**(11):1218-24, 2016.



PATIENTS WITH ANTERIOR SHOULDER INSTABILITY ADOPT COMPENSATORY SCAPULA MOTION DURING UPPER LIMB FUNCTION

¹Fraser W. Francis-Pester, ^{2,3}Lukas Ernstbrunner, ⁴Aaron Fox, ²Karl Wieser, ⁵David C. Ackland

¹Australian National University Medical School, Acton, Canberra, Australia; ²Department of Orthopedics, Balgrist University Hospital, University of Zurich, Zurich, Switzerland; ³Melbourne Orthopaedic Group, Windsor, Melbourne, Australia; ⁴Centre for Sport Research, Deakin University, Warrn Ponds, Geelong, Australia; ⁵Department of Biomedical Engineering, University of Melbourne, Melbourne, Australia

email: fraser.francis-pester@anu.edu.au

INTRODUCTION

Increased scapulothoracic rhythm has been observed in pathological conditions affecting the glenohumeral joint and is thought to be a compensatory mechanism associated with reduced glenohumeral function [1, 2]. Studies have questioned whether scapula and humeral head kinematics may be pathologically coupled in patients with recurrent anterior glenohumeral instability, though this remains to be proven [3, 4]. To answer this question, which will provide a strong basis for diagnosing joint instability and predicting long-term joint function in these patient, this study aimed to employ open computed tomography (CT) to quantify *in vivo* scapulothoracic and glenohumeral joint positions in patients with recurrent anterior shoulder instability and healthy control subjects.

METHODS

Twenty patients with recurrent anterior instability (19 male, 1 female; mean age: 28 years; range: 19-49) were recruited for the study along with a further 5 healthy control subjects (4 male, 1 female; mean age: 39 years; range: 30-60). Shoulders of participants were imaged using Open CT (Balgrist University Hospital, Zürich) in six static positions: Neutral shoulder elevation and full external rotation, lift off position (hand touching one's back), 90° abduction, 90° flexion, maximum flexion, and 90° abduction with full external rotation (ABER).

Three-dimensional computer models of the scapula and proximal humerus were generated for each subject by digitally segmenting and reconstructing the CT scans of each participant for each shoulder position (Mimics, Materialise, Belgium). Anatomic scapular and humeral coordinate systems were defined in accordance with ISB recommendations to calculate scapulothoracic position in the scapular plane and humeral head position relative to the glenoid for each limb position. Independent sample t-tests were used to evaluate the differences between glenohumeral joint angle, scapulothoracic angle and glenohumeral-scapulothoracic ratios between patients with recurrent anterior instability and healthy controls, with significance level set at $p < 0.05$.

RESULTS AND DISCUSSION

The shoulder instability patients demonstrated significantly less glenohumeral abduction (mean difference: 13.30, 95% CI [0.82, 25.80], $p = 0.038$) and significantly increased upward scapulothoracic rotation compared to the control subjects (mean difference: 13.29, 95% CI [-25.74, -0.83], $p = 0.038$) when the upper limb was positioned in 90° abduction. Less overall humeral head translation was observed in instability patients compared to control subjects across all tasks, although none of the comparisons reached significance ($p > 0.05$).

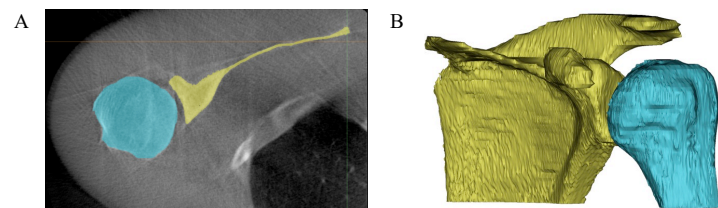


Figure 1: Segmentation of humerus (blue) and scapula (yellow) (A) and three-dimensional computer reconstruction (B) for analysis of glenohumeral and scapulothoracic position.

CONCLUSIONS

Patients with recurrent instability demonstrate significantly increased scapulothoracic angles during arm elevation, which patients may adopt to compensate for reduced glenohumeral joint motion. These findings suggest that the glenohumeral muscles ought to be a target for rehabilitation in patients with recurrent anterior instability. A novel method of measuring glenohumeral joint position using Open CT has also been described and may be useful for evaluating glenohumeral joint function in other joint conditions.

REFERENCES

1. Robert-Lachaine, X., et al., Journal of Shoulder and Elbow Surgery, 2016. **25**(10): p. 1616-1622.
2. Walker, D., et al., Journal of Shoulder and Elbow Surgery, 2015. **24**(7): p. 1129-1134.
3. Paletta, G.A., et al., Journal of Shoulder and Elbow Surgery, 1997. **6**(6): p. 516-527.
4. von Eisenhart-Rothe, R., et al., Clinical Orthopaedics and Related Research, 2005. **433**.



HIP FRACTURE AND DEMENTIA: PREVALENCE, CLINICAL PROFILE, IN-HOSPITAL OUTCOMES AND READMISSIONS

¹Kiran Rajesh, ²Wichat Srikusalanakul and ^{1,2,3}Alexander Fisher

¹ANU Medical School, Australian National University, Canberra, ACT, Australia

Departments of ²Geriatric Medicine and ³Orthopaedic Surgery, The Canberra Hospital, Canberra, ACT, Australia

email: Kiran.Rajesh@act.gov.au

INTRODUCTION

Dementia is traditionally thought to be associated with poor surgical outcomes, however, the literature regarding hip fracture (HF) repair is limited and inconsistent [1-4]. This study had three aims: 1) to determine the prevalence and clinical profile of HF patients with dementia; 2) to ascertain whether there are differences in outcomes between patients with and without dementia, and 3) to determine whether dementia affects the incidence of surgical and/or medical causes of readmissions.

METHODS

In 522 consecutive HF patients (mean age 82.2 ± 9.2 [SD] years, 70.7% females) admitted in 2017-2018, we analysed sociodemographic, clinical and laboratory data as well as in-hospital outcomes (mortality, inflammatory response, length of stay [LOS]) and readmissions (over a 6-month period). In total, 66 parameters were investigated. Statistical analyses including multivariate regressions has been performed using Stata software version 16 (USA)

RESULTS AND DISCUSSION

Of 522 HF patients, 132 (25.3%) were diagnosed with dementia. Patients with dementia, compared to the rest of the cohort, were significantly older ($+3.6$ years, $p < 0.0001$), more often living in a permanent residential care facility (PRCF, 73.5% vs. 14.0%, $p < 0.001$), using walking aids (34.6% vs. 25.9%, $p = 0.053$), and having anaemia (49.3% vs. 37.4%, $p = 0.015$), chronic kidney disease (CKD, 41.2% vs. 30.7%, $p = 0.025$), and hypoalbuminaemia (on average -5.9 g/L; < 33 g/L: 30.9% vs. 21.5%, $p = 0.026$), but were less likely to have vitamin D insufficiency (26.7% vs. 36.8%, $p = 0.033$), chronic obstructive pulmonary disease (COPD, 11.8% vs. 18.7%, $p = 0.062$), a history of smoking (7.4% vs. 19.0%, $p = 0.025$) or alcohol overuse (0.7% vs. 4.7%, $p = 0.033$). The prevalence of other chronic conditions such as cardiovascular (coronary artery disease [CAD], history of myocardial infarction, hypertension), cerebrovascular (stroke, TIA), Parkinson's, type 2 diabetes mellitus, as well as hip fracture type were similar in both groups. Postoperatively, more patients with dementia demonstrated a high inflammatory response (CRP > 150 mg/L: 59.8% vs. 45.1%, $p = 0.005$), but the LOS did not differ between the groups and the mortality rate in patients with dementia was not significantly higher (7.4% vs. 3.7%, $p = 0.084$). In the total cohort, independent risk factors for in-hospital death (after adjustment for age, gender, dementia, COPD, hyperparathyroidism [PTH > 6.8 pmol/L], high postoperative

inflammatory response and living in a PRCF) were CAD (OR 3.06, 95% CI 1.32-7.09, $p = 0.009$) and CKD (OR 2.55, 95% CI 1.05-6.18, $p = 0.039$). For HF patients with dementia, CAD was the only significant and independent prognostic factor for in-hospital death (OR 6.44, 95% CI 1.55-26.86, $p = 0.011$).

Within 6 months after HF repair, 100 (19.5%) of 512 discharged patients were readmitted; among them there were 31 (31%) individuals with dementia. The re-admitting rates in patients with and without dementia did not differ significantly (23.0% vs. 17.2%, $p = 0.148$), despite the patients with dementia being significantly older ($+5.1$ years, $p = 0.004$) and the majority above 80 years of age (87.1% vs. 65.2%, $p = 0.024$). The causes of readmissions were mainly medical (87%) and similar in both groups; the most common were genitourinary infection (19%), falls (18%), chest infection (15%), and gastrointestinal diseases (13%). CKD was the only significant risk factor for readmission (OR 1.59, 95% CI 1.02-2.48, $p = 0.044$), but this characteristic lost its prognostic value after adjustment for age and gender (OR 1.45, 95% CI 0.91-2.32, $p = 0.107$). Surgical causes contributed to 13% of readmissions ($n = 13$), the need for surgical correction ($n = 6$) being the most common reason. Postoperatively, patients with dementia, compared to non-demented subjects, more often developed a haematoma and wound infection (6.5% vs. 0.0%, $p = 0.033$) requiring readmission.

CONCLUSIONS

About 25% of elderly HF patients had a diagnosis of dementia; although this group is significantly older, more often anaemic, malnourished, and have CKD, the LOS, rates of in-hospital mortality and re-admission are similar to those without dementia, indicating that dementia *per se* may not predict poor outcome.

ACKNOWLEDGEMENTS

This research was not funded.

REFERENCES

1. Morioka N, et al., *PloS one*. **16**: e0249364, 2021
2. Delgado A, et al., *Injury*. **51**: S19-S24, 2020
3. Fisher A, et al., *J Trauma Manag Outcomes*. **6**: 1-12, 2012
4. Rasu R, et al., *BMC Geriatr*. **20**: 1-9, 2020



PREOPERATIVE KINEMATICS INFLUENCES POSTOPERATIVE KINEMATICS OF THE KNEE. A PROSPECTIVE RANDOMISED CLINICAL TRIAL OF TOTAL KNEE ARTHROPLASTY.

¹ Pouya Saeedian, ² Joe Lynch ² Diana Perriman, ^{2,3} Mark Pickering, ² Paul Smith, ^{1,2} Jennie Scarvell

¹ Faculty of Health, University of Canberra, Canberra, ACT, Australia

² Trauma and Orthopaedic Research Unit, Canberra Hospital, Canberra, ACT, Australia

³ School of Engineering and Information Technology, University of NSW, NSW, Australia

email: Pouya.saeedian@outlook.com

INTRODUCTION

Regaining postoperative kinematics is an important postoperative outcome after total knee arthroplasty (TKA) [1]. Preoperative maximum flexion is known to correlate with postoperative maximum flexion [2]. However, the influence of other preoperative kinematic factors on postoperative TKA kinematics has not been established.

METHODS

This longitudinal study recruited 68 participants who had been randomised prior to total knee arthroplasty to receive cruciate retaining fixed bearing (CR-FB), cruciate retaining rotating platform (CR-RP) or posterior stabilised fixed bearing (PS-FB) implants. Participants were imaged pre and postoperatively using single-plane fluoroscopy while kneeling into full flexion from 90° and with computed tomography preoperatively..

Shape-matching 2D-3D registration was used to register the native knee (CT) and implant (computer aided design) to the fluoroscopy frames preoperatively and at two years follow-up postoperatively. Only 55 participant's data were available for analysis at two years. Analysis included multivariate regression models and Pearson's correlation coefficients.

RESULTS AND DISCUSSION

Overall postoperative flexion during kneeling was less at 2 year follow-up but not significantly ($p=0.06$).

Postoperative maximum flexion was associated with preoperative maximum flexion ($r=0.58$, $p<0.001$) for the cohort overall (Figure 1). Similar associations were found for each implant group: CR-FB ($r=0.61$, $p<0.006$), CR-RP($r=0.60$, $p<0.009$) and PS-FB($r=0.58$, $p<0.01$). Pre and postoperative anterior-posterior translation were associated for both the descending and ascending phases of kneeling. For descending the cohort strength of association was $r=0.70$, $p<0.001$; and for each implant group: CR-FB ($r=0.69$, $p<0.001$), CR-RP ($r=0.81$, $p<0.001$) and PS-FB ($r=0.81$, $p<0.001$). For the ascending phase the association for the cohort was $r=0.70$, $p<0.001$; and for each implant group: CR-FB ($r=0.60$, $p<0.001$); CR-RP ($r=0.70$, $p<0.001$) and PS-FB ($r=0.78$, $p<0.001$).

Preoperative maximum flexion was the strongest predictor of postoperative maximum flexion (Beta=0.5, $p<0.001$). The adjusted model predicted that for every 1° of preoperative maximum flexion, there was a relative increase of 0.5° of

postoperative maximum flexion plus a constant of 61 degrees. Preoperative anterior-posterior translation was the second strongest predictor of postoperative maximum flexion (Beta=0.7, $p<0.001$). The adjusted model indicated that for every 1 mm of preoperative anterior-posterior translation there was a 0.7° increase in postoperative maximum flexion plus a constant of 122 degrees.

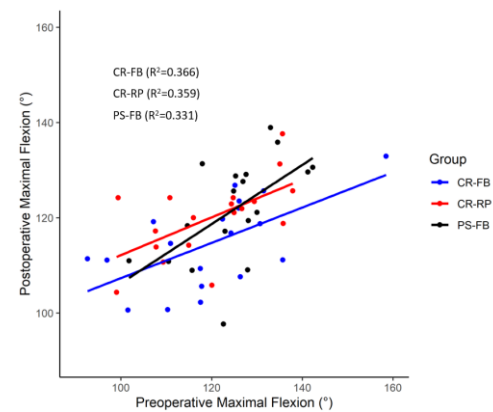


Figure 1: Associations between preoperative and postoperative maximum flexion.

CONCLUSIONS

This study confirmed that greater preoperative flexion during kneeling predicts greater postoperative flexion with an additional 0.5 degrees for every preoperative degree. Similarly, anterior-posterior translation was an important predictor of post-op flexion. However, post-op flexion during kneeling in this cohort was not increased overall compared to preoperative. The distribution of the data (Figure 1) supports previous findings that knees with low preoperative flexion improve more than knees with a good preoperative flexion [1]. There were no important differences between TKA designs indicating that it is probably the person and not the implant which predicts kinematic outcomes.

ACKNOWLEDGEMENTS

This research has received financial support from Zimmer Biomet Pty Ltd.

REFERENCES

1. Wimmer MA, *Biomed Res Int.* 2015;2015:157541-157541.
2. Ritter MA, *J Bone Joint Surg Am.* 2003;85(7):1278-1285.

CONFLICT OF INTEREST DECLARATION

In the interests of transparency and to help reviewers assess any potential bias, all authors of original research papers are required to declare any competing commercial interests in relation to the submitted work. Referees are also asked to indicate any potential conflict they might have reviewing a particular paper.

If you have accepted any support such as funds or materials, tangible or intangible, concerned with the research by the commercial party such as companies or investors, choose YES below, and state the relation between you and the commercial party.

If you have not accepted any support such as funds or materials, choose NO.

Do you have a conflict of interest to declare?

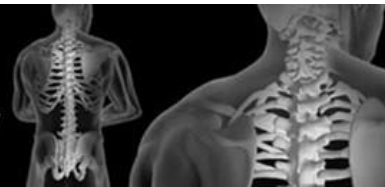
YES

If YES, please complete as appropriate:

1. A commercial entity paid or directed, or agreed to pay or direct, any benefits to any research fund, foundation, educational institution, or other charitable or nonprofit organization with which the authors are affiliated or associated.



Australian & New Zealand
Orthopaedic Research Society



DAY 2

POSTERS



DELAYED FRACTURE HEALING IN ZUCKER DIABETIC FATTY (ZDF) RATS IS ASSOCIATED WITH PERSISTENT UP-REGULATED PRO-INFLAMMATORY MARKER EXPRESSION

¹Jonghoo Sung, ²Gerald J. Atkins, ³Paul H. Anderson, ⁴Chantal Chenu, ⁵Ines Reichert, ¹Stephen M. Pederson and ⁶Peter J. Smitham

¹Adelaide Medical School, The University of Adelaide, Adelaide, SA, Australia

²Centre For Orthopaedic and Trauma Research, The University of Adelaide, SA, Australia

³Clinical and Health Sciences, University of South Australia, Adelaide, SA, Australia

⁴Department of Comparative Biomedical Sciences, The Royal Veterinary College, London, United Kingdom

⁵Department of Trauma and Orthopaedic Surgery, King's College Hospital, London, United Kingdom

⁶Orthopaedic and Trauma Service, The Royal Adelaide Hospital, Adelaide, SA, Australia

email: a1695343@student.adelaide.edu.au

INTRODUCTION

Type 2 Diabetes Mellitus (T2DM) is associated with increased fracture risk, interference with bone formation, and impairment and delay in fracture healing [1,2] Little is currently known regarding gene expression associated with impaired fracture healing in T2DM. The aim of this study was to identify the gene expression profile associated with delayed fracture healing in the Zucker Diabetic Fatty (ZDF) rat model.

METHODS

Zucker rats, 6 wild-type (WT) and 6 homozygous for leptin receptor mutation (ZDF), were raised on a high fat diet to induce T2DM in the ZDF animals. Open femoral fractures were simulated using osteotomy in one femur of each animal and stabilised with an external fixator. Animals were culled at 4 weeks post-surgery and the fractured and unfractured femurs were harvested. Radiographs were taken of all specimens and 3 whole callus per group were assessed for gene expression using mRNA sequencing (RNA-Seq).

RESULTS AND DISCUSSION

Radiographs and histology clearly demonstrated delayed fracture healing in ZDF rats. RNA-Seq revealed 1002 genes that were differentially expressed (DE). Using a false discovery rate threshold of 20.0% identified 18 genes as DE, 16 being upregulated in ZDF rats, while two, *Pnpla2* (logFC -7.193) and *Rcor2* (logFC -5.115), were downregulated. Upregulated genes included proinflammatory genes such as *Il6*, *Mmp3* and *Cxcl1* (Figure 1) (Table 1).

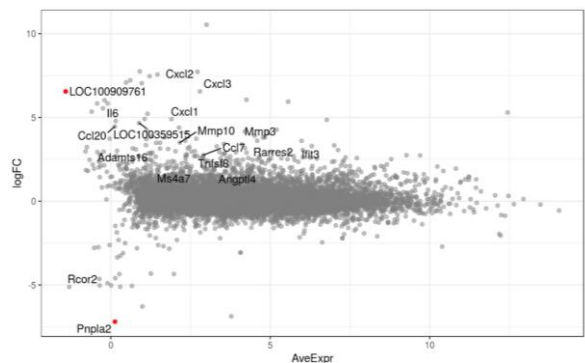


Figure 1: RNA Seq dot plot showing average gene expression as a function of log fold-change in ZDF rats compared to non-diabetic controls. Confidently significant genes (FDR <0.05) are indicated in red, whilst others are labelled to an FDR of 20.0%.

CONCLUSIONS

Using an unbiased mRNA sequencing approach, our study identified 16 genes that were upregulated in ZDF fracture samples, including proinflammatory genes *Il6*, *Mmp3* and *Cxcl1*, among others, with the *Rcor2* and *Pnpla2* were downregulated. These findings may be utilised as potential biomarkers and/or therapeutic targets to monitor and treat delayed fracture healing in diabetic patients.

ACKNOWLEDGEMENTS

This research was partly funded by Joint Action from the British Orthopaedic Association.

REFERENCES

1. Compston, *J intern Med.* **283**:140-153, 2018.
2. Napoli, et al., *Nat Rev Endocrinol.* **4**:208-219, 2016.

Table 1: Top 3 most highly ranked genes when sorting by p-value. This represents an FDR of up to 20.0%. logFC >0 indicates upregulation in diabetic samples relative to control.

Name	logFC	AveExpr	T value	P value	FDR
<i>Pnpla2</i>	-7.193	0.1297	-13.05	3.334e-06	0.02846
LOC100909761	6.555	-1.417	12.52	4.326e-06	0.02846
<i>Mmp10</i>	3.502	2.164	8.791	3.768e-06	0.1653

LATERAL FENESTRATION OF LUMBAR INTERVERTEBRAL DISCS IN RABBITS: DEVELOPMENT AND CHARACTERISATION OF A PRECLINICAL MODEL

¹James D. Crowley, ¹Matthew H. Pelletier, ¹Rema A. Oliver, ¹Tian Wang and ¹William R. Walsh

¹Surgical and Orthopaedic Research Laboratories, UNSW Sydney

email: james.crowley@unsw.edu.au

INTRODUCTION

Intervertebral disc degeneration (IVDD) is common to dogs and humans; Zoobiquity. Hansen Type 1 IVDD, common in chondrodystrophic dog breeds, is characterised by chondroid metaplasia of the nucleus pulposus. Extrusion of nucleus material into the vertebral canal causes compression and/or contusion of the spinal cord and subsequent neurological dysfunction.

Fenestration is the surgical removal of the nucleus pulposus via annulotomy. Multiple veterinary studies strongly support the prophylactic effect of fenestration in dogs with previous episodes of symptomatic IVDD [1]. In humans, fenestration discectomy, is the most common spinal surgical procedure for symptomatic lumbar disc herniation [2]. There is a paucity of veterinary and human literature describing the biological and biomechanical implications of fenestration. Therefore, the objective of this study was to develop and characterise a preclinical rabbit model of lateral fenestration of lumbar IVDs to 1) investigate the biological and biomechanical effect of fenestration in dogs and humans and 2) develop a preclinical rabbit model of human IVDD.

METHODS

In vitro: The surgical technique of lateral lumbar IVD fenestration (L2/3, L3/4, L4/5) was developed using New Zealand White (NZW) Rabbit cadavers (n=6) weighing 3.5-4.5kg. Briefly, a left lateral approach to each lumbar disc was performed by a muscle splitting approach through the transverse abdominis, external abdominal oblique and internal abdominal oblique muscles. Next, the psoas muscle was retracted ventrally (Fig 1) from the vertebral transverse process(es) to expose the IVD.

Fenestration was performed by making a 1.5 x 2mm window in the lateral annulus and removing the nucleus pulposus with a spinal curette. The soft tissues were closed routinely.

In vivo: Single level (L2/3; n=12) and multi-level (L2/3, L3/4, L4/5; n=12) fenestration was performed in vivo in skeletally mature NZW rabbits (n=24 total). Rabbits were culled at 6- and 12-week timepoints. Endpoint analysis included pre-operative and

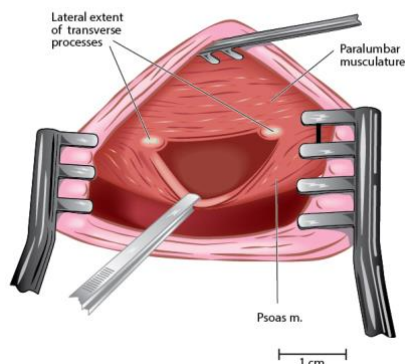


Figure 1: Ventral retraction of the psoas muscle to expose the lumbar intervertebral disc (IVD).

cull bloodwork, high-resolution faxitron radiography, micro-CT, micro-MRI, biomechanical robotic range of motion and histology.

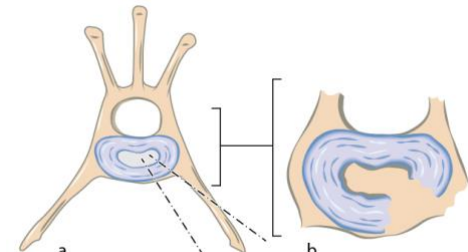


Figure 2: Working angle for left lateral/ventrolateral fenestration of the lumbar IVD

RESULTS AND DISCUSSION

The surgical technique of lateral fenestration of lumbar IVDs was developed in vitro and successfully extrapolated to the in vivo setting. The procedure was well-tolerated by all rabbits, with all rabbits surviving the procedure and reaching their respective timepoints. The lateral approach allowed for sufficient depth of the fenestration into the nucleus pulposus to ensure maximal nucleus pulposus was retrieved. No post-operative complications were observed.

Mean surgical time was 30.8 +/- 19 mins and 41.5 +/- 9.6 mins for the single level and multi-level fenestration groups respectively. Faxitron radiography and micro-CT revealed significant biological osseous reactions at all treated levels at both timepoints. Micro-MRI demonstrated marked loss of the normal nucleus pulposus T2 hyperintensity at all treated sites compared to intact IVDs. Biomechanical robotic range of motion was significantly reduced in operated animals compared to intact in vivo specimens.

CONCLUSIONS

We describe an in vitro and in vivo preclinical rabbit model of lateral fenestration of lumbar IVDs. Veterinary surgeons should consider biological and biomechanical implications of prophylactic fenestration in their canine patients. The described technique represents a suitable preclinical model that could be utilised to evaluate new treatment strategies, including nucleus pulposus augmentation strategies for IVDD in humans.

ACKNOWLEDGEMENTS

The authors thank Marcus Cremonese for the anatomical illustrations and Rebekah Smith and James O'Connor for animal husbandry, and anaesthesia duties.

REFERENCES

1. Jeffery, N.D. and Freeman, P.M., 2018. The role of fenestration in management of type I thoracolumbar disk degeneration. *VCNA* **48**(1), pp.187-200.
2. Hamawandi, S.A., et al 2020. Open fenestration discectomy versus microscopic fenestration discectomy for lumbar disc herniation: a randomized controlled trial. *BMC Musculoskeletal Disorders*, **21**(1), pp.1-11.



IN VIVO KINEMATICS OF THE SCAPHOID IN SCAPHOLUNATE INSTABILITY USING 4D-CT PRELIMINARY RESULTS

¹Melanie Amarasooriya, ²Rami Al-Dirini, ¹Kimberley Bryant and ¹Gregory Bain

¹College of Medicine and Public Health, Flinders University, Adelaide, SA, Australia

²Medical Device Research Institute, College of Science and Engineering, Flinders University, Adelaide, SA, Australia

email: amar0041@flinders.edu.au

INTRODUCTION

Scapholunate instability is the most common carpal instability. In vivo kinematics of the scaphoid in scapholunate instability (SLI) is only studied using quasi-static models [1]. Dynamic CT provides a better understanding of wrist instabilities and impingement [2].

METHODS

The study sample included 08 4D CT scans of wrists with SLI and 03 scans of healthy wrists. Analyzed motion sequences were wrist radioulnar deviation (RUD) and flexion and extension.

Images were analyzed using 3D slicer and MATLAB_R2020b. Image segmentation, registration and transformation matrix were used to calculate the displacement of the scaphoid in relation to the neutral wrist position.

Primary outcome measures were

1. Rotations (Euler angles) and translations of the scaphoid with reference to the radius
2. Contribution of the scaphoid to the global wrist motion
3. The joint proximity of the radio scaphoid joint during wrist motion

RESULTS AND DISCUSSION

During wrist radioulnar deviation, the scaphoid had more radioulnar deviation than flexion. (RUA=28.5°±8.6° and Flexion =20.8°±3.7°, $P=0.037$)

During extension of the wrist, the scaphoid had more pronation compared to the healthy wrist. (11.8°±5.17°, $P=0.023$)

The scaphoid in-plane motion contributed 67% (+/-1) to the RUD of the wrist and 88% (+/-6) to the flexion and extension of the wrist.

During wrist extension, joint proximity analysis demonstrated abnormal radio scaphoid proximity at the radial styloid region (Fig1).

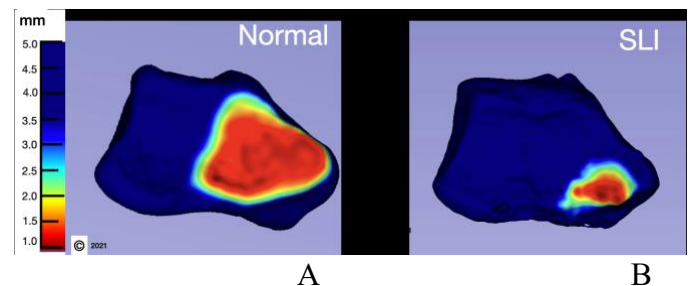


Figure 1: Changes in radio scaphoid joint proximity during wrist extension. A. Normal wrist. B. SLI wrist. Note the joint proximity in the radial styloid region during wrist extension in SLI (B).

CONCLUSIONS

4D CT can be used as an objective and reproducible method of studying kinematics in SLI.

There was more in-plane motion of the scaphoid than out of plane motion during wrist radioulnar deviation.

Extension of the wrist worsened the rotational malalignment of the scaphoid and led to abnormal radio scaphoid joint proximity in SLI.

ACKNOWLEDGEMENTS

NA

REFERENCES

1. Omori S et al. In vivo 3-dimensional analysis of dorsal intercalated segment instability deformity secondary to scapholunate dissociation: a preliminary report. *J Hand Surg Am.* **2013**;**38**(7):1346-55.
2. Carr R et al. Four-Dimensional Computed Tomography Scanning for Dynamic Wrist Disorders: Prospective Analysis and Recommendations for Clinical Utility. *J Wrist Surg.* **2019**;**8**(2):



DESIGN WORKFLOW FOR 3D PRINTABLE PATIENT-SPECIFIC VORONOI BONE SCAFFOLDS

Buddhi Herath^{1,2,4}, Sinduja Suresh^{1,2}, Beat Schmutz^{1,2,4}, J. Paige Little^{1,2,3}, Prasad KDV Yarlagadda^{1,2}, Mark A. Knackstedt^{1,5}, Dietmar W. Hutmacher^{1,2}, Marie-Luise Wille^{1,2}

¹ARC Training Centre for Multiscale 3D Imaging, Modelling, and Manufacturing, Brisbane, Australia

²School of Mechanical, Medical, and Process Engineering, Faculty of Engineering, QUT, Brisbane, Australia

³Biomechanics and Spine Research Group, Centre for Children's Health Research, School of MMPE, QUT, Brisbane, Australia

⁴Jamieson Trauma Institute, Metro North Hospital and Health Service, Brisbane, Australia

⁵Research School of Physics, Department of Applied Mathematics, The Australian National University, Canberra, Australia
email: b.herath@qut.edu.au

INTRODUCTION

The Voronoi structure is gaining popularity within the bone tissue engineering community to develop bone scaffolds, given its close resemblance to trabecular bone. Bone scaffold meshes designed for 3D printing should possess certain qualities such as being manifold and closed. This paper presents a semi-automated generative design workflow to design Voronoi bone scaffolds based on a CT imaged bone defect, including the fixation flanges if required. The output design is closed and manifold, which does not need any further mesh repairing operations, thereby making it readily 3D printable.

METHODS

Aside from the image segmentation step, the core design workflow is set up in the software *Rhinoceros 3D* along with its visual programming module *Grasshopper*. Based on the OpenVDB [1, opendb.org] library and the *Grasshopper* plugin Dendro (ecrlabs.com/dendro), a custom plugin was developed in-house for *Grasshopper* that uses signed distance fields to represent and manipulate a geometry implicitly.

The DICOM data is segmented with a suitable medical image processing software, and the 3D reconstructed mesh of the bone defect is exported in STL format. This is imported into *Rhinoceros 3D* and by using Boolean operations, SUB-D functions and the in-house developed plugin, a solid geometry of the scaffold region including the fixation flanges is constructed manually (Figure 1.1). Within *Rhinoceros 3D*, "Surface" geometries are created to demarcate the fixation flanges that are to remain solid (Figure 1.2) and are assigned to the respective node in the *Grasshopper* workflow, which will be used to split the mesh. Once the number of Voronoi seed points is selected using a number slider, they will be randomly distributed within the region (Figure 1.3) and the geometry will be partitioned into Voronoi cells (Figure 1.4). The edges of these cells and the curve intersections of the split mesh are isolated (Figure 1.5), and a level set is wrapped around them to form a solid lattice. Using implicit Boolean operations, the pores of the scaffold (Figure 1.6) and the porous lattice (Figure 1.7) and are created, converted back to a closed manifold mesh and 3D printed (Figure 1.8). Finally, the porosity, surface area of the scaffold and the effective pore diameters are computed.

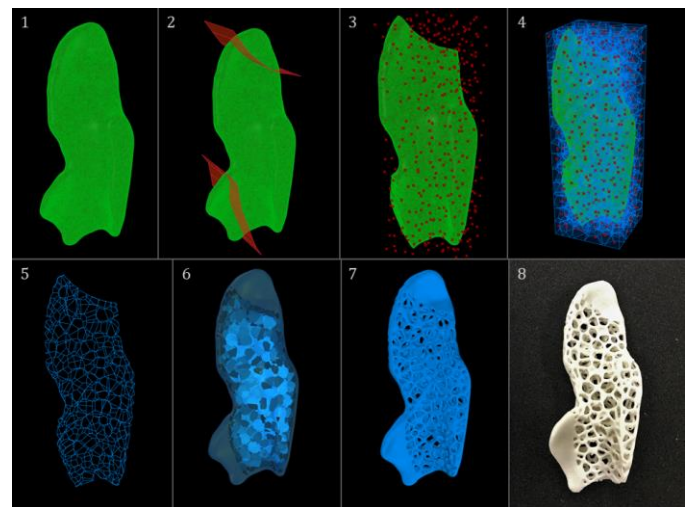


Figure 1: Steps of the workflow. 1) Solid scaffold geometry. 2) Surfaces demarcating the flanges. 3) Voronoi seed points. 4) Voronoi Cells. 5) Curves intersected with the geometry. 6) Pores of the scaffold. 7) Porous scaffold. 8) 3D printed sample.

RESULTS AND DISCUSSION

The resultant mesh is a closed manifold mesh that does not need any mesh repairing operations prior to 3D printing. The implicit Boolean operations are computationally fast and robust. Once setup, the workflow functions as a semi-automated process where any variable such as the strut diameter, number of seed points, demarcations of the fixation flanges, scaffold geometry, etc. can be changed by the user and the generative workflow will regenerate the design accordingly.

CONCLUSIONS

The developed generative design workflow uses signed distance fields to efficiently design patient-specific Voronoi bone scaffolds that are readily 3D printable.

ACKNOWLEDGEMENTS

This work was supported by the ARC ITTC for Multiscale 3D Imaging, Modelling, and Manufacturing [IC 180100008], and the Jamieson Trauma Institute.

REFERENCES

1. K. Museth, ACM Trans. Graph., vol. 32, no. 3, 2013.



DOUBLE SCREW FIXATION IN AN UNSTABLE SCAPHOID FRACTURE MODEL: A BIOMECHANICAL COMPARISON OF TWO SCREW CONFIGURATIONS

Lachlan S. Huntington^{1,3,4} BSc (Hons), MD ;Carsten Surke^{2,3} MD; Xin Zhang⁴ BEng;

Eugene Ek^{3,5} MBBS PhD; David Ackland⁴ PhD; Stephen Tham^{3,5,6} MBBS

¹Department of Surgery, Western Health, Footscray, Victoria, Australia

²Department of Plastic and Hand Surgery, Inselspital, University Hospital Bern, University of Bern, Switzerland

³Hand and Wrist Biomechanics Laboratory, O'Brien Institute, Fitzroy, Victoria, Australia

⁴Department of Biomedical Engineering, University of Melbourne, Parkville, Victoria, Australia

⁵Division of Hand Surgery, Department of Orthopaedic Surgery, Monash University, Dandenong Hospital, Dandenong, Australia

⁶Department of Plastic and Hand Surgery, St Vincent's Hospital, Fitzroy, Victoria, Australia

email: lachlanhuntington@gmail.com

INTRODUCTION

While there is evidence that a single headless compression screw is sufficient for fixation of most scaphoid fractures¹, double screw osteosynthesis has been shown to result in higher failure strength and stiffness compared to that of a single screw². However, the biomechanical effect of different screw configurations has not been determined.

METHODS

A standardized unstable fracture model was produced in 28 cadaveric scaphoids. Specimens were randomly allocated to one of two fixation groups using two internal compression screws positioned in either the sagittal or coronal planes. A subject-specific 3D printed customized screw placement and osteotomy device was developed using computer-aided design generated models derived from computed tomography scan data of each individual scaphoid (Figure 1). Load to failure and stiffness of the repair constructs was evaluated using a mechanical testing system.

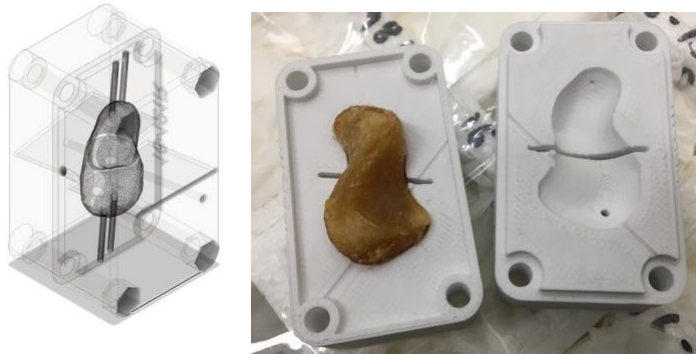


Figure 1: LEFT: 3D model of scaphoid sitting within osteotomy jig. RIGHT: Hemisections of 3D printed custom osteotomy and screw placement jig with accompanying 3D cadaveric scaphoid.

RESULTS AND DISCUSSION

There were no significant differences in the size, weight and density between the scaphoid specimens. The average distance between screws was significantly greater in the sagittal group than in the coronal group. There were no significant differences in load to 2 mm displacement (mean coronal 180.9 N \pm 109.7, mean sagittal 156.0 N \pm 85.8), load to failure (mean coronal 275.9 N \pm 150.6, mean sagittal 248.0 \pm 109.5), stiffness (mean coronal 111.7 N/mm \pm 67.3, mean sagittal 101.2 N/mm \pm 45.1) and energy absorption (mean coronal 472.6 mJ \pm 261.4, mean sagittal 443.5 mJ \pm 272.7), between the coronal and sagittal aligned double screws ($p > 0.05$).

CONCLUSIONS

There are no significant biomechanical differences between the sagittal or coronal aligned double headless compression screws in a scaphoid fracture model with bone loss. In cases where double screw fixation of the scaphoid is considered, placement of double screws can be at the discretion of the surgeon, and be dictated by ease of access, surgical preference and fracture orientation.

ACKNOWLEDGEMENTS

The authors would like to acknowledge Medartis for the generous donation of screws for use in this study.

REFERENCES

1. McCallister WV, Knight J, Kaliappan R, Trumble TE. Central placement of the screw in simulated fractures of the scaphoid waist: a biomechanical study. *J Bone Joint Surg Am.* 2003;85(1):72-77. doi:10.2106/00004623-200301000-00012
2. Mandaleson A, Tham SK, Lewis C, Ackland DC, Ek ET. Scaphoid Fracture Fixation in a Nonunion Model: A Biomechanical Study Comparing 3 Types of Fixation. *J Hand Surg.* 2018;43(3):221-228. doi:10.1016/j.jhsa.2017.10.005



HIGH TIBIAL OSTEOTOMY AND DISTAL FEMORAL OSTEOTOMY USING PATIENT-SPECIFIC INSTRUMENTS: PILOT DATA FROM A BIOMECHANICAL STUDY OF THE LOWER LIMBS, PELVIS AND LUMBAR SPINE

¹Hugo Wiggins, ²William Lu, ³Mustafa Alttahir ^{2,3}Munjed Al Muderis, ¹Richard Appleyard, ¹Joseph Cadman, ¹Dane Dabirrahmani
¹Department of Biomedical Sciences, Faculty of Medicine, Health and Human Sciences, Macquarie University, Sydney, NSW, Australia
²Osseointegration International, North Ryde, Sydney, NSW, Australia
³Macquarie University Hospital, Macquarie University, Sydney, NSW, Australia
 Email correspondence to: hugo.wiggins@hdr.mq.edu.au

INTRODUCTION

The high tibial osteotomy (HTO) and distal femoral osteotomy (DFO) are common surgical procedures for the treatment of varus/valgus (VV) lower limb malalignment and/or unilateral knee osteoarthritis [1]. HTO/DFO using patient-specific instruments (PSI) is a novel technique aiming to increase surgical accuracy and reduce complications [2], yet, an Australian study of this technique has not been conducted. Furthermore, effects on pelvic and spinal alignment following HTO/DFO has received insufficient attention in the literature, despite similar studies showing changes after total knee and total hip replacements. We hypothesise that the PSI approach will achieve post-operative alignment within 4° of the planned correction. We also hypothesise that changes (towards nomological values) in pelvic and spinal alignment in the coronal and sagittal planes will be observed post-operatively.

METHODS

Patients undergoing HTO/DFO procedures with the lead surgeon (MA) were invited to participate in this study. Full-spine EOS scans were taken pre and twelve-weeks post-operatively (Figure 1), and analysed on IntelViewer (Intelrad, Montreal, Quebec, Canada). The fifteen measurements of interest are: hip-knee-ankle angle (HKA); functional leg length; anatomical femur length; anatomical tibia length; anatomical leg length; mechanical medial proximal tibial angle; mechanical lateral distal femoral angle; knee joint line convergence angle; pelvic obliquity (PO); lumbar scoliosis; tibial slope; knee flexion angle (KFA); sacral slope (SS); pelvic tilt; lumbar lordosis. These measurements represent a comprehensive biomechanical assessment to determine the effects of HTO/DFO on the lower-limbs, pelvis and spine. This study has been ethically approved by the Macquarie University Human Research Ethics Committee (RE: 52021982328611).

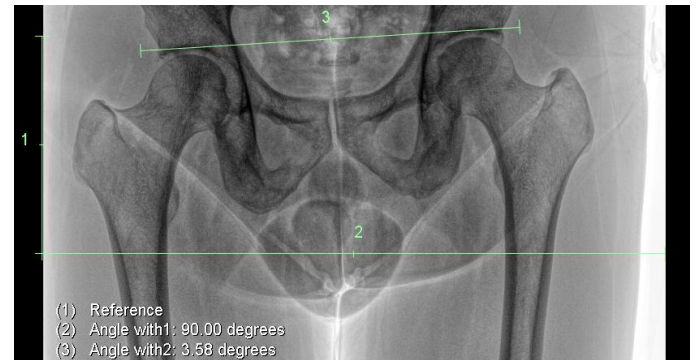


Figure 1: Example of measurement method showing pelvic obliquity of 3.58 degrees

RESULTS AND DISCUSSION

Pilot testing involved five participants and four measurements of interest: HKA; PO; KFA; SS (Table 1). Average HKA correction error of 2.70° was seen. Changes towards nomological values in PO, KFA and SS were also observed, highlighting the positive effects of correcting VV knee malalignment beyond the knee. This excluded one outlier that involved a 14.77° increase to SS post-operatively, which suggested incorrect patient stance during imaging acquisition.

CONCLUSIONS

The HTO/DFO using PSI is an accurate, safe and effective technique for VV knee correction. Pelvic changes appear minimal, yet positive, and are sensitive to change if imaging protocols are not strictly adhered to.

REFERENCES

1. Abramoff B, et al., *Medical Clinics*. **104**:293-311, 2020.
2. Victor J and Premanathan, *The Bone and Joint Journal*. **95**: 153-8, 2013.

Table 1: Hip-knee-ankle angle error and pre/post-operative alignment changes

Case	Hip-knee-ankle angle error (°)	Pelvic obliquity (°)	Knee flexion angle (°)	Sacral slope (°)
1	4.66	1.29	2.07	1.48
2	3.54	1.28	1.48	1.38
3	0.35	0.87	0.86	14.77
4	3.18	2.31	5.57	2.92
5	1.8	1.38	8.77	2.03
Averages	2.70	1.42	3.75	4.52



BIOMECHANICAL IMPROVEMENTS IN GAIT FOLLOWING MEDIAL PIVOT KNEE IMPLANT SURGERY

¹Sara Farshidfar, ¹Joseph Cadman, ¹Hamed Shahidian, ²Lauren Kark, ³James Sullivan, ¹Richard Appleyard and ¹Danè Dabirrahmani

¹Faculty of Medicine, Health and Human Sciences, Macquarie University, Sydney, NSW, Australia

²Graduate School of Biomedical Engineering, UNSW, Sydney, NSW, Australia

³Macquarie University Hospital, Sydney, NSW, Australia

email: sara.farshidfar@hdr.mq.edu.au

INTRODUCTION

Total knee replacements (TKRs) are designed to be functional, whilst ensuring comfort [1] with successful results in providing pain relief, correct deformity and basic mobility and stability to patients. However, despite improvements in designing the TKR implants, knee instability, abnormal feeling [2] and patient dissatisfaction [3] has been reported. Alteration of the knee articular geometry after TKR may result in kinematic changes in the biomechanical behaviour of the knee joint [4]. This unnatural biomechanics has the potential to lead to long-term failure. In an effort to improve knee biomechanics in TKR patients, some designs have focused on altering the articular surface geometries to encourage medial pivoting, such as the medial stabilising knee implants [5]. Therefore, this study used gait analysis to investigate the knee kinematics & kinetics of a medially stabilising knee, comparing it to a healthy control group, as well as to its pre-operative state. It was hypothesised that the TKR knees would experience moments which are similar to healthy (asymptomatic) controls.

METHODS

This study recruited two cohorts of participants: TKR patients (n=13) and an age-matched healthy control cohort (n=8). The TKR patient cohort included patients who were assessed as having late-stage knee osteoarthritis (OA) and scheduled for primary TKA with a medially stabilising knee implant (GMK Sphere, Medacta Int.), all operated on by a single surgeon (JS). Patients participated at two time-points: once 4-6 weeks prior to surgery and again at the 12 months post-surgery time point. For data collection, participants performed walking barefoot at a comfortable, self-selected speed in the gait laboratory. Kinematic data was collected using an 8 camera Vicon motion capture system (Vicon, Oxford, UK) and kinetic data was collected using three force platforms (Kistler, Winterthur, Switzerland).

For each patient, the knee joint moments in the sagittal, frontal and transverse planes during stance phase were computed for every pre and post op trial in Opensim [6] using a modified version of Gait 2392 model, and then averaged for each condition. Joint angles and joint moments were evaluated using Statistical Parametric Mapping (SPM) which is based on Random Field Theory [7] and validated for 1D data [8]. A SPM one-way-ANOVA was performed to determine whether there was a difference between the pre-operative and post-operative joint angles and moments, as well as post-operative results and the healthy, control cohort.

RESULTS

The TKA group showed a marked increase in the peak flexion moment when compared to their OA time-point (Figure 1A), aligning closely with the control group. The peak extension moment for the TKA group was also very different to the OA time-point, but even more so when compared to the control group, which was statistically significant (p=0.033). As expected, higher knee adduction moments (KAM) were generally observed in the OA cohort. A significant difference (p=0.043 and p=0.04) was observed for both the 1st and 3rd KAM peaks during stance phase when comparing the OA vs TKA groups (Figure 1B). The peak internal rotation moment was significantly different between both the OA vs TKA (p=0.32) (Figure 1C) and between the TKA vs control (p=0.039).

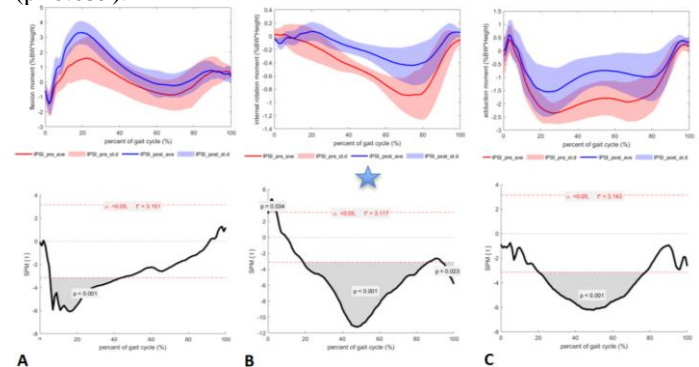


Figure 1: Average \pm SD knee joint moments in A) sagittal, B) transverse, and C) frontal planes for walking.

CONCLUSIONS

This study found the medial stabilising TKR to produce knee moments closer to that of a healthy knee, compared with an osteoarthritic knee, in both the sagittal and coronal planes. The increase in knee flexion moment after surgery suggest an improved ability to load the knee joint, as is evident in confidence shown by patients when they present for their post-operative data collection. This data suggests that medially stabilised TKR implants has features which assist in loading the joint more naturally.

ACKNOWLEDGEMENTS

Authors would like to acknowledge research funding from Medacta International and Macquarie University.

REFERENCES: [1] Feng et al 2018; [2] Nam et al 2014; [3] Bourne et al 2010; [4] Dunbar et al 201 ; [5] Fan et al 2010; [6] Delp et al 2007 ; [7] Flandin et al 2008 ; [8] Pataky et al 2016



THE EFFECT OF SPINE CAGE POSITION ON THE MECHANICAL RESPONSE OF THE SUPERIOR LUMBAR ENDPLATE AFTER LUMBAR INTERBODY FUSION

¹Yihang Yu, ¹Dale Robinson, ¹David Ackland, ¹Yi Yang, ²Eric Bert, ¹Peter Vee Sin Lee

¹Department of Biomedical Engineering, The University of Melbourne, Melbourne, VIC, Australia

²3DMediTech, Melbourne, VIC, Australia

email: yihangy@student.unimelb.edu.au

INTRODUCTION

Lumbar interbody fusion (LIF) with interbody cages is an established treatment for lumbar degenerative disc disease. However, the use of interbody cages may result in complications such as cage migration and subsidence. Previous studies of surgical outcomes of LIF have shown that rates of post-operative complications can be influenced by interbody cage positioning [1]. This study aims to evaluate the effect of cage positioning on the mechanical response of superior lumbar endplate using a spine finite element (FE) model.

METHODS

Computed tomographic (CT) scans of a healthy male subject (18 years old) was used to develop a FE model of the L5 vertebra. The 3D geometry of the vertebra was reconstructed in Mimics 21.0 software, and the model was meshed with tetrahedral elements (HyperMesh 2017). The meshed model was imported into a FE modelling software package (Abaqus CAE 2017) and the material properties of the vertebra were assigned based on the Hounsfield units (HU) of the CT scans [2]. The interbody cage in the model was based on a kidney-shaped Polyether-ether-ketone (PEEK) cage. The cage was meshed in tetrahedral elements and assigned material properties of PEEK. The cage was placed in four different positions on the superior endplate of L5 (Figure 1a). The interface between the cage and endplate was simulated by surface-to-surface contact [3]. The lower surface of L5 was clamped while a 1000N axial compression load was applied directly to the cage in the inferior direction. The final FE model comprised 41,183 nodes and 209,707 elements.

RESULTS AND DISCUSSION

The resultant stresses and strains of the endplate were obtained (Table 1) along with the stress contour on the endplate for middle position (Figure 1b). Lower minimum (Min) principal strains (7.9% - 27.3%) and higher von Mises stresses (21.4% - 26.4%, except posterior position) were observed for models with the cage located on the peripheral region of the endplate compared to the medial region. The lower minimum principal strains related to lower compressive deflections on the endplates for models with cages located on peripheral regions. This is consistent with the clinical outcomes of cages located on the medial region of the endplate having higher migration and subsidence rates [1].

The higher stresses on the endplate for models with cages located on peripheral regions are consistent with previous studies that show peripheral regions of the lumbar endplate have larger strength and thickness compared to medial regions [4].

Table 1: Major mechanical responses of the endplate with four cage positions.

Cage position	Peak value	
	Von Mises stress (MPa)	Min principal strain ($\mu\epsilon$)
Anterior	72.2	46500
Middle	57.1	50600
Posterior	47.8	46600
Lateral	69.3	36800

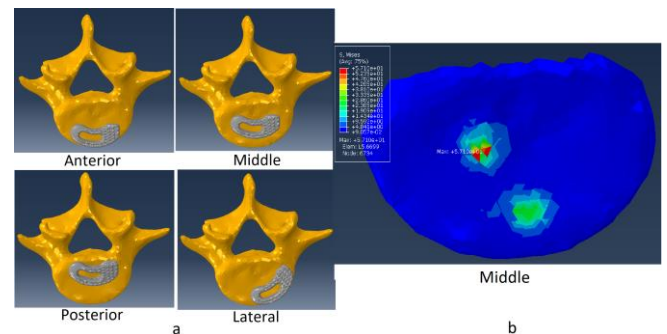


Figure 1: (a) Four cage positions on L5 superior endplate, (b) Stress contour on the endplate for middle position.

CONCLUSIONS

Cages located at peripheral positions of the vertebral endplate lead to lower minimum principal strains on the endplate. To reduce post-operative complication rates such as cage migration and subsidence, minimum principal strains on the endplate derived from computational modelling may be used to guide cage design. Experimental validation of the model will be examined in the future.

REFERENCES

1. Yao Y C, et al., *Spine*, **45**(19), E1279-E1285, 2020.
2. Morgan E F, *J. Biomech.* **36**(7), 897-904, 2003.
3. Calvo-Echenique, A, *Biomed. Eng. Online.* **18**(1), 1-17, 2019.
4. Grant J P, et al., *Spine*, **26**(8), 889-896, 2001.

CONFLICT OF INTEREST DECLARATION

In the interests of transparency and to help reviewers assess any potential bias, all authors of original research papers are required to declare any competing commercial interests in relation to the submitted work. Referees are also asked to indicate any potential conflict they might have reviewing a particular paper.

If you have accepted any support such as funds or materials, tangible or intangible, concerned with the research by the commercial party such as companies or investors, choose YES below, and state the relation between you and the commercial party.

If you have not accepted any support such as funds or materials, choose NO.

Do you have a conflict of interest to declare? (DELETE TEXT as appropriate)

YES

If YES, please complete as appropriate:

1. The author(s) did receive payments or other benefits or a commitment or agreement to provide such benefits from a commercial entity.

State the relation between you and the commercial entity:

This research was partially founded by 3DMediTech (Australia).

FAILURE OF TENDON GRAFTS FIXED WITH 3MM TENODESIS SCREWS: DOES SCREW PLACEMENT MAKE A DIFFERENCE?

¹Joseph Cadman, ²Dennis Brouwers, ¹Dane Dabirrahmani, ²Nicholas Smith and ¹Richard Appleyard

¹Orthopaedics Biomechanics Research Group, FMHHS, Macquarie University, NSW, Australia

²Macquarie Hand unit, Macquarie University, NSW, Australia

email: joseph.cadman@mq.edu.au

INTRODUCTION

Several soft tissue reconstruction techniques in the wrist/hand rely on strong fixation of tendon/suture via tenodesis screws in the carpal bones [1, 2]. There are several screw types and also different tunnel options [2-4]. Few studies have compared the different devices and techniques with regards to fixation strength.

This study will consider two different techniques for interference screw placement; screw placement on the near side of the bone resulting in pull-out testing vs placement on the far side for pull-through testing (Figure 1). The hypothesis was that the pull-through test would achieve a higher failure load than the pull-out test, as the pull-through test would likely bed the screw further into the bone increasing the resistance to pull-through.

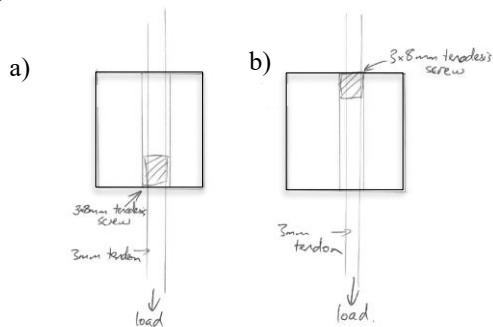


Figure 1: The two different loading configuration tested are described as a) pull-out (with the screw near the applied load) and b) pull-through (with the screw on the far side of the bone)

METHODS

Carpal bones including the scaphoid, lunate, capitate, triquetrum and hamate were dissected from 5 cadaveric wrists. Bones were only used if they were large enough to drill two parallel 3mm holes through, as both methods were tested in each bone to provide an internal control.

Flexor tendons were also dissected, including flexor digitorum superficialis, flexor digitorum profundus, palmaris longus and flexor carpi radialis. Flexor tendons were only used if they had a diameter of at least 3mm, appropriate for a typical repair, and a length of at least 130mm, required to fit into the testing jig. A total of 14 constructs were tested.

The tendons were passed through the drilled tunnels and fixed in place with 3mm tenodesis screws (Arthrex, USA). The screws were placed on either the near side or far side of the bone (Figure 1).

The tendon was then passed through a 15mm hole drilled through a 10mm thick plastic sheet fixed to the base of a mechanical testing machine. The free end of the tendon was passed over a capstan grip attached to the linear actuator, and a constant displacement rate of 10mm/min was applied until failure was observed.

RESULTS AND DISCUSSION

No significant difference was detected between the pull-out and pull-through. The pull-out tests had an average ultimate failure load of 88 ± 33 N compared to 98 ± 46 N for the pull-through tests ($p=0.55$). Similar results were observed for yield loads.

BMD measurements suggested no correlation between density and failure load.

The mode of failure was the tendon slipping past the tenodesis screw, which is why the placement of the screw did not result in any difference in failure load.

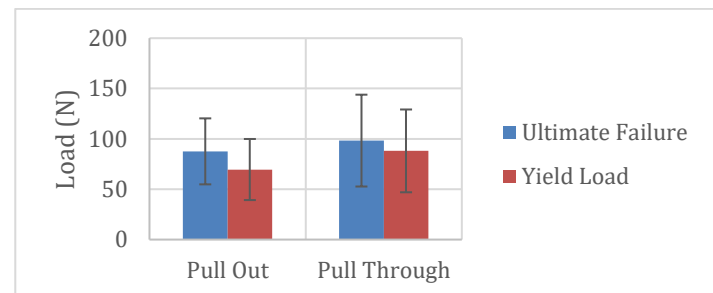


Figure 2: The ultimate Failure Load and Yield Load for Pull-Out and Pull-Through tests

CONCLUSIONS

This study shows that the location of the screw is not critical to the failure load of the construct in the case of soft tissue anchoring in the wrist.

REFERENCES

1. Skoff, H.D., et al., *The Journal of Hand Surgery: British & European Volume*, **20(2)**: 245-248, 1995.
2. Abboud, J.A., et al., *The Journal of Hand Surgery*, **27(1)**: 43-48, 2002.
3. Azato, F.N., et al., *Acta Ortopédica Brasileira*, **11**: 25-31, 2003.
4. Poukalova, M., et al., *Journal of Biomechanics* **43(6)**: 1138-1145, 2010.

CONFLICT OF INTEREST DECLARATION

In the interests of transparency and to help reviewers assess any potential bias, all authors of original research papers are required to declare any competing commercial interests in relation to the submitted work. Referees are also asked to indicate any potential conflict they might have reviewing a particular paper.

If you have accepted any support such as funds or materials, tangible or intangible, concerned with the research by the commercial party such as companies or investors, choose YES below, and state the relation between you and the commercial party.

If you have not accepted any support such as funds or materials, choose NO.

Do you have a conflict of interest to declare? (DELETE TEXT as appropriate)

YES

Dr Nicolas Smith uses the Arthrex tenodesis screws that were used in this testing. However, no funding was provided by Arthrex for this study.



THE EFFECT OF MODELLING PARAMETERS IN THE DEVELOPMENT AND VALIDATION OF KNEE JOINT MODELS ON LIGAMENT MECHANICS: A SYSTEMATIC REVIEW

¹Sara Farshidfar, ¹Joseph Cadman, ²Danny Deng, ¹Richard Appleyard and ¹Danè Dabirrahmani

¹Faculty of Medicine, Health and Human Sciences, Macquarie University, Sydney, New South Wales, Australia

²Faculty of Medicine and Health, The University of Sydney, Sydney, New South Wales, Australia

email: sara.farshidfar@hdr.mq.edu.au

INTRODUCTION

Background: The knee joint is a crucial, load-bearing joint comprising of hard (bone) and soft tissue (cartilage, capsule, tendons and ligaments). The ligaments in the knee are particularly prone to injury and rupture during dynamic activities, resulting in patients experiencing increased knee instability, which profoundly impacts a patient's daily living and functional capacity activities. Musculoskeletal knee modelling is a valuable tool for non-invasively investigating ligament force-strain behaviour under various applied boundary conditions and identifying potentially high-risk scenarios. However, despite the development and validation of many musculoskeletal knee models, the effect of modelling parameters on ligament mechanics has not yet been systematically reviewed.

The current systematic review's primary aim was to evaluate the knee joint's musculoskeletal models and focus on ligaments mechanics and modelling parameters in various simulated movements. Secondly, this review aimed to determine whether the predicted loading pattern depended on the investigation techniques used to validate their outcomes? Furthermore, this study aimed to identify the parameters with a higher impact on the ligament mechanics, which in turn affects clinical decision making.

Data sources: MEDLINE, ScienceDirect, and IEEE Xplore

Eligibility criteria for selecting studies: Databases were searched for musculoskeletal knee modelling articles, including both the femur and tibia and the ligaments, reporting any numerical ligaments strain or force data. The studies modelled the intact, ACL-deficient, PCL-deficient, or lateral extra-articular reconstructed (LER) knee joints and were published between the 1st of January 1995 and 31st of July 2021.

METHOD

A customised data extraction table was developed to obtain the critical parameters of each selected study. Specific parameters of the musculoskeletal knee model development used in each eligible study were independently extracted, including the (1) musculoskeletal model definition including geometry, joint boundary conditions and ligament modelling, (2) sensitivity analysis, (3) validation approaches, (4) predicted ligament mechanics and (5) clinical applications, where available.

RESULTS

From the 993 articles retrieved by the initial electronic search, only 19 met all the inclusion criteria. This systematic review

shows that a large variety of modelling techniques applying different boundary conditions have been used to predict knee joint kinematics and ligament mechanics. Because of the differences in the models, there is considerable variability in the predicted ligament mechanics. Geometric input (such as articular contact surfaces, wrapping objects, number of ligament bundles, and ligament insertion points), boundary conditions (including DoFs and type of activity), and ligament modelling parameters (including ligament stiffness and reference values, and method of strain calculation) has been used to define the unique characteristics of each specific musculoskeletal model. All of these parameters have, to varying degrees, been found to affect the predicted ligament force-elongation behaviour.

Different bundles of the ACL, PCL, MCL and LCL exhibit different force/strain patterns during *active* walking and squatting and *passive* knee flexion tests. For example, a model representing the MCL with lower numbers of bundles [1] showed larger ranges of motion in the varus-valgus and mediolateral directions during walking compared to other studies [2-4]. Also, higher MCL force values were seen in a model during active squatting, which modelled the MCL with superficial and deep layers [5], compared to forces within MCL bundles of another study [6], which didn't consider the deep layers of MCL. Moreover, by comparing the knee joint DoFs and ligament strain values reported among studies modelling *passive* flexion test, it was seen those two models [7,8] reported acceptable strain results within ACL, PCL, MCL and LCL with a higher number of unlocked DoFs.

CONCLUSION

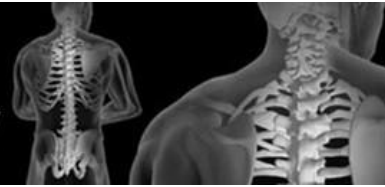
This review aids in our understanding of various modelling parameters on ligament loading predictions and assists in defining and improving protocols for developing these models, validating the outcomes and the reconstruction and rehabilitation techniques.

REFERENCES

1. Hu, J., et al., *Journal of Engineering in Medicine*, 232(5):508-519, 2018.
2. Shelburne, K.B., et al., *Journal of Biomechanics*, 37(3):313-319, 2004.
3. Shao, Q., et al., *Annals of Biomedical Engineering*, 39(1):110-121, 2011.
4. Vignos, M.F., et al., *Am J Sports Med*, 48(14): 3503-3514, 2020.
5. Bersini, S., et al., *Computer Methods in Biomechanics and Biomedical Engineering*, 19(5): 571-579, 2016.
6. Shelburne, K.B., et al., *Computer Methods in Biomechanics and Biomedical Engineering*, 5(2): 149-159, 2002.
7. Kia, M., et al., *Journal of Biomechanical Engineering*, 138(5), 2016.
8. Schmitz, A., et al., *IEEE Trans Biomed Eng*, 63(10): 2056-67, 2016.



Australian & New Zealand
Orthopaedic Research Society



DAY 3

POSTERS



MULTI LENGTH SCALE STRUCTURAL INVESTIGATION OF ARTICULAR CARTILAGE: HOW STRUCTURE INFLUENCES THE SWELLING RESPONSE OF MILDLY DEGENERATE BOVINE ARTICULAR CARTILAGE

¹Emma Brown, ¹Ashvin Thambyah and ²Joni Simons

¹ Department of Chemical and Materials Engineering, University of Auckland, 5 Grafton Road, Auckland 1010, New Zealand.

² Orthopaedic Biomechanics Group, Department of Biomedical Engineering, Eindhoven University of Technology, P.O. Box 513, 5600 MB Eindhoven, the Netherlands

Corresponding author email: emma.brown@auckland.ac.nz

INTRODUCTION

Some of the known influencing factors on cartilage mechanics include the structural and compositional variation through the tissue depth [1,2]. Indeed, recently by studying the collagen fibrillar network architecture, we were able to demonstrate how the transverse collagen fibrillar network interconnectivity and packing density was itself a significant influencing factor governing cartilage swelling behavior [3]. Acknowledging this mechanically significant collagen network we seek to understand how changes associated with degeneration, such as a loss in lateral interconnectivity might influence the tissue swelling response. For the present study, three collagen network structure related aspects are investigated in relation to the biomechanics of swelling strain and these are: (1) degenerative changes at the surface zone (SZ) (2) loss of fibrillar matrix interconnectivity, and (3) change in deep zone (DZ) tissue microstructure.

METHODS

Thin strips of articular cartilage were harvested from adult bovine patellae (n=30) which demonstrated pre-osteoarthritic degenerative changes at the macro scale. The swelling induced strain responses, following two-hour equilibrations in 0.15M saline solution followed by distilled water, were obtained. Multi-scale structural analysis was carried out on chemically-fixed 30- μ m cross sections via differential interference contrast microscopy (DIC) to image chondrocytes, and scanning electron microscopy (SEM) to image collagen fibrillar network interconnectivity. The healthy tissue data reported in an earlier study [3] was used as a control, consisting of 40 sample strips harvested from healthy patellae where half were tested intact and half were tested with SZ removed.

RESULTS AND DISCUSSION

For the degenerate samples, SZ strain decreased with increasing curvature while DZ strain increased with increasing sample curvature. Values of strain tended to be greater than those from the earlier study using healthy patellae [3], these differences correlating to differences in micro and ultrastructure. As an example, see ultrastructural differences captured in Fig. 1.

With degenerative changes at the tissue surface, the gross tissue response is different compared to when healthy cartilage has its surface layer removed. The reason for this difference is due to the fact that matrix lateral interconnectivity influences the cartilage swelling mechanics. Finally, our data demonstrates how there are consistent differences between healthy and degenerate tissue, in the microstructures of the DZ cartilage and zone of calcified cartilage.

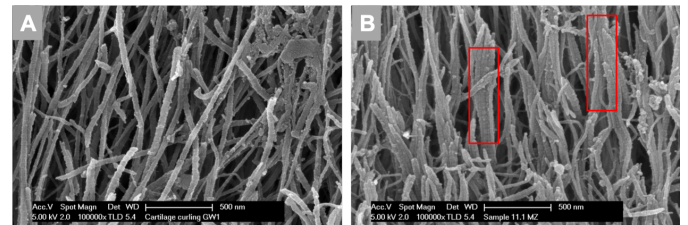


Fig. 1: (A) SEM image of the fibrillar network within pristine articular cartilage. Fibrils are well dispersed and radially aligned. (B) SEM image of the fibrillar network within more degenerate articular cartilage. Fibrils are radially oriented but clustered together (see red boxes)

CONCLUSIONS

This micro and ultrastructural investigation revealed that key influences over the tissue swelling induced strain response was (1) the thickness and extent of disruption to the surface layer and (2) the amount of fibrillar network destructuring, highlighting the importance of the collagen and tissue matrix structure in restraining cartilage swelling

ACKNOWLEDGEMENTS

The authors are grateful for a University Faculty Doctoral Scholarship for author Brown.

REFERENCES

1. Benninghoff, A. *Z Zellforsch Mik Ana.* **2**, 783–862 (1925)
2. Mow, V C et al. *Sports Med. Arthrosc. Rev* **2**(3) 189-202 (1994)
3. Brown, E et al. *Clin Biomech.* **79**, p. 104926. (2020)

REFERENCE POINT INDENTATION FOR THE DETECTION OF EARLY OSTEOARTHRITIS

¹Josh Workman, ¹Thomas Loho and ¹Ashvin Thambyah

¹Chemical and Materials Engineering, The University of Auckland, Auckland, NZ

email: j.workman@auckland.ac.nz

INTRODUCTION

Osteoarthritis (OA) is a common joint degenerative disease, for which few effective preventative interventions exist. The detection of early OA in articular joints is a key step towards providing solutions to slow down or even halt the progress of this debilitating disease [1,2]. The advancement of the zone of calcified cartilage, and subsequent changes to the subchondral bone may lead to detectable changes in the mechanical properties of the joint tissue beneath the articular cartilage.

Reference point indentation (RPI) is a mechanical characterization technique that may be able to identify these early changes using a tool that may be clinically relevant [3]. In RPI, a test probe is encased within a reference probe that penetrates soft tissue surrounding the bone. The test probe indents the bone relative to the reference probe. A cyclical load is applied to measure dynamic mechanical properties that can provide insight into the viscoelastic properties of the material.

METHODS

A total of 36 bovine patellae exhibiting various stages of OA were obtained and sorted into groups according to the Outerbridge scale. Sample blocks were extracted from the distal lateral quadrant and mounted in stainless steel sample holders. RPI characterization was carried out using the BioDent reference point indenter as seen in Figure 1. The reference probe was used to pierce the articular cartilage until it reached the calcified region. A nominal load of 3.5N was then applied and 10 indentation cycles completed. This was repeated 9 times for each sample.

RESULTS AND DISCUSSION

The characterization identified four key parameters that could be compared between groups as seen in Table 1. There was a statistically significant decrease in all the key parameters from healthy G0 samples through to more degenerate G2 and G3 samples. This reflects the subtle structural changes occurring at the soft-hard tissue junction during early OA.

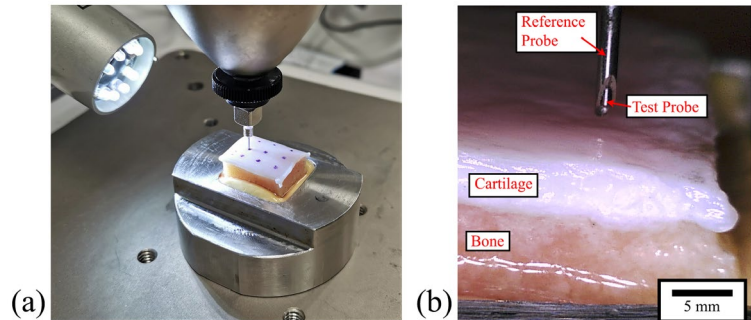


Figure 1: (a) BioDent test set-up. (b) Image taken using built-in optical microscope. The reference probe penetrates the cartilage to allow the test probe to indent the underlying bone without removing the cartilage.

CONCLUSIONS

Using this RPI technique, early OA may be detectable before presentable clinical symptoms occur. This may also be applied to identify cases of post-traumatic OA, and enable the early intervention of novel therapies to prevent further articular cartilage degeneration.

REFERENCES

1. M. Lotz, Posttraumatic osteoarthritis: pathogenesis and pharmacological treatment options, *Arthritis Res Ther.* **12**:211, 2010.
2. L. Ryd, M. Brittberg, K. Eriksson, J. Jurvelin, A. Lindahl, S. Marlovits, P. M'oller, J. Richardson, M. Steinwachs, M. Zenobi-Wong, Pre-osteoarthritis: Definition and diagnosis of an elusive clinical entity, *Cartilage.* **6**, 2015.
3. S. Tang, P. Mathews, C. Randall, E. Yurtsev, K. Fields, A. Wong, A. Kuo, T. Alliston, P. Hansma, In situ materials characterization using the tissue diagnostic instrument, *Polymer Testing.* **29**:2, 2010.

Table 1: Obtained data from RPI measurements, reported as mean \pm standard error. CID1 = 1st cycle indentation distance, US1 = 1st cycle unloading slope, IDI = indentation distance increase, TID = total indentation distance.

Grade	CID1 (μm)	US1 ($\text{N}/\mu\text{m}$)	IDI (μm)	TID (μm)
G0	35.67 \pm 0.97	0.2098 \pm 0.2295	91.46 \pm 4.72	570.02 \pm 5.43
G1	32.62 \pm 1.41	0.1421 \pm 0.1867	68.07 \pm 3.92	545.73 \pm 4.57
G2	30.14 \pm 1.38	0.1006 \pm 0.0109	48.19 \pm 4.08	536.15 \pm 4.56
G3	27.57 \pm 0.84	0.0674 \pm 0.0044	33.74 \pm 3.97	538.63 \pm 3.60



THE THERMAL PROFILE OF SELF-TAPPING SCREWS: THE EFFECT OF INSERTION SPEED, POWER INSERTION, AND SCREW GEOMETRY ON HEAT PRODUCTION AT THE BONE-SCREW INTERFACE

Daniel J Wills BVSc¹, Anshula Prasad BS², Brian B Gilmer MD³, William R. Walsh PhD¹

¹Surgical and Orthopaedic Research Laboratory, University of New South Wales, Australia.

²University of Nevada, Reno School of Medicine.

³Mammoth Orthopaedic Institute, Mammoth Lakes, CA, United States.

Email: d.wills@unsw.edu.au

INTRODUCTION

Power insertion of screws using high-speed saves time and increases efficiency during operative fixation of fractures compared to manual insertion. Heat production during screw insertion may cause thermal damage at the critical bone-screw interface, reducing fixation strength, delaying healing, or increasing infection risk. Currently, the thermal impact of screw insertion is incompletely understood. This study investigated the thermal profiles of self-tapping screws at varying insertion speeds, utilizing manual versus power insertion, and with differing cutting flute geometries to determine which variables may save time while mitigating thermal injury.

METHODS

Thermal and biomechanical profiles were obtained during insertion of 24mm length, 3.5mm stainless steel screws into 50 PCF polyurethane after pre-drilling. Power insertion at low (30RPM) and high (300RPM) speed, manual screwdriver insertion and high-speed power insertion, and two flute geometries were compared. Infrared thermography was used to measure maximum surface temperatures and mean temperature change (°C). Time (s) was measured to compare manual versus power insertion. Means were compared using a two-tailed independent t-test.

RESULTS AND DISCUSSION

Maximum surface temperature of high-speed insertion ($55.42 \pm 5.58^{\circ}\text{C}$) was significantly greater ($p < 0.001$) than low-speed ($41.07 \pm 2.33^{\circ}\text{C}$). Similarly, mean temperature rise of high-speed insertion ($29.52 \pm 5.39^{\circ}\text{C}$) was greater than that of low-speed ($15.13 \pm 2.63^{\circ}\text{C}$) ($p < 0.001$). There was no statistical difference in maximum surface temperature between manually inserted screws ($56.58 \pm 5.53^{\circ}\text{C}$) and high-speed power inserted screws ($55.42 \pm 5.58^{\circ}\text{C}$) ($p = 0.155$), while insertion speeds were almost 5 times faster with high-speed power insertion (6.75 ± 1.84 seconds) than with manual insertion (30.3 ± 4.06 seconds)

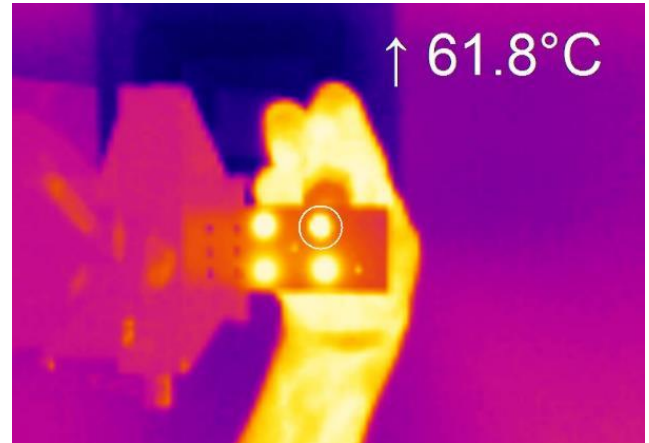


Figure 3 – Infrared thermography of the exit-surface of 24mm length, 3.5mm AO self-tapping locking screw, hand-driven into PCF50 density polyurethane block.

($p < 0.001$). There were no differences detected between the geometry groups in any outcome measure tested.

CONCLUSION

High speeds for screw insertion create significantly greater maximum temperatures and greater temperature rise than slower speeds. Surprisingly, the thermal profile of manual insertion was similar to high-speed insertion, while requiring significantly longer for insertion. Low-speed insertion generated significantly lower maximal temperatures and temperature rise. Surgeons could consider utilizing low-speed when inserting orthopedic screws with a power driver to minimize thermal impact to bone while optimizing efficiency.

ACKNOWLEDGEMENTS

The SMARTDrill® Research Prototype 4.3 used in the study was provided by Smart Medical Devices Inc.

TABLE 1 – Thermal profile of manual, low and high-speed power insertion of AO 3.5mm locking screws in 50PCF polyurethane medium

Outcome: mean (±SD)	Manual Insertion	Low-speed – 30RPM	High-speed– 300RPM
Starting temperature (°C)	27.38 (±0.29)	25.93 (±0.58)	25.9 (±0.25)
Maximum temperature (°C)	56.58 (±5.53)	41.07 (±2.33)	55.42 (±5.58)
Temperature rise (°C)	29.2 (±5.33)	15.13 (±2.63)	29.52 (±5.39)
Duration of insertion (s)	30.3 (±4.06)	48.02 (±2.79)	6.75 (±1.84)
Average insertion speed (RPM)	48.25 (±6.50)	30	300

CONFLICT OF INTEREST DECLARATION

In the interests of transparency and to help reviewers assess any potential bias, all authors of original research papers are required to declare any competing commercial interests in relation to the submitted work. Referees are also asked to indicate any potential conflict they might have reviewing a particular paper.

If you have accepted any support such as funds or materials, tangible or intangible, concerned with the research by the commercial party such as companies or investors, choose YES below, and state the relation between you and the commercial party.

If you have not accepted any support such as funds or materials, choose NO.

Do you have a conflict of interest to declare? (DELETE TEXT as appropriate)

YES

If YES, please complete as appropriate:

1. The author(s) did receive payments or other benefits or a commitment or agreement to provide such benefits from a commercial entity.

State the relation between you and the commercial entity:

The SMARTDrill® Research Prototype 4.3 used in the study was provided by Smart Medical Devices Inc.

No other funds or benefits were received by any authors or institutions.



A POPULATION-BASED STUDY ON TOTAL KNEE REPLACEMENT ATTRIBUTABLE TO OBESITY IN AUSTRALIA

¹Lianzhi Chen, ²Monica Zheng, ¹Ziming Chen, ^{3,5}Yi Peng, ⁴Christopher Jones, ⁵Stephen Graves, ¹Peilin Chen, ¹Rui Ruan, ^{1,6}John Papadimitriou, ⁷Richard Carey-Smith, ⁷Toby Leys, ¹Christopher Mitchell, ⁸Yi-Gang Huang, ¹David Wood, ²Max Bulsara, ^{1,9}Minghao Zheng

¹Centre for Translational Orthopaedic Research, Medical School, University of Western Australia, Perth, Western Australia, Australia

²Institute for Health Research, Medical School, University of Notre Dame, Fremantle, Western Australia, Australia

³South Australian Health and Medical Research Institute (SAHMRI), Adelaide, South Australia, Australia

⁴Department of Orthopaedic Surgery, Fiona Stanley Hospital Group, Perth, Western Australia, Australia

⁵Australian Orthopaedic Association National Joint Replacement Registry, Adelaide, South Australia, Australia

⁶Pathwest Laboratories, Perth, Western Australia, Australia

⁷Department of Orthopaedic Surgery, Sir Charles Gardner Hospital, Perth, Western Australia, Australia

⁸Department of Orthopaedic Surgery, Shanghai Jiao Tong University Affiliated Sixth People's Hospital, Shanghai, China

⁹Perron Institute for Neurological and Translational Science, Perth, Western Australia, Australia

email: Minghao.zheng@uwa.edu.au

INTRODUCTION

Obesity is a risk factor for osteoarthritis (OA) [1,2]. To determine the risk of total knee replacement (TKR) for primary OA associated with obesity in Australia, we conducted a population-based study used data collected from the AOA National Joint Replacement Registry and Australian Bureau of Statistics.

METHODS

We analyzed 191,723 adult Australians with OA who had a TKR from 2015-2018. Age- and gender-specific incidence rate (IR) and incidence rate ratio (IRR) for each body mass index (BMI) category were calculated to determine time-trend changes in incidence of TKR and the contribution of obesity. The population attributable fraction (PAF) was calculated to estimate the effect of obesity reduction on TKR incidence [3].

RESULTS AND DISCUSSION

The total number of TKRs increased by 28.33%, with the greatest increase seen in obesity class III patients. The impact of obesity was most significant in the younger population. When compared to patients with normal weight, those aged 18-54 years, the overweight, obesity class I&II and obesity class III showed a 3.751-, 13.811- and 28.683-times the risk, respectively. Obesity was associated with a higher incidence of TKR in female compared to male populations. Females in obesity class III were 1.7 times more likely to undergo TKR compared to similarly classified males. The PAFs of TKR

associated with overweight or obesity was 35%, estimating over 10,000 cases of TKR attributable to obesity. The proportion of TKRs could be reduced by 20% if overweight and obese population move down one BMI category.

CONCLUSIONS

Obesity contributed to a large proportion of TKR for OA in young and in female patients.

ACKNOWLEDGEMENTS

The authors would like to acknowledge of the staffs from Australian Orthopaedic Association National Joint Replacement Registry for assisting data collection.

REFERENCES

1. Cooper C, et al. Risk factors for the incidence and progression of radiographic knee osteoarthritis. *Arthritis Rheum* 2000; 43(5):995-1000.
2. Chen L, et al. Horizontal fissuring at the osteochondral interface: a novel and unique pathological feature in patients with obesity-related osteoarthritis. *Ann Rheum Dis* 2020 ;79(6):811-818.
3. Barnes DE, Yaffe K. The projected effect of risk factor reduction on Alzheimer's disease prevalence. *Lancet Neurol* 2011; 10(9):819-28.



SCOPING REVIEW OF IMAGING TECHNIQUES TO ASSESS MUSCLE DAMAGE POST-TOTAL HIP ARTHROPLASTY

^{1,2}Ross Hamilton, ^{2,3}Stuart Callary, ^{2,3}Peter Smitham and ^{2,3}Bodgan Solomon

¹Adelaide Medical School, The University Adelaide, Adelaide, SA, Australia

²Centre for Orthopaedic and Trauma Research, The University of Adelaide, Adelaide, SA, Australia

³Department of Orthopaedics and Trauma, Royal Adelaide Hospital, Adelaide, SA, Australia

email: ross.hamilton@adelaide.edu.au

INTRODUCTION

There has been a recent increase in the importance of assessing soft tissue damage during total hip replacement surgery. Common imaging modalities such as, Computed Tomography (CT), Magnetic Resonance Imaging (MRI) and Ultrasound (US) have been used since the 1990's in conjunction with a number of other clinical outcome measures. While these imaging modalities aim to assess soft tissue structures; muscle, tendon, articular capsule and ligaments, each have their strengths and weaknesses.

The aim of this review is to provide clinicians with recommendations towards best practice to assess muscle and soft tissue damage which may have occurred because of surgical intervention and to monitor healing post Total Hip Arthroplasty (THA).

METHODS

A systematic review of the literature was performed using EMBASE, PUBMED and SCOPUS. Studies were included if medical imaging was used as an outcome measure to assess hip musculature damage following primary THA. After exclusion of duplicates, our initial review of literature found 511 studies for screening.

RESULTS AND DISCUSSION

This review identified a large variation in the image sequencing parameters, anatomic locations for muscular region of interest and definitions for muscle damage in almost all 49 papers eligible for full text review (see Figure 1 for PRISMA flow-chart). The review found an equal distribution of studies retrospectively (n=20) and prospectively (n=19) analysing post-surgical soft tissue atrophy/repair, at an average of 14 months (range: post-operative day 1 – 10 years) comparing contralateral and surgical sides, and most commonly of the Gluteus Medius muscle (n=34). Furthermore, MRI (n=38) and/or CT (n=8) were used in all cohorts in the review except one, which solely used US. Of the 38 studies which used MRI,

one used CT and two used US in conjunction or to determine efficacy between the two modalities. The remaining studies, of which seven used CT and one used ultrasound to assess muscle damage in isolation did so without the use of a secondary imaging assessment modality.

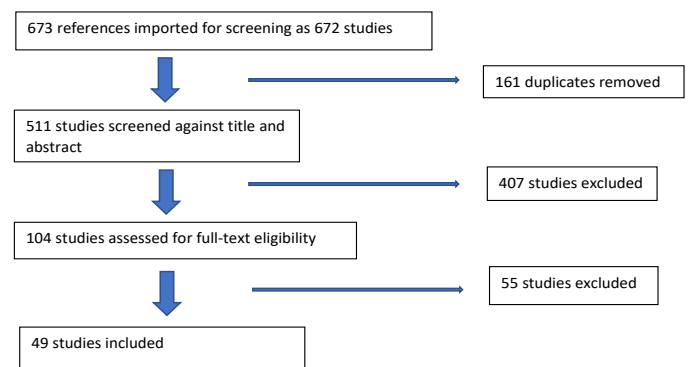


Figure 1: PRISMA flow-chart for systematic search.

CONCLUSIONS

We identified that MRI is currently the most popular imaging modality as a primary or secondary outcome measure for assessing muscular alterations after THA. However, the literature suggests that there are still questions surrounding study protocol and therefore analysis and definition of trophic changes in hip musculature as a result of surgical intervention. Recommendations for assessing muscle or soft tissue damage around the hip with regards to study protocol, region of interest, defining muscle damage and imaging sequencing parameters, therefore, requires further investigation.



IN-VIVO KINEMATICS DURING STEP-UP AND DOWN IN THREE TOTAL KNEE REPLACEMENT DESIGNS: A RANDOMISED CLINICAL TRIAL

Joe Lynch¹; Diana Perriman¹; Jennie Scarvell²; Mark Pickering³; Jeremy Ripper¹; Catherine Galvin¹; Paul Smith¹

¹Australian National University, Canberra

²University of Canberra, Canberra

³University of New South Wales at ADFA, Canberra.

Email: joseph.lynch@anu.edu.au

INTRODUCTION

Modern total knee replacement prostheses are designed to reduce pain and restore kinematic function (1). However, randomised clinical trials are rarely conducted to control for bias in patient selection. Implant choice is guided by implant survival, surgeon preference and kinematic performance (2). However, the debate over which implant to use is still unresolved. Surgeons' choice of prosthesis typically does not have the benefit of the information from clinical trials. Therefore, this clinical trial aimed to prospectively compare outcomes, but also kinematics of three common designs: posterior-stabilised fixed-bearing (PS-FB), cruciate-retaining fixed-bearing (CR-FB) and cruciate-retaining rotating-platform (CR-RP) designs. Here we present kinematics of a step-up and step-down task.

METHOD

68 participants were randomised to receive either cruciate retaining (CR-FB), rotating platform (CR-RP) or posterior stabilised (PS-FB) knee prostheses. Image quality was sufficient for 49 of these patients to be included in the final analysis following a minimum 1-year follow-up. Patients completed a step-up and down task while being imaged using single-plane fluoroscopy. Femoral and tibial computer-aided design (CAD) models for each of the TKR designs were registered to the fluoroscopic images using bespoke software OrthoVis to generate six-degree-of-freedom kinematics. Differences in kinematics between design were compared as a function of flexion.

RESULTS

There were no differences in terminal extension or clinical outcomes (Oxford knee score, Pain or Satisfaction) between the groups. The CR-FB was further posterior and the CR-RP was more externally rotated at terminal extension compared to the other designs (Table 1). Furthermore, the femoral component of CR-FB designs was more posteriorly positioned at each flexion angle compared to both CR-RP and PS-RB designs during both

movements. Additionally, the CR-RP design had more external femoral rotation throughout flexion when compared with both fixed bearing designs. However, there were no differences in total rotation for either step-up or down. Visually, it appears there was substantial variability between participants in each group, indicating unique patient-specific movement patterns (Figure 1).

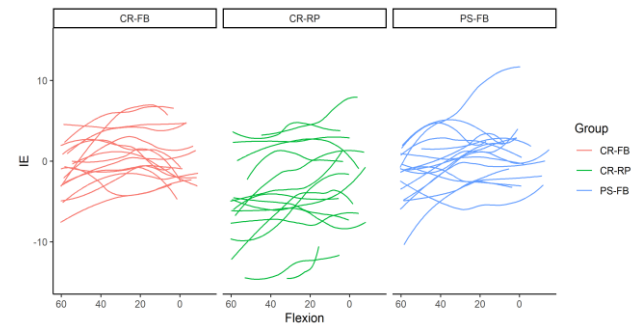


Figure 1. Individual kinematic curves for all three designs for internal- external rotation

CONCLUSIONS

This study found that CR-FB designs were more posterior across both movements compared the other designs, while CR-RP designs remained relatively more externally rotated than the fixed bearing designs. Although there were differences in step-up and down kinematics between designs, the inter-individual variation was high indicating that individual motor control factors are an important determinant of kinematic outcome.

REFERENCES

- [1] Lange T et al. J Arthroplasty **32**(7):2093-2099. 2017
- [2] Vertullo CJ et al. J Arthroplasty **32**:2980–2989. 2017

Table 1: Kinematics at Terminal Extension

	Cruciate Retaining Fixed Bearing	Cruciate Retaining Rotating Platform	Posterior Stabilised Fixed Bearing
Anterior-Posterior(mm)	4.2 (2.6 to 5.8)	8.9 (7.3 to 10.5)#	8.6 (7.0 to 10.1) #
Abduction/Adduction (°)	0.9 (0.0 to 1.7)	1.1 (0.3 to 1.9)	0.2 (-0.6 to 1.0)
Internal External (°)	0.2 (-2.2 to 2.5)	-2.8 (-5.1 to -0.5) ¥	1.5 (-0.8 to 3.7)
Medial Lateral (mm)	2.4 (1.1 to 3.7)	2.9 (1.6 to 4.2)	2.8 (1.5 to 4.1)
Superior Inferior (mm)	16.2 (14.9 to 17.5)	18.1 (16.8 to 19.3)	16.9 (15.6 to 18.1)

CONFLICT OF INTEREST DECLARATION

In the interests of transparency and to help reviewers assess any potential bias, all authors of original research papers are required to declare any competing commercial interests in relation to the submitted work. Referees are also asked to indicate any potential conflict they might have reviewing a particular paper.

If you have accepted any support such as funds or materials, tangible or intangible, concerned with the research by the commercial party such as companies or investors, choose YES below, and state the relation between you and the commercial party.

If you have not accepted any support such as funds or materials, choose NO.

Do you have a conflict of interest to declare? (DELETE TEXT as appropriate)

YES

1. A commercial entity (ZimmerBiomet) paid or directed, or agreed to pay or direct, any benefits to any research fund, foundation, educational institution, or other charitable or nonprofit organization with which the authors are affiliated or associated.



DANGERS OF BEING AN OUTLIER; MORTALITY RISK IN HIP FRACTURE PATIENTS BASED OFF THE ORTHOPAEDIC WARD. A COHORT STUDY.

Peggy Emily Miller¹, Evelyn Patricia Murphy¹, Robert Murphy², Ben Murphy¹, Conor Hurson¹

1. Department of and Orthopaedics, St. Vincent's University Hospital, Elm Park, Dublin 4, Ireland

2. University Hospital Limerick, Limerick City, Ireland

email: p.miller2@nuigalway.ie

Introduction

Fragility fractures remain one of the most prevalent and devastating injuries in an ageing population. They are associated with reduced quality of life, increased mortality and high economic burden to the health service. Adherence to best practice guidelines for hip fracture management in Ireland is audited by the Irish Hip Fracture (IHFD) database. A key recommendation is to transfer a patient to the ward within four hours.

Methods

To assess if a patient based on a non-orthopaedic ward has a higher mortality risk at 30 days and at 1 year, relative to a patient based on a specialist orthopaedic ward for the duration of their hospital stay. Methods: This was a single centre retrospective cohort study including all patients presenting with fragility hip fractures between 2015-2019. Exclusion criteria consisted of patients with polytrauma or atypical femoral fractures. Mortality rates at 30 days and at 1 year were compared in the two cohorts. Univariate and multi-variate logistic regression was used to control for variables such as age, American Society of Anaesthesia grade, gender and fracture type.

Results

In this cohort 69 patients were based on a non-orthopaedic ward, while 895 were based on an orthopaedic ward. The mean age of those outlier patients was 76.84 years with a distribution of 68% (47) female patients to 31.8% (22) male patients. Mean age of patients on Orthopaedic ward is 80.5 years and gender distribution is 70% (628) female and 30% (267) male. 20.2% (14) outlier patients were dead at 1 year, while 18.5% (166) of patients based on the orthopaedic ward were dead at 1 year. 23% (16) outlier patients were

discharged home directly, while 17.5% (157) were discharged home directly from the Orthopaedic ward.

Discussion

Mortality rate at 1 year is similar in both groups, 20% for those on outlier wards and 18.5% for those on the specialist ward. Gender distribution is also reflective in both cohorts, however it is important to note the mean age in both cohorts. Patients on the outlier wards were 76.8 years old on average, while those on the Orthopaedic ward 80.5 years old. Larger numbers of outlier patients would be required to understand the significance of this information.

Conclusion

This study compares mortality rate based on patient location on and off the orthopaedic ward. This study highlights the need for further efforts to cohort orthopaedic patients on specialist wards.

References

1. Metcalfe D, Zogg CK, Judge A, Perry DC, Gabbe B, Willett K, et al. Pay for performance and hip fracture outcomes. *Bone Joint J.* 2019 Aug;**101-B(8):1015–23.**
<https://www.ncbi.nlm.nih.gov/pmc/articles/PMC5473829/>
2. Johnell O, Kanis JA. An estimate of the worldwide prevalence and disability associated with osteoporotic fractures. *Osteoporos Int.* 2006 Dec;**17(12):1726–33.**



PRELIMINARY OUTCOMES FOR PATIENTS UNDERGOING VERTEBRAL BODY TETHERING FOR IDIOPATHIC SCOLIOSIS

Megan Roser, Paige Little, Geoffrey Askin, Robert Labrom, Maree Izatt

Biomechanics and Spine Research Group, Centre for Children's Health Research, Brisbane, QLD, Australia
Orthopaedics Department, Queensland Children's Hospital, South Brisbane, QLD, Australia
email: megan.rosier@health.qld.gov.au

INTRODUCTION

Anterior vertebral body tethering (AVBT) is a procedure used to halt progression and correct idiopathic scoliosis by applying a flexible tether to the convex surface of the spine in skeletally immature patients¹.

This, in contrast to traditional fusion methods, allows patients to retain flexibility and to continue growing². The purpose of this study is to determine the preliminary clinical outcomes for an adolescent patient cohort.

METHODS

18 patients with idiopathic scoliosis underwent AVBT and of this cohort, 6 had reached a minimum follow up of 2 years at the time of analysis, 7 had reached 18 months follow up, 2 had reached 1 year follow up and 1 had reached 6 months follow up. This subset of patients all demonstrated a primary thoracic deformity, were skeletally immature, and were analysed in this preliminary study of coronal plane deformity correction.

Using open-source image analysis software (ImageJ, NIH) PA radiographs taken pre-operatively and at regular follow-up visits post-operatively (1 week, 2 months, 6 months, 1 year, 1.5 years and 2 years) were used to measure the coronal plane deformity of the major and compensatory curves.

RESULTS AND DISCUSSION

Pre-operatively, the mean age was 12.0 years (S.D. 10.7 – 13.3), Risser 0.3 (S.D. 0-0.9), Sanders 2.6 (S.D. 1.8-3.4), pre-

menarchal, with a main thoracic scoliosis curve angle of 52° (S.D. 44.2-59.8°). Post-operatively the main curve angle decreased to 25.4° (S.D. 18.4-32°) at 1 week, 29.8° (S.D. 21.6-38°) at 2 months, 24° (S.D. 17.1-30.9°) at 6 months, 27.5° (S.D. 16.5-38.5°) at 12 months, and 31.4° (S.D. 20.4-42.4°) at 18 months and 44.5° (S.D. 39.6-49.4°) at 2 years.

There was an average of 8 levels tethered (7-9) the highest level was T5 and the lowest level was L1. The average surgical time was 163.5 minutes (S.D. 138.5-188.5), average intra-op blood loss 106.7mls (S.D. 21.3-192.2), X-ray time 68.6 seconds (S.D. 58.4-78.9), and hospital stay 3.67 days (S.D. 2.85-4.5).

One patient was required to wear a brace at final follow up due to curve progression and there were 4 tether breakages identified.

CONCLUSIONS

AVBT is a promising new technique for skeletally immature patients with progressive AIS. This study has demonstrated a reduction in scoliosis severity with no unplanned returns to theatre.

REFERENCES

1. Samdani, A et al., *Spine*. **39**:1688-1793, 2014.
2. Newton, P, et al., *The Journal of Bone and Joint Surgery*. **100**:1691-7, 2018.

3D PRINTED HANDHELD MODELS DO NOT IMPROVE RECOGNITION OF SPECIFIC CHARACTERISTICS AND PATTERNS OF THREE-PART AND FOUR-PART PROXIMAL HUMERUS FRACTURES

¹ Reinier W. A. Spek, ¹ Bram J. A. Schoolmeesters, ² Jacobien H. F. Oosterhoff, ³ Job N. Doornberg, ⁴ Michel P. J. van den Bekerom MD, ¹ Ruurd L. Jaarsma, ⁵ Denise Eygendaal MD, PhD, ³ Frank IJpma, and the Traumaplatform 3D Consortium

¹ Department of Orthopaedic Surgery, Flinders University and Flinders Medical Centre, Adelaide, Australia

² Department of Orthopaedic Surgery, Massachusetts General Hospital, Harvard Medical School, Boston, MA, USA

³ Department of Orthopaedic Surgery, University of Groningen and University Medical Centre Groningen, Groningen, the Netherlands

⁴ Shoulder and Elbow Expertise Centre, Department of Orthopaedic Surgery, OLVG, Amsterdam, the Netherlands

⁵ Department of Orthopaedic Surgery, Amsterdam University Medical Centre, Amphia Hospital, Breda, the Netherlands

email: reinierspek@gmail.com

INTRODUCTION

Reliably recognizing the overall pattern and specific characteristics of proximal humerus fractures may aid in surgical decision-making. With conventional onscreen imaging modalities, there is considerable and undesired interobserver variability, even when observers receive training in the application of the classification systems used. It is unclear whether three-dimensional (3D) models, which now can be fabricated with desktop printers at relatively little cost, can decrease interobserver variability in fracture classification. To fill this knowledge gap, we asked: do 3D-printed handheld models of proximal humerus fractures improve agreement among residents and attending surgeons regarding (1) specific fracture characteristics and (2) patterns according to the Neer and Hertel classification systems?

METHODS

Plain radiographs, as well as two-dimensional (2D) and 3D CT images were collected from 20 patients (aged 18 years or older) who sustained a three-part or four-part proximal humerus fracture which were treated at a Level I trauma center between 2015 and 2019. The included images were chosen to comprise images from patients whose fractures were considered as difficult-to-classify, displaced fractures. Consequently, the images were assessed for eight fracture characteristics and categorized according to the Neer and Hertel classifications by four orthopaedic residents and four attending orthopaedic surgeons during two separate sessions. In the first session, the assessment was performed with conventional onscreen imaging (radiographs and 2D and 3D CT images).

In the second session, 3D-printed handheld models were used for assessment, while onscreen imaging was also available (Fig. 1).

RESULTS AND DISCUSSION

Using 3D-printed models in addition to conventional imaging did not improve interobserver agreement of the following fracture characteristics: more than 2 mm medial hinge displacement, more than 8 mm metaphyseal extension, surgical neck fracture, anatomic neck fracture, displacement of the humeral head, more than 10 mm lesser tuberosity displacement, and more than 10 mm greater tuberosity displacement. Agreement regarding the presence of a humeral head-splitting fracture was improved but only to a level that was insufficient for clinical or scientific use (fair-to-substantial, delta kappa = 0.33 [95% CI 0.02 to 0.64]). Assessing 3D-printed handheld models in adjunct to onscreen conventional imaging did not improve the interobserver agreement for pattern recognition according to Neer (delta kappa = 0.02 [95% CI -0.11 to 0.07]) and Hertel (delta kappa = 0.01 [95% CI -0.11 to 0.08]).

CONCLUSIONS

Using 3D-printed handheld fracture models in addition to conventional onscreen imaging of three-part and four-part proximal humerus fractures does not improve agreement among residents and attending surgeons on specific fracture characteristics and patterns. Therefore, we do not recommend that clinicians expend the time and costs needed to create these models if the goal is to classify or describe patients' fracture characteristics or pattern.

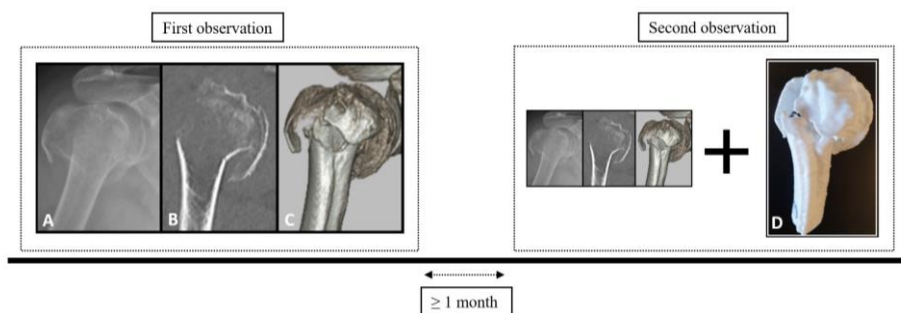


Fig. 1 The image labelled with the letter A represents the trauma radiograph, B the 2D CT image (coronal plane), C the 3D CT image (anterolateral aspect) and D the 3D-printed handheld model.

CONFLICT OF INTEREST DECLARATION

In the interests of transparency and to help reviewers assess any potential bias, all authors of original research papers are required to declare any competing commercial interests in relation to the submitted work. Referees are also asked to indicate any potential conflict they might have reviewing a particular paper.

If you have accepted any support such as funds or materials, tangible or intangible, concerned with the research by the commercial party such as companies or investors, choose YES below, and state the relation between you and the commercial party.

If you have not accepted any support such as funds or materials, choose NO.

Do you have a conflict of interest to declare? (DELETE TEXT as appropriate)

YES

If YES, please complete as appropriate:

1. The author(s) did receive payments or other benefits or a commitment or agreement to provide such benefits from a commercial entity.
State the relation between you and the commercial entity:

One author (RWAS) has received payments, during the study period, in an amount of less than USD 10,000 from the Michael van Vloten Foundation (Rotterdam, the Netherlands). One author (BJAS) received a payment of less than USD 10,000 from the Traumaplatform Foundation and Anna Foundation.
Three authors (RWAS, BJAS, JFFO) received a payment of between USD 10,000-USD 100,000 from Prins Bernhard Cultuurfonds.
One author (RLJ) received personal fees from Smith & Nephew and DePuy Synthes in the form of paid lectures.
One author (DE) received an institutional research grant from Zimmer Biomet and Stryker and received educational research support from Lima.
2. A commercial entity paid or directed, or agreed to pay or direct, any benefits to any research fund, foundation, educational institution, or other charitable or nonprofit organization with which the authors are affiliated or associated.



CT MEASURED ACETABULAR BONE DENSITY FOLLOWING TOTAL HIP ARTHROPLASTY: A SCOPING REVIEW AND META-ANALYSIS

Thomas Robertson^{1,2}, Bogdan Solomon^{1,2}, Rob Nelissen³, Zachary Munn^{2,4} Stuart Callary^{1,2}

¹Department of Orthopaedics and Trauma Royal Adelaide Hospital, Adelaide, SA, Australia

²Faculty of Health and Medical Sciences, The University of Adelaide, Adelaide, SA, Australia

³Department of Orthopaedics, Leiden University Medical Center, Leiden, Netherlands

⁴Joanne Briggs Institute, Adelaide, SA Australia

email: thomas.robertson@sa.gov.au

INTRODUCTION

With the increasing numbers of total hip arthroplasty and revision arthroplasty being performed in Australia accurate and repeatable measurements of acetabular bone quality is imperative. Despite advancements in polyethylene liner design, loosening and bone lysis continues to be the most frequent cause of revision of THA.¹ Measurements of bone quality in the periacetabular region provide potentially useful information in predicting failure of implants as well as planning revision surgery. The aim of this study was to perform a scoping review to identify all studies which had measured bone density around total hip arthroplasty using quantitative computer tomography (CT). Secondly to identify the regions of interest defined to measure density and perform of a meta-analysis of the change of density over time between cemented vs uncemented acetabular components.

METHODS

Using Embase, Scopus and Pubmed a systematic search was conducted to identify all studies measuring bone density in the acetabular region using CT following total hip arthroplasty. The Covidence system was used by two blinded reviewers which identified 19 unique studies. Of these 19 studies all reviewed for the regions of interest identified and the standards of reporting CT measured density. A meta-analysis was performed on the 9 unique studies which reported bone density measurements at immediately post operatively and at subsequent follow up. To facilitate correlation between studies the regions of interest were simplified to; cranial to the level of the cup or at the level of the cup, those at the level of the cup were further classified as either ventral or dorsal. Further

analysis was performed on separate regions relative to the top of the acetabular component.

RESULTS AND DISCUSSION

There is a paucity in consistency of data reporting of CT related measurements. Of all studies reviewed there were great disparity in the regions of interest reported, units and CT parameters. In the meta-analysis acetabular bone density of both cemented and uncemented components decreases over time. This is disproportionately seen in the dorsal region at the level of the cup for all types of acetabular components in both cortical and cancellous bone.

CONCLUSIONS

Bone density disproportionately decreases dorsally at the level of the acetabular component over time. Standardized reporting of quantitative CT studies of bone density should include all parameters of CT function, patient factors and regions of interest. A standardized region of interest system splitting the acetabulum into zones relative to the top of the acetabular component is proposed.

ACKNOWLEDGEMENTS

Nil

REFERENCES

1. Australian Orthopaedic Association National Joint Replacement Registry (AOANJRR) **Hip, Knee & Shoulder Arthroplasty: 2020 Annual Report**. AOA, Adelaide 2020



TWO NOVEL DESIGNS OF IMPROVING PATELLA RESECTION TOOLS

¹Yuan Chai, ¹Mounir Boudali, ²David A. Parker and ¹William L. Walter

¹Kolling Institute of Medical Research, Faculty of Medicine and Health, The University of Sydney, St. Leonards, NSW, Australia

²Sydney Orthopaedic Research Institute, Chatswood, NSW, Australia

email: yuan.chai@sydney.edu.au

INTRODUCTION

In total knee arthroplasty (TKA), the patella resection is difficult due to the small size of the patella bone and its attached soft tissue. Although the current preoperative planning technique has developed a reasonable precision, the majority of the market available tools are designed to perform resection using freehand. The quality of patella resurfacing in TKA is mainly managed by the experience and dexterity of a surgeon. The procedure is usually not reproducible nor accurately quantifiable onsite [1]. A tilted patella resection affects the bone thickness in different quadrants, which is likely to reduce implant function and cause pain, thus increasing the likelihood of a revision [2]. There is therefore a need for novel patella resection tools that allow reproducible and consistent cuts.

METHODS

This project overviewed current patella resurfacing techniques using a saw blade and off-the-shelf tools through an online search and surgery observations. Then a survey was designed to collect data of patella resection preference from 9 surgeons with different experience levels. We used data from the survey result to guide our design of novel patella cutting devices. Two possible solutions were proposed that have a good potential to improve the patella resection accuracy without increasing the complexity of use. These solutions were 3D modeled using CAD software for demonstration purposes (Figure 1 and 2).

RESULTS AND DISCUSSION

We identified two main features of improvement regarding the design of current patella resection tools: firmly holding the patella bone while positioning the resection plane, and maintaining the saw blade on the cutting plane. Findings from the survey showed the predominance of the sawing technique as opposed to milling. Furthermore, an average of two cuts is necessary before obtaining a satisfactory resected plane. Participating surgeons requested improving the accuracy and reproducibility of cuts while maintaining the simplicity of each tool used. These findings guided two improved designs of patella resection tools: saw blade with guiding arms (Figure 1), and resection plane positioning clamp (Figure 2).

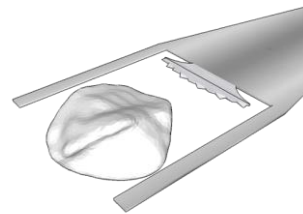


Figure 1: Saw blade with guiding arms

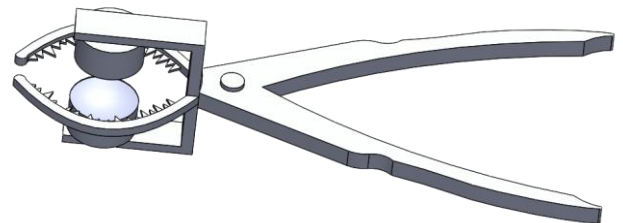


Figure 2: Resection plane positioning clamp

Compared to the market available patella resection tools, the proposed designs are likely to solve two major causes of imperfect patella cuts by applying a novel resection plane positioning device (Figure 2) and an arm-guided saw blade (Figure 1). Neither of the designs requires extra learning. Although feedback from 9 surgeons was consistent, more data input, a prototype realization, and a clinical trial are necessary to validate our design.

CONCLUSIONS

In this project, we proposed two novel patella cutting tool designs that have a high potential of improving the patella resection quality and repeatability. The designs improve the consistency of the patella resection by reducing the vertical drift of the saw blade and avail a better realization of resection plane positioning of the pre-operative planning. The improved reproducibility is likely to provide a better training environment for residents and a more objective assessment criterion of the patella resection performance.

REFERENCES

1. Kandhari V, et al., *The Knee*, **27**: S4, 2020.
2. Rex E L, et al., *Bioengineering*, **5**(2): 38, 2018.



ESTABLISHING AN EVIDENCE-BASED APPROACH TO IMPROVE THE STABILITY OF ACETABULAR COMPONENTS USED AT REVISION SURGERY

Stuart Callary, John Abrahams, Donald Howie, Bogdan Solomon

Centre for Orthopaedic and Trauma Research, The University of Adelaide and the Department of Orthopaedics and Trauma, The Royal Adelaide Hospital, Adelaide, SA, Australia

email: stuart.callary@sa.gov.au

INTRODUCTION

An evidence based stepwise introduction of new implants has been effective when applied to implants used at primary total hip arthroplasty (THA) [1]. The initial step included preclinical testing, followed by three sequential clinical steps 1) prospective randomized trials, 2) multicentre studies and 3) register studies (Figure 1). The hypothesis of this evidence based introduction was that it would allow more precise and careful evaluation of new implant technology and reduce the number of patients at risk for unexpected failures.

The survivorship of implants used at revision THA is inferior to those used at primary THA [2], especially for acetabular components in the presence of large bone defects. It is more difficult to apply the stepwise algorithm of introduction of new technology to implants used at revision THA due to the smaller volume of surgeries; the small number of long-term follow-up studies due to older frailer patients; and the confounding potentially complicating factors that exist due to previous surgery. As a result, there are very few published prospective randomized or multicentre studies required as part of clinical steps I and II in the stepwise algorithm. Additionally, step III registry studies have been limited by the fact that patients may not undergo re-revision surgery despite a poor performing implant.

An important aspect of the stepwise introduction proposed by Malchau was the use of early implant migration as a surrogate for long term aseptic loosening. Prior to the beginning of our body of work, it was difficult to interpret the limited literature as many small single-institution cohort studies used inaccurate manual radiographic migration measurements and only reported early outcomes. While established acceptable migration thresholds have been described for acetabular components used at primary THA, there were no validated thresholds for components used at revision THA prior to our studies.

METHODS

We conducted a large longitudinal study with radiological and clinical follow-up that spanned over 30 years [3,4]. Uniquely, loosening status for patients in our study were validated using intraoperative implant loosening confirmed at the time of re-revision surgery, and not based on radiographic loosening like all other reports. We determined that >1mm proximal migration within the first two years is predictive of later loosening [4]. Proximal migration >3mm or sagittal rotation >5 degrees were each found to be diagnostic of loosening [3]. These migration thresholds allowed us to interpret the outcomes of our own

prospective cohort of patients that had undergone sensitive radiostereometric analysis (RSA) measurements prospectively between 2003 and 2018.

RESULTS AND DISCUSSION

Used a novel combination of the most sensitive methods available, RSA and CT scans, we identified factors that influenced early stability including the severity of the existing bone defects, the presence of pelvic discontinuity and the fixation of the component to the pelvic bones. When first introduced in our institution, porous tantalum components had comparable early failure rates with the other literature reports [5]. Our results improved after establishing the importance of three-point fixation including inferior ischial and pubic contact [5]. Preoperative assessment of the defect being treated is important and we have implemented CT imaging protocols that improve peri-prosthetic metal artefact.

CONCLUSION

Our studies provide an evidence base to assess the outcomes of the implants and surgical techniques used currently and when conducting clinical step I prospective randomized or step II multicentre studies. The advantage of accurately monitoring early stability of new implants and surgical techniques to address large acetabular defects at revision THA have been demonstrated with our increased understanding of the failure mechanisms, and evidence supporting the necessity for three-point implant-to-bone contact with the ilium, ischium and pubis.

ACKNOWLEDGEMENTS

We thank the RAH for supporting this study, our Orthopaedic surgeons and nursing staff, the Orthopaedic Quality Assurance and Research Unit at the RAH.

REFERENCES

1. Malchau H et al., *J Arthroplasty*. 2011;26:825-831.
2. AOANJRR Annual Report. Adelaide: AOA, 2019.
2. Abrahams J et al., *Bone Joint J*. 2017;99-B:458-464.
3. Kim SY, et al., *Bone Joint J*. 2017;99-B:465-474.
4. Solomon LB et al., *JBJs Am*. 2018;100:1926-1933.

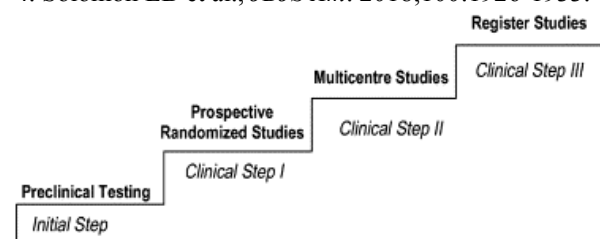


Figure 1: The algorithm for introducing new treatment techniques into clinical practice

ANZORS 26th Annual Scientific Meeting

List of Registered Delegates

(at the time of printing, surname ordered alphabetically)

Title	First Name	Surname	Institution	E-mail
A/Prof	David	Ackland	The University of Melbourne, Australia	dackland@unimelb.edu.au
Dr	Rami	Al-Dirini	Flinders University, Australia	rami.aldirini@flinders.edu.au
Dr	Ian	Al'Khafaji	Hip Arthroscopy Australia	ialkhafa@gmail.com
Mr	Mitchell	Almond	The University of Melbourne, Australia	malmond@student.unimelb.edu.au
Dr	Jayalathge	Amarasooriya	Flinders University, Australia	melanieamarasooriya@gmail.com
Dr	Maged	Awadalla	Flinders University, Australia	Awad0001@flinders.edu.au
Dr	Martina	Barzan	Griffith University, Australia	m.barzan@griffith.edu.au
Dr	Samuel	Bennett	The University of Western Australia	samuel.bennett@research.uwa.edu.au
Mr	Kieran	Bennett	The University of Adelaide, Australia	kieran.bennett@adelaide.edu.au
Prof	Thor	Besier	The University of Auckland, New Zealand	t.besier@auckland.ac.nz
Dr	Carina	Blaker	Kolling Institute, University of Sydney, Australia	carina.blaker@sydney.edu.au
Dr	Scott	Bolam	The University of Auckland, New Zealand	s.bolam@auckland.ac.nz
Mr	Marco	Branni	Queensland University of Technology, Australia	marco.branni@qut.edu.au
Ms	Alexis	Brierty	Griffith University, Australia	alexis.brierty@griffithuni.edu.au
Ms	Emma	Brown	The University of Auckland, New Zealand	emma.brown@auckland.ac.nz
Ms	Francesca	Bucci	Flinders University, Australia	francesca.bucci@flinders.edu.au
Dr	Joseph	Cadman	Macquarie University, Australia	joseph.cadman@mq.edu.au
Dr	Stuart	Callary	Royal Adelaide Hospital, Australia	stuart.callary@sa.gov.au
Dr	Yuan	Chai	The University of Sydney, Australia	76383250@qq.com
Dr	Audrey	Chan	The University of Melbourne, Australia	audrey.chan@unimelb.edu.au
Mr	Peilin	Chen	The University of Western Australia	peilin.chen@research.uwa.edu.au
Dr	Lianzhi	Chen	The University of Western Australia	lianzhi.k.chen@outlook.com
Dr	Kai	Chen	The University of Western Australia	kai.chen@uwa.edu.au
Dr	Julie	Choisne	The University of Auckland, New Zealand	j.choisne@auckland.ac.nz
A/Prof	Claire	Clarkin	The University of South Hampton, UK	c.e.clarkin@soton.ac.uk
Prof	Jillian	Cornish	The University of Auckland, New Zealand	j.cornish@auckland.ac.nz
A/Prof	John	Costi	Flinders University, Australia	john.costi@flinders.edu.au
Mrs	Kerry	Costi	Royal Adelaide Hospital, Australia	kerry.costi@sa.gov.au
A/Prof	Tania	Crotti	The University of Adelaide, Australia	tania.crotti@adelaide.edu.au
Dr	James	Crowley	University of New South Wales, Australia	james.crowley@unsw.edu.au
Mr	Bailey	Deverell	The University of Adelaide, Australia	bailey.deverell@adelaide.edu.au
Mr	William	du Moulin	Griffith University, Australia	will.dumoulin@griffithuni.edu.au

Mr	Pholpat	Durongbhan	The University of Melbourne, Australia	pdurongbhan@student.unimelb.edu.au
Mrs	Julie	Edwards	Children's Health Queensland, Australia	Julie.Edwards@health.qld.gov.au
Ms	Sara	Farshidfar	Macquarie University, Australia	sara.farshidfar@hdr.mq.edu.au
Mr	Ben	Ferguson	The University of Sydney, Australia	ben.ferguson@sydney.edu.au
Prof	David	Findlay	Retired	david.findlay@adelaide.edu.au
Dr	Aaron	Fox	Deakin University, Australia	aaron.f@deakin.edu.au
Mr	Fraser	Francis-Pester	Australian National University, Australia	fraser.francispester@gmail.com
Mrs	Michelle	Gordon	Queensland Children's Hospital, Australia	michelle.gordon@health.qld.gov.au
Dr	Hans	Gray	The University of Melbourne, Australia	hans.gray@unimelb.edu.au
Prof	Farshid	Guilak	Washington University, St. Louis, USA	guilak@wustl.edu
Prof	Saman	Halgamuge	The University of Melbourne, Australia	saman@unimelb.edu.au
Mr	Ross	Hamilton	The University of Adelaide, Australia	ross.hamilton@adelaide.edu.au
Miss	Samantha	Hefferan	Kolling Institute, University of Sydney, Australia	samantha.hefferan@sydney.edu.au
Mr	Buddhi	Herath	Queensland University of Technology, Australia	b.herath@qut.edu.au
Miss	Salindi	Herath	Flinders University, Australia	salindi.herath@flinders.edu.au
Dr	Lachlan	Huntington	Western Health, Australia	lachlanhuntington@gmail.com
Mr	Niveda	Jeyamanoharan	Curtin University, Australia	nivedanj@gmail.com
Dr	Claire	Jones	The University of Adelaide, Australia	claire.jones@adelaide.edu.au
Dr	Azadeh	Kian	Victoria University, Australia	azadeh.kian@vu.edu.au
Mr	Subhajit	Konar	The University of Auckland, New Zealand	s.konar@auckland.ac.nz
Mr	Adam	Kositsky	Griffith University, Australia	adam.kositsky@griffithuni.edu.au
Miss	Melody	Labrune	Macquarie University, Australia	melody.labrune@students.mq.edu.au
Miss	Tyra	Lange	Flinders University, Australia	tyralange@me.com
Mr	Joshua	Lee	Monash University, Australia	jlee0134@student.monash.edu
Prof	Peter	Lee	The University of Melbourne, Australia	pvlee@unimelb.edu.au
Dr	Jiao Jiao	Li	University of Technology Sydney, Australia	jiaojiao.li@uts.edu.au
A/Prof	Rachel	Li	Australian National University, Australia	rachel.li@anu.edu.au
Prof	Christopher	Little	Kolling Institute, University of Sydney, Australia	christopher.little@sydney.edu.au
Dr	Joe	Lynch	Trauma & Orthopaedic Research Unit, Australia	joseph.lynch@anu.edu.au
Dr	Sheanna	Maine	Griffith University, Australia	sheanna.maine@gmail.com
Dr	Peggy	Miller	St Vincent's University Hospital, Dublin, Ireland	peggy.miller0496@gmail.com
Miss	Daniela	Mini	Flinders University, Australia	mini0017@flinders.edu.au
Dr	Saeed	Miramini	The University of Melbourne, Australia	s.miramini@unimelb.edu.au
Dr	Sam	Mischewski	The University of Sydney, Australia	sam.mischewski@gmail.com
Dr	Luca	Modenese	Imperial College London, United Kingdom	l.modenese@imperial.ac.uk
Dr	Dzenita	Muratovic	The University of Adelaide, Australia	dzenita.muratovic@adelaide.edu.au
Dr	David	Musson	The University of Auckland, New Zealand	d.musson@auckland.ac.nz
Dr	Azadeh	Nasseri	Griffith University, Australia	a.nasseri@griffith.edu.au
Dr	Dermot	O'Rourke	Flinders University, Australia	dermot.orourke@flinders.edu.au
A/Prof	Nathan	Pavlos	The University of Western Australia, Australia	nathan.pavlos@uwa.edu.au
A/Prof	Egon	Perilli	Flinders University, Australia	egon.perilli@flinders.edu.au
Dr	Diana	Perriman	Australian National University, Australia	diana.perriman@anu.edu.au
Ms	Teresa	Phillips	Queensland Children's Hospital, Australia	teresa.phillips2@health.qld.gov.au
Mr	Heng	Qiu	The University of Western Australia, Australia	heng.qiu@research.uwa.edu.au

Dr	Ryan	Quarrington	The University of Adelaide, Australia	ryan.quarrington@adelaide.edu.au
Mr	Kiran	Rajesh	Australian National University, Australia	u6402061@anu.edu.au
Ms	Sophie	Rapagna	Flinders University, Australia	sophie.rapagna@flinders.edu.au
Miss	Amy	Ribet	The University of Western Australia, Australia	amyribet@gmail.com
Dr	Thomas	Robertson	Limestone Coast Local Health Network, Australia	thomas.robertson@sa.gov.au
Dr	Dale	Robinson	The University of Melbourne, Australia	drobinson@unimelb.edu.au
Dr	Iman	Roohani	The University of Sydney, Australia	i.roohani@sydney.edu.au
Dr	Megan	Roser	Queensland Children's Hospital and Centre for Children's Health Research	mjnroser@gmail.com
Ms	Harshi	Rupasinghe	The University of Melbourne, Australia	harshirs99@gmail.com
Mr	Michael	Russo	Flinders University, Australia	michael.russo@flinders.edu.au
Mr	Pouya	Saeedian	The University of Canberra, Australia	pouya.saeedian@outlook.com
Dr	Ladan	Sahafi	Flinders Medical Centre, Australia	ladan.sahafi@sa.gov.au
Prof	Jennie	Scarvell	The University of Canberra, Australia	jennie.scarvell@canberra.edu.au
Dr	Damith	Senanayake	The University of Melbourne, Australia	damithasanka@unimelb.edu.au
Mr	Kyle	Shapland	Materialise Australia, Australia	kyle.shapland@materialise.com.au
Dr	David	Shen	Royal North Shore Hospital, Australia	david.b.shen@gmail.com
Prof	Natalie	Sims	St. Vincent's Institute, Australia	nsims@svi.edu.au
Mr	Arjun	Sivakumar	The University of Adelaide, Australia	arjun.sivakumar@adelaide.edu.au
Prof	Bogdan	Solomon	Royal Adelaide Hospital, Australia	bogdan.solomon@sa.gov.au
MD	Reinier	Spek	Flinders Medical Centre, Australia	reinierspek@gmail.com
Dr	Kathryn	Stok	The University of Melbourne, Australia	kstok@unimelb.edu.au
Mr	Jonghoo	Sung	The University of Adelaide, Australia	a1695343@student.adelaide.edu.au
Dr	Chi Pang	Tai	Perron Institute, Australia	andrew.tai@perron.uwa.edu.au
Prof	Ashvin	Thambyah	The University of Auckland, New Zealand	ashvin.thambyah@auckland.ac.nz
A/Prof	Dominic	Thewlis	University of Adelaide, Australia	dominic.thewlis@adelaide.edu.au
Mr	Darcy	Thompson-Bagshaw	The University of Adelaide, Australia	darcy.thompson-bagshaw@adelaide.edu.au
Mr	Simon	Thwaites	The University of Adelaide, Australia	simon.thwaites@adelaide.edu.au
Mr	Jacob	Trend	University Of Southampton, United Kingdom	jt4n19@soton.ac.uk
Dr	Dane	Turner	Macquarie University, Australia	saneh.turner@mq.edu.au
Ms	Lauren	Wearne	Flinders University, Australia	lauren.wearne@flinders.edu.au
Mr	Hugo	Wiggins	Macquarie University, Australia	hugo.wiggins@hdr.mq.edu.au
Dr	Daniel	Wills	The University of New South Wales, Australia	d.wills@unsw.edu.au
Dr	Josh	Workman	The University of Auckland, New Zealand	j.workman@auckland.ac.nz
Prof	Jiake	Xu	The University of Western Australia, Australia	jiake.xu@uwa.edu.au
Mr	Yihang	Yu	The University of Melbourne, Australia	yihangy@student.unimelb.edu.au
Mr	Jun	Yuan	The University of Western Australia, Australia	jun.yuan@research.uwa.edu.au
Mr	Faseeh	Zaidi	The University of Auckland. New Zealand	szai535@aucklanduni.ac.nz
Dr	Sanaa	Zaki	University of Sydney, Australia	sanaa.zaki@sydney.edu.au
Dr	Ju	Zhang	Formus Labs Ltd, New Zealand	ju@formuslabs.com
Prof	Minghao	Zheng	The University of Western Australia, Australia	minghao.zheng@uwa.edu.au
Dr	Yinhong	Zhou	Queensland University of Technology, Australia	yinhongzhou@qut.edu.au